



**UNIVERSIDADE FEDERAL DO PARÁ  
INSTITUTO DE GEOCIÊNCIAS  
PROGRAMA DE PÓS-GRADUAÇÃO EM GEOLOGIA E GEOQUÍMICA**

---

**DISSERTAÇÃO DE MESTRADO Nº 607**

**ICNOLOGIA, ESTRATIGRAFIA E PALEOAMBIENTE DA  
FORMAÇÃO PASTOS BONS, JURÁSSICO SUPERIOR -  
CRETÁCEO INFERIOR DA BACIA DO PARNAÍBA**

**Dissertação apresentada por:**

**NOME: ARGEL DE ASSIS NUNES SODRÉ**

**Orientador: Prof. Dr. Joelson Lima Soares (IG/UFPA)**

---

**BELÉM – PA  
2021**

**Dados Internacionais de Catalogação na Publicação (CIP) de acordo com ISBD  
Sistema de Bibliotecas da Universidade Federal do Pará  
Gerada automaticamente pelo módulo Ficat, mediante os dados fornecidos pelo(a) autor(a)**

---

S679i Sodré, Argel de Assis Nunes.

Iconologia, estratigrafia e paleoambiente da Formação Pastos Bons, Jurássico Superior -Cretáceo Inferior da Bacia do Parnaíba / Argel de Assis Nunes Sodré. — 2021.

xv; 69 f. : il. color.

Orientador(a): Prof. Dr. Joelson Lima Soares  
Dissertação (Mestrado) - Universidade Federal do Pará, Instituto de Geociências, Programa de Pós-Graduação em Geologia e Geoquímica, Belém, 2021.

1. Sistema lacustre. 2. Icnofósseis. 3. Formação Pastos Bons. 4. Jurássico Superior. 5. Cretáceo Inferior. I. Título.

CDD 551.700981

---



**Universidade Federal do Pará**  
**Instituto de Geociências**  
Programa de Pós-Graduação em Geologia e Geoquímica

**ICNOLOGIA, ESTRATIGRAFIA E PALEOAMBIENTE DA  
FORMAÇÃO PASTOS BONS, JURÁSSICO SUPERIOR -  
CRETÁCEO INFERIOR DA BACIA DO PARNAÍBA**


**Dissertação de mestrado apresentada por:**


**ARGEL DE ASSIS NUNES SODRÉ**


**Como requisito parcial à obtenção do Grau de Mestre em Ciências na Área de  
GEOLOGIA, linha de pesquisa ANÁLISE DE BACIAS SEDIMENTARES**

**Data da Aprovação: 05 / 11 /2021**

**Banca Examinadora:**

  
Prof. Dr. Joelson Lima Soares  
(Orientador – UFPA)

  
Prof. Dr. José Bandeira Cavalcante da Silva Júnior  
(Membro - UFPA)

  
Dr. Rafael Costa da Silva  
(Membro – CPRM-RJ)

Dedico à minha família e aos meus amigos, que me dão todo apoio na jornada da vida acadêmica.

## AGRADECIMENTOS

O presente trabalho foi realizado com apoio da Coordenação de Aperfeiçoamento de Pessoal de Nível Superior - Brasil (CAPES) - Código de Financiamento 001.

Agradeço primeiramente aos meus pais, Raimundo Sodré e Edna Nunes, que nunca mediram esforços para que eu alcançasse os meus objetivos.

À minha irmã, Amaranta Sodré; à minha avó Marlene Nunes; aos meus primos/irmãos Victor e Letícia Nunes.

À minha noiva, Brenda Costa, por todo o amor, companheirismo, carinho e companhia, força e aconselhamentos durante esses dois longos anos de mestrado.

Ao orientador Prof. Dr. Joelson Lima Soares, pela amizade, orientações, sugestões e oportunidades.

Ao Prof. Dr. Afonso Nogueira, pela amizade, companheirismo, orientações e pelas oportunidades.

Ao Programa de Pós-graduação em Geologia e Geoquímica, ao Instituto de Geociências da Universidade Federal do Pará.

Aos amigos do GSED, que foram essenciais em várias fases deste trabalho, principalmente durante esses tempos tão difíceis, em especial ao Alexandre Ribeiro, Pedro Augusto, Renan Fernandes, Lucas Cunha, Antonio Gonçalves e Walmir Lima, Ailton Brito, Guilherme Raffaelli e Gabriel Leal.

Aos técnicos do Laboratório de Sedimentologia, Everaldo Cunha, e Laboratório de Laminação, Joelma Lobo e Bruno Fernandes, pelo auxílio na preparação de amostras.

Aos Geol. Dr. Clóvis Maurity pela amizade, incentivo e oportunidades desde o início da graduação.

Aos amigos da turma de 2014, em especial Dominique Ferreira, Artur Sarmiento, Victor Coutinho, Ádria Mori, Ismayla Carneiro, Sanmya Dias, Jhoseph Costa, Murilo Henrique e Matheus Moura; e aos amigos de fora da geologia, Bruce Morais, Maíra Ferraz, Luan Sanches, Alana Menezes, Vitória Mendes, Manuela Gaya, Laura Quaresma, Camila Cravo, Daniel Kahwage, Brendo Gaia; aos amigos de Barcarena, Maura, Caio, Kayse, Bruna, Eive e Cauê por todo o amor e por tornarem esta caminhada mais agradável.

Aos demais professores do IG, pelos ensinamentos; e aos funcionários do IG, especialmente ao Afonso Quaresma, pelo apoio.

Agradeço a todos que direta ou indiretamente me ajudaram a ingressar e concluir mais essa etapa da vida acadêmica.

*“Quem costuma vir de onde eu sou, às vezes não tem  
motivo pra seguir, então levanta e anda”*

(Emicida)

## RESUMO

Após a implantação de volumosas quantidades de magma, relacionadas à Província Magmática do Atlântico Central (CAMP), no Triássico-Jurássico (~ 200 Ma), uma grande área de subsidência foi formada no Gondwana Ocidental, possibilitando a instalação do sistema lacustre do Jurássico Superior-Cretáceo Inferior da Bacia do Parnaíba, representado pela Formação Pastos Bons. Apesar dos recentes avanços, esses depósitos ainda precisam ser investigados detalhadamente com base no conteúdo icnológico, combinado com a análise de fácies, e na estratigrafia de sequência lacustre, refinando a interpretação paleoambiental e contribuindo para o entendimento das condições pós-CAMP no Gondwana Ocidental. Nesse sentido, a análise de fácies baseada em afloramentos permitiu o reconhecimento de quatro paleoambientes: lago central, margem do lago, fluvial entrelaçado e frente deltaica. A margem do lago concentra a assembleia icnológica, que consiste em oito icnofósseis, organizados em três icnofácies: *Mermia* (*Cochlichnus anguineus* e *Lockeia siliquaria*); *Scoyenia* (*Agrichnium* isp., *Gyrochorte comosa*, *Palaeophycus tubularis*, *Planolites berveleyensis* e *Rusophycus* isp.), e *Skolithos* (*Skolithos linearis*). Essa sucessão lacustre é organizada em cinco ciclos deposicionais, caracterizados por ciclos de escala milimétrica a métrica, delimitados por superfícies erosivas ou superfícies de inundação. Quatro ciclos definem um padrão retrogradacional e agradacional que compõe o trato de sistema transgressivo; e um ciclo indica o padrão progradacional, constituindo o trato do sistema de máxima inundação. A estratigrafia de sequências sugere que a subsidência térmica pós-CAMP é responsável pela criação do espaço de acomodação, controle do suprimento sedimentar e da entrada e saída de água, bem como a relação proporcional entre eles. Na base, predomina o trato de sistema transgressivo, formando as bacias lacustres do tipo *underfilled*, caracterizada por lago central fossilífero e margens de lagos com icnofósseis; no topo, após a subsidência máxima, ocorre o trato do sistema de máxima inundação, configurando-se a bacia lacustre do tipo *overfilled* caracterizada pelo domínio de arenito com estratificações cruzadas que compõem o sistema fluvio-deltaico.

Palavras-chave: Formação Pastos Bons; Jurássico-Cretáceo; Pós-CAMP; *Mermia*; *Scoyenia*; *Skolithos*.

## ABSTRACT

After the voluminous lava eruption related to the Central Atlantic Magmatic Province (CAMP), in the Triassic–Jurassic (~200 Ma), a large subsiding area formed in West Gondwana, allowing the Upper Jurassic–Lower Cretaceous lacustrine system of the Pastos Bons Formation, in the Parnaíba Basin. Despite recent studies on this lacustrine system, these deposits still need to be investigated in detail with palaeoenvironmental mapping based on the ichnological content, facies analysis and lacustrine sequence stratigraphy. Outcrop-based facies analysis allowed the identification of four palaeoenvironments: central lake, lakeshore, braided fluvial, and delta front. The ichnological content is concentrated in the lakeshore deposits and includes of eight ichnofossils, organized in three ichnofacies: *Mermia* (*Cochlichnus anguineus* and *Lockeia siliquaria*), *Scoyenia* (*Agrichnium* isp., *Gyrochorte comosa*, *Palaeophycus tubularis*, *Planolites berveleyensis*, and *Rusophycus* isp.), and *Skolithos* (*Skolithos linearis*). This lacustrine succession is organized in five millimeter- to meter-scale depositional cycles bounded by erosive surfaces or flooding surfaces. Four cycles define a retrogradational and aggradational stratal stacking pattern composing the transgressive systems tract, and one cycle indicates the progradational stratal stacking pattern constituting the highstand systems tract. The sequence stratigraphy suggests that post-CAMP thermal subsidence and responsible for creating the accommodation space, controlling the sedimentary supply and water inflow/outflow, and the proportional relationship between them. At the base of this system, an underfilled lacustrine basin characterized by fossil and ichnofossil-bearing layers and thick mudstones predominated, and after the maximum subsidence, an overfilled lacustrine basin characterized by cross-laminated sandstone of the fluvio-deltaic system was established.

Keywords: Pastos Bons Formation; Jurassic-Cretaceous; Post-CAMP; *Mermia*; *Scoyenia*; *Skolithos*.



## LISTA DE ILUSTRAÇÕES

- Figura 1.1 – Mapa de localização da área de estudo. (A) Mapa geográfico do Brasil, estado do Piauí de cor amarela. (B) Mapa geológico da Bacia do Parnaíba, destacando as superseqüências sedimentares, o retângulo vermelho delimita a área de estudo (modificado de Santos & Carvalho 2004). (C) Mapa paleoambiental da área de estudo, sudeste da Bacia do Parnaíba. Fonte: Produzido pelo autor. .... 3
- Figura 1.2 – Carta estratigráfica da Bacia do Parnaíba. Fonte: Góes & Feijó (1994). .... 5
- Figura 1.3 – Bloco diagrama que apresenta a distribuição dos ambientes de sedimentação em contextos lacustres. Fonte: Nichols (2009). .... 11
- Figura 1.4 – Exemplos de ciclos deposicionais recorrentes em lagos atuais. Fonte: Renaut & Gierlowski-Kordesch (2010). .... 12
- Figura 1.5 – Diagrama que sumariza as características estratigráficas e ambientais dos três tipos de bacias lacustres, *overfilled* ( $A_p < S_s$ ), *balanced-fill* ( $A_p \sim S_s$ ) e *underfilled* ( $A_p > S_s$ ) *lake basins*, segundo Carroll & Bohacs (1999) e Bohacs *et al.* (2000). Fonte: Bohacs *et al.* (2000). .... 13
- Figura 1.6 – Icnotaxobases utilizadas para classificação morfológica dos icnofósseis. Fonte: Bromley (1996). .... 14
- Figura 1.7 – Terminologia para classificação estratinômica de icnofósseis conforme seu modo de preservação segundo Seilacher (1964) e Martinsson (1970). Fonte: Ekdale *et al.* (1984). .... 15
- Figura 1.8 – Bloco diagrama com os principais icnogêneros que compõem a icnofácies *Mermia*. Me, *Mermia*; He, *Helminthoidichnites*; Go, *Gordia*; Co, *Cochlichnus*; Ac, *Archaeonassa*; Wa, *Warvichnium*; Cr, *Cruziana*; Pl, *Planolites*; Pa, *Palaeophycus*; Tr, *Treptichnus*; Va, *Vagorichnus*; Lo, *Lockeia*; Un, *Undichna*. Fonte: Scott *et al.* (2012). .... 16
- Figura 1.10 – Bloco diagrama com os principais icnogêneros que compõem a icnofácies *Skolithos*. Ar, *Arenicolites*; Es, estruturas de escape; Po, *Polykladichnus*; Ps, *Psilonichnus*; Sk, *Skolithos*. Fonte: Scott *et al.* (2012). .... 17
- Figura 1.11 – Modelo de icnofácies para a estratigrafia de seqüência de ambientes lacustres, conforme a classificação de bacias lacustres postulada por Bohacs *et al.* (2000). Fonte: Buatois & Mángano (2007). .... 18

- Figure 2.1 – Location map of the study area. A. Geographic map of Brazil, with Piauí State marked in yellow. B. Parnaíba Basin, north-eastern Brazil, and geological mapping of the local sedimentary supersequences; the red rectangle delimits the study area (modified from Santos and Carvalho, 2004). C. Palaeoenvironmental map of the study area, south-eastern Parnaíba Basin. .... 23
- Figure 2.2 – The stratigraphic context of measured sections of the Upper Jurassic–Lower Cretaceous Pastos Bons Formation in the eastern Parnaíba Basin, Brazil. .... 28
- Figure 2.3 – Sedimentary facies. A. Central lake. Grey mudstone interbedded with laminated limestone, forming millimeter- to centimeter-thick shallowing/salinization-upward cycles (white triangles). B and C. Fragments of *Lepidotes piauihyensis* (white arrows). D and E. Central lake (FA1). Grey to green laminated mudstone (Ml), grading to grey to red massive sandstone (Ms), arranged in coarsening-upward cycles (white triangles). F. Lakeshore (FA2). Mudstone with complete, nonorthogonal, and nonoriented desiccation cracks (white arrows). .... 29
- Figure 2.4 – Ichnofossils in outcrops. A. At the base, red to green laminated mudstone is overlain by red sandstone with bioturbated wave ripples (0–5%) and trace fossils of *Scoyenia* ichnofacies. B. and C. Sandstone with 3D current crest ripples with horizontal trace fossils (*Cochlichnus anguineus*) B2 (10–15%). D. and E. Bioturbated sandstone (Sb). Red to yellow sandstone with vertical bioturbation (*Skolithos linearis*); B3-B4 (40–50%). F. Bioturbated sandstone (Sb). Red to yellow sandstone with vertical bioturbation (*Skolithos linearis*), in plant visualization, B3-B4 (40–50%). .... 31

Figure 2.5 – Sedimentary facies. A. FA3 braided fluvial system. Thinning-upward of set of the Sandstone with tabular cross-stratification (Sta.) B. Detail of the sandstone with trough cross-stratification (St). C. Conglomerate with trough cross-stratification (Ct). D. Structureless conglomerate with subrounded mudstone and quartz clasts (Ci). E. Grey sandstone with sigmoidal cross-stratification (Ssg-FA4) overlain by grey laminated mudstone (MI-FA1). This transition of FA4 to FA1 marks the Lacustrine Flooding Surface (LFS), characterizing the retrogradational pattern (C4). F. Sandstone with sigmoidal cross-stratification (Ssg), overlying laminated mudstone (MI). The transition of MI-FA1 to Ssg-FA4 marks the Maximum Lacustrine Flooding Surface (MLFS), characterizing the progradational pattern (C5). G and H. FA4 delta front. Sandstone with sigmoidal cross-stratification (Ssg). I. FA4 delta front. Grey to red sandstone showing supercritical climbing ripple cross-lamination (Scr)..... 35

Figure 2.6 – Ichnofossils of the Pastos Bons Formation. A. *Agrichnium* isp. (Ag) showing V-shaped, in cross-sections, preserved as negative epirelief. B. *Agrichnium* isp. showing sinuous shaped, in longitudinal sections. C. and D. *Cochlichnus anguineus* (Co), simple meandering burrows, preserved as positive epirelief (E. showing bifurcation). E. *Gyrochorte comosa* (Gr) curved and horizontal burrow, preserved as positive epirelief. F. *Lockeia siliquaria* (red arrows), small horizontal trace, seed-like or almond-shaped, preserved as positive epirelief. G. *Palaeophycus tubularis* (Pa), subhorizontal and bifurcated burrows, preserved as a positive epirelief. .... 39

Figure 2.7 – Ichnofossils of Pastos Bons Formation. A. *Planolites beverleyensis* (Pl), subhorizontal, straight burrows with active fill, preserved as positive hyporelief. B. *Rusophycus* isp. (Rs), horizontal, oval, and slightly elongate and bilobate burrow, preserved as positive hyporelief. C. and D. The *Skolithos linearis* show a circular to subcircular structure, in the transverse section, and a grey to green clay wall. E. and F. The *Skolithos linearis* show funnel-shaped apertures grading to a cylindrical shape towards the base, the longitudinal section, and grey to green clay walls. .... 44

Figure 2.9 – A. Composite profile, sequence stratigraphic stages of the lacustrine system, and the depositional cycles, retrogradational and aggradational cycles, compose the TST; and the progradational cycles compose the HST. B. Overfilled Lake phase. C. Underfilled lake phase. .... 48

Figure 2.10 – A. CAMP deposition dikes and sills extension in Parnaíba Basin, causing the CAMP induced uplift; adapted from Nogueira *et al.* 2021; B. Underfilled Lacustrine basins with retrogradational stacking pattern. Ichnofacies model. *Mermia* ichnofacies: Co: *Cochlichnus anguineus*. Lo: *Lockeia siliquaria*. *Scoyenia* ichnofacies: Ag: *Agrichnium* isp. Gr: *Gyrochorte comosa*; Pa: *Palaeophycus tubularis*; Pl: *Planolites beverleyensis*; Rs: *Rusophycus* isp.; *Skolithos* ichnofacies: Sk: *Skolithos linearis*. Fish-fossils of *Lepidotes piauhyensis*. C. Overfilled lacustrine basin phase with a progradational stacking pattern.....50

**LISTA DE TABELAS**

Table 2.1 – Facies, facies associations and depositional processes of Upper Jurassic – Lower Cretaceous lacustrine succession Pastos Bons Formation, of the Parnaíba Basin, Northeastern Brazil.....	24
Table 2.2 – Ichnospecies, number total of specimens described <i>in situ</i> and in samples of the ichnofossils of Upper Jurassic – Lower Cretaceous lacustrine succession Pastos Bons Formation, of the Parnaíba Basin, Northeastern Brazil.....	36
Table 2.3 – Palaeoenvironments; trace fossil assemblage; ethology; ichnofacies; and bioturbation index (BI) of the Upper Jurassic–Lower Cretaceous lacustrine succession in the Pastos Bons Formation of the Parnaíba Basin, north-eastern Brazil.....	41

## SUMÁRIO

<b>DEDICATÓRIA</b> .....	iv
<b>AGRADECIMENTOS</b> .....	v
<b>EPIÍGRAFE</b> .....	vi
<b>RESUMO</b> .....	vii
<b>ABSTRACT</b> .....	viii
<b>LISTA DE ILUSTRAÇÕES</b> .....	ix
<b>LISTA DE TABELAS</b> .....	xiii
<b>1 INTRODUÇÃO</b> .....	1
1.1 LOCALIZAÇÃO DA ÁREA DE ESTUDO .....	2
1.2 OBJETIVOS.....	2
1.3 GEOLOGIA REGIONAL .....	3
1.3.1 Grupo Mearim .....	6
1.3.2 Formação Corda .....	6
1.3.3 Formação Pastos Bons.....	7
1.3.4 Folhelhos Muzinho .....	8
1.4 MATERIAIS E MÉTODOS.....	10
1.4.1 Análise de Fácies.....	10
1.4.2 Estratigrafia de sequências em ambientes lacustres .....	11
1.4.3 Icnologia .....	13
1.4.3.1 Classificação icnotaxonômica .....	13
1.4.3.2 Classificação estratinômica .....	14
1.4.3.3 Classificação etológica .....	15
1.4.4 Icnofácies .....	15
<b>2 THE EARLY CRETACEOUS LACUSTRINE FACIES AND ICHNOFOSSILS OF THE PARNAÍBA BASIN, BRAZIL: A record of bioactivity in response to post-CAMP thermal subsidence in West Gondwana</b> .....	19
<b>ABSTRACT</b> .....	19

2.1 INTRODUCTION .....	20
2.2 GEOLOGICAL SETTING .....	20
2.3 METHODS .....	21
2.4 FACIES ASSOCIATION .....	23
2.4.1 FA1- <b>Central Lake</b> .....	26
2.4.2 FA2 – <b>Lakeshore</b> .....	28
2.4.3 FA3 – <b>Braided fluvial</b> .....	32
2.4.4 FA4 – <b>Delta front</b> .....	32
2.5 ICHNOLOGY .....	35
2.5.1 <i>Agrichnium</i> Pfeiffer, 1968 – <i>Agrichnium</i> isp. ....	35
2.5.2 <i>Cochlichnus</i> Hitchcock, 1848 – <i>Cochlichnus anguineus</i> , Hitchcock, 1858 .....	36
2.5.3 <i>Gyrochorte</i> Heer, 1865 – <i>Gyrochorte comosa</i> Heer, 1865 .....	37
2.5.4 <i>Lockeia</i> James, 1879 – <i>Lockeia siliquaria</i> James, 1879 .....	37
2.5.5 <i>Palaeophycus</i> Hall, 1847 – <i>Palaeophycus tubularis</i> Hall, 1847 .....	38
2.5.6 <i>Planolites</i> Nicholson, 1873 – <i>Planolites beverleyensis</i> Billings, 1862.....	40
2.5.7 <i>Rusophycus</i> Hall, 1852 – <i>Rusophycus</i> isp. ....	40
2.5.8 <i>Skolithos</i> Haldemann, 1840 – <i>Skolithos linearis</i> Haldemann, 1840 .....	41
2.6 LACUSTRINE DEPOSITIONAL CYCLES .....	44
2.6.1 <b>Retrogradational-aggradational cycles</b> .....	44
2.6.2 <b>Progradational cycles</b> .....	44
2.7 PALAEOENVIRONMENTAL RECONSTRUCTION .....	45
2.7.1 <b>Underfilled lake ichnofacies model</b> .....	46
2.7.2 <b>Interpretation of the staking pattern</b> .....	47
2.7.3 <b>Lacustrine basin evolution</b> .....	49
2.8 CONCLUSIONS .....	50
<b>3 CONCLUSÕES</b> .....	52
<b>REFERÊNCIAS</b> .....	54

## 1 INTRODUÇÃO

A transição Triássico-Jurássico é marcada pela fragmentação do supercontinente Gondwana e consequente abertura do Oceano Atlântico, que culminou em importantes alterações paleoclimáticas, geológicas e biológicas a níveis globais (Torsvik & Cocks 2013, Holz 2015). Esse evento foi acompanhado por um intenso magmatismo, denominado como Província Magmática do Atlântico Central (CAMP), uma das mais significativas LIPs (Grande Província Ígnea – *Large Igneous Province*) e que provavelmente desencadeou processos geológicos que contribuíram para a extinção em massa do Triássico, ~200 Ma (Buatois & Mángano 2016, Capriolo *et al.* 2020).

Os registros do CAMP são geralmente basaltos toleíticos que afloram na América do Norte, Europa, África e na América do Sul (Marzoli *et al.* 1999). No Brasil, o CAMP é registrado nas bacias sedimentares do Solimões e Amazonas, na Bacia do Parecis, na Bacia Lavras da Mangabeira e na Bacia do Parnaíba (Moura Silva *et al.* 2020, Rezende *et al.* 2021).

O registro pós-CAMP na Bacia do Parnaíba é representado por áreas que experimentaram subsidência térmica (Klöcking *et al.* 2018), o que permitiu a implantação de depósitos fluvio-eólicos da Formação Corda (Rabelo & Nogueira 2015) e fluviolacustres da Formação Pastos Bons (Cardoso *et al.* 2017, 2019a). Sucessão similar ocorre nos depósitos da Bacia do Parecis (Rubert *et al.* 2019) e Lavras da Mangabeira (Moura Silva *et al.* 2020).

Embora essa unidade seja razoavelmente bem interpretada do ponto de vista paleoambiental, ainda não existe um contexto paleogeográfico adequado que possibilite o entendimento da distribuição destes depósitos. Os trabalhos mais recentes acerca da Formação Pastos Bons consistem em análises paleontológicas (Petra 2006, Bernardes-de-Oliveira *et al.* 2007, Petra & Gallo 2012, Montefeltro *et al.* 2013, Cardoso *et al.* 2020), mapeamentos regionais (Góes & Feijó 1994, Vaz *et al.* 2007) e análises faciológicas pontuais (Cardoso *et al.* 2017), aliadas à estratigrafia de sequências (Cardoso *et al.* 2019a), além de análise de minerais pesados e leves para caracterizar a proveniência sedimentar (Cardoso *et al.* 2019b).

Portanto, pretendeu-se ampliar o conhecimento estratigráfico da Formação Pastos Bons, apresentando sua distribuição paleogeográfica, bem como correlacioná-la com os eventos pós-CAMP que afetaram esta região do Gondwana Ocidental. As reconstruções destes paleoambientes fornecem um conjunto de informações cruciais para a compreensão dos últimos eventos sedimentares relacionados ao CAMP.



## 1.1 LOCALIZAÇÃO DA ÁREA DE ESTUDO

A Formação Pastos Bons foi investigada em uma área central da Bacia do Parnaíba, a cerca de 300 Km ao sul de Teresina, capital do estado do Piauí. Os afloramentos dessa unidade ocorrem ao longo de uma zona com orientação SW-NE com aproximadamente 50 km de extensão, na Microrregião de Floriano, nas adjacências do município de Nazaré do Piauí - PI e Oeiras do Piauí - PI (Fig. 1.1). O principal acesso à região dá-se por meio da BR-230, e para acessar os afloramentos distantes da rodovia principal, foram utilizadas estradas vicinais, que dão acesso às áreas rurais dos municípios.

## 1.2 OBJETIVOS

Os objetivos deste trabalho incluem a interpretação paleoambiental da Formação Pastos Bons na porção centro-leste da Bacia do Parnaíba. Discutir e interpretar a ocorrência de icnofósseis e propor um modelo faciológico e icnofaciológico. Pretende-se também discutir a origem dos ciclos deposicionais da unidade estudada, assim como interpretar o padrão de empilhamento estratal e o significado das superfícies estratigráficas.

Adicionalmente, pretende-se discriminar os controles autogênicos e alogênicos e propor uma história deposicional para a bacia lacustre. Por fim, busca-se contribuir para as relações estratigráficas da Bacia do Parnaíba e compreender as implicações paleogeográficas desta sucessão no contexto do supercontinente Gondwana Ocidental durante o intervalo Jurássico Superior-Cretáceo Inferior.

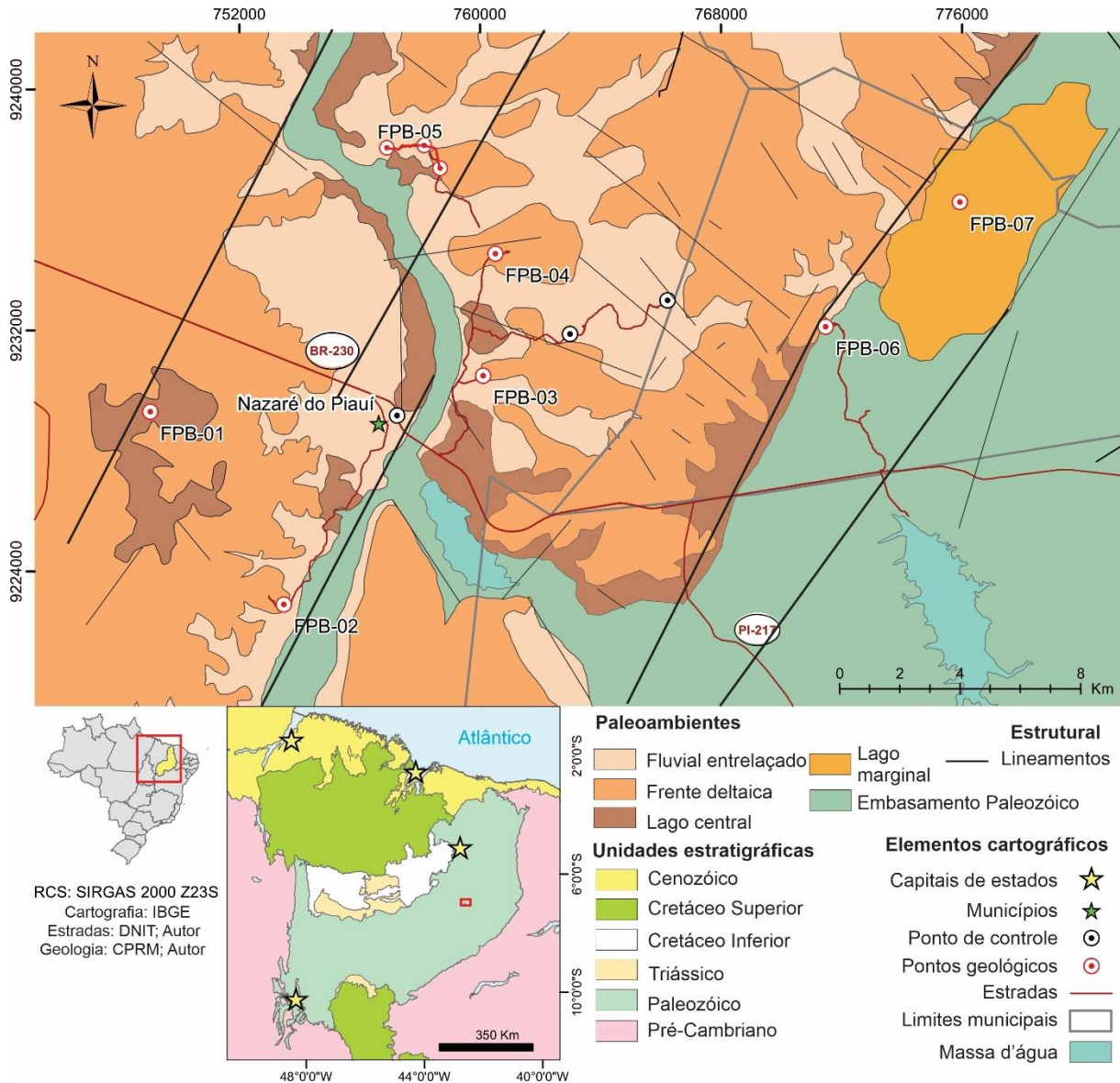


Figura 1.1 – Mapa de localização da área de estudo. (A) Mapa geográfico do Brasil, estado do Piauí de cor amarela. (B) Mapa geológico da Bacia do Parnaíba, destacando as superseqüências sedimentares, o retângulo vermelho delimita a área de estudo (modificado de Santos & Carvalho 2004). (C) Mapa paleoambiental da área de estudo, sudeste da Bacia do Parnaíba. Fonte: Produzido pelo autor.

### 1.3 GEOLOGIA REGIONAL

A Bacia do Parnaíba é uma bacia intracratônica paleozoica, de formato semicircular do tipo *sag*, situada no nordeste do Brasil. Ela abrange cerca de 600.000 km<sup>2</sup> e distribui-se pelos estados do Pará, Tocantins, Maranhão, Piauí, Ceará e Bahia (Aguiar 1969, Góes & Feijó 1994, Oliveira & Mohriak 2003, Pereira *et al.* 2012).

A espessura média da bacia é cerca de 2 km, mas pode atingir de 3,4 a 3,5 km de espessura no seu depocentro (Vaz *et al.* 2007, Pereira *et al.* 2012). Ela é separada em sua porção norte, pelo arco tectônico de Ferrer-Urbano Santos, das Bacias de São Luís e de Barreirinhas;

na porção nordeste, é circundada pelo Arco Tocantins, que a separa da Bacia do Marajó, e, na porção sul, o Arco São Francisco a separa da Bacia do São Francisco (Vaz *et al.* 2007).

Essa bacia instala-se sobre uma discordância regional subplanar datada do Neoproterozoico/Paleozoico inferior, que foi gerada sob um embasamento formado por rochas ígneas, metamórficas e sedimentares com idades arqueanas a ordovicianas. O embasamento foi formado e/ou retrabalhado durante o Ciclo Brasileiro, sendo constituído de rochas do Cinturão Araguaia-Tocantins, dos crátons Amazônico e São Francisco, Província Borborema e Bloco Parnaíba, além das bacias Riachão e Jaibas (Oliveira & Mohriak 2003, Vaz *et al.* 2007, Daly *et al.* 2014, Daly *et al.* 2018, Porto *et al.* 2018).

Essa unidade geotectônica abarca sedimentos marinhos rasos a continentais em longas histórias de subsidência (Góes & Feijó 1994, Vaz *et al.* 2007, Daly *et al.* 2014). O registro sedimentar da Bacia do Parnaíba foi dividido por Góes & Feijó (1994) em cinco sequências: Siluriana (Grupo Serra Grande), Devoniano (Grupo Canindé), Carbonífero-Triássico (Grupo Balsas), Jurássico (Grupo Mearim) e Cretáceo (Grupo Itapecuru); que são delimitadas por discordâncias regionais (Fig. 1.2). Por outro lado, Vaz *et al.* (2007), mais recentemente, adicionaram dados de subsuperfície e propuseram uma outra subdivisão estratigráfica para a Bacia do Parnaíba: Sequência Siluriana; Sequência MesoDevoniana-EoCarbonífera; Sequência NeoCarbonífera-EoTriássica; Sequência Jurássica e Sequência Cretácea.

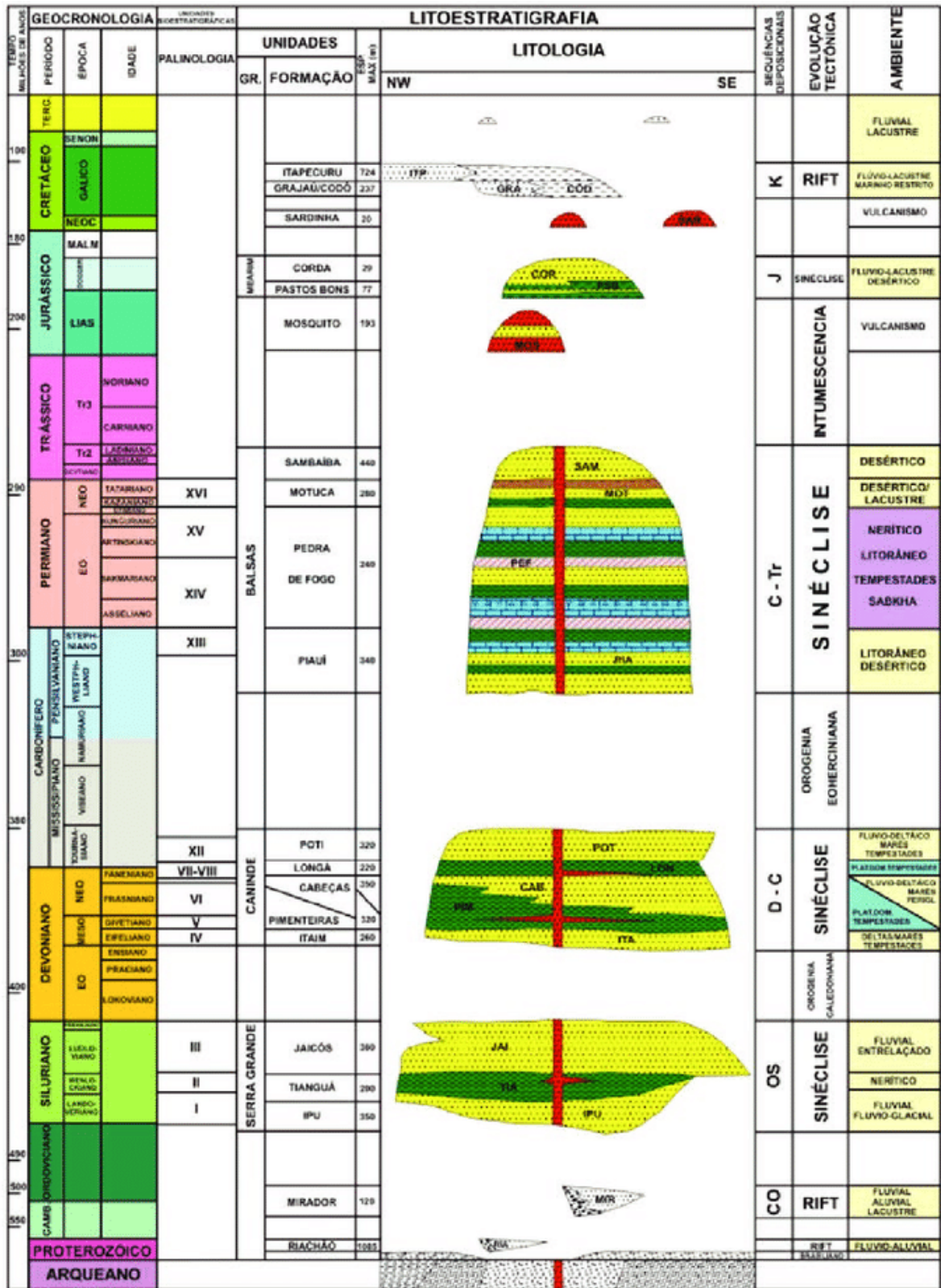


Figura 1.2 – Carta estratigráfica da Bacia do Parnaíba. Fonte: Góes & Feijó (1994).

### 1.3.1 Grupo Mearim

Lisboa (1914) criou o termo Série Mearim para englobar arenitos vermelhos e basaltos amigdaloidais, datados do Triássico, que afloram no Rio Mearim, no estado do Maranhão. Aguiar (1969), sob outra perspectiva, utiliza a denominação Grupo Mearim para agrupar os basaltos intercalados com arenitos da Formação Mosquito, os arenitos da Formação Corda, diques de basalto da Formação Sardinha e arenitos e folhelhos da Formação Pastos Bons. Segundo o referido autor, essa unidade é limitada pelas unidades paleozoicas na base e pela Formação Grajaú (Cretáceo) no topo e apresenta idade Jurássica-Cretácea.

Seguindo a mesma linha, Góes *et al.* (1990) definem o Grupo Mearim como o conjunto das formações supracitadas relacionadas com distensão crustal e magmatismo relacionados à abertura do oceano Atlântico. Góes & Feijó (1994) sugeriram que o Grupo Mearim é datado do Jurássico e é composto pelas formações Corda e Pastos Bons, interdigitadas e sobrepostas discordantemente sobre a Formação Mosquito e o Grupo Balsas, além de serem sotopostas, em discordância, pelos depósitos cretáceos das formações Sardinha, Grajaú, Codó e do Grupo Itapecuru.

Vaz *et al.* (2007) sugerem que somente a Formação Pastos Bons compõe a sequência Jurássica, propondo a idade cretácea para a Formação Corda. Romero Ballén (2012), Rabelo & Nogueira (2015) e Cardoso *et al.* (2019b), mais recentemente, com base nos estudos estratigráficos e de assembleias de minerais pesados, sugerem que a Formação Corda e a Formação Pastos Bons pertencem ao Grupo Mearim, datadas do Jurássico Superior ao Cretáceo Inferior.

### 1.3.2 Formação Corda

A Formação Corda (Lisboa 1914) compreende arenitos finos a médios, bimodais, cinza-esbranquiçados, creme a avermelhados, com grãos arredondados e foscos de quartzo, com alguns níveis de sílex e eventuais níveis de seixos facetados (Góes & Feijó 1994, Santos & Carvalho 2004). O ambiente deposicional é interpretado como desértico úmido, com dunas eólicas e interdunas e subambientes fluviolacustres (Góes & Feijó 1994, Romero Ballén 2012, Rabelo & Nogueira 2015).

### 1.3.3 Formação Pastos Bons

Lisboa (1914), inicialmente, denominou “Camadas Pastos Bons” os calcários e folhelhos verdes e marrons intercalados com arenitos esbranquiçados que afloram em drenagens nas proximidades do município homônimo, no estado do Maranhão. Posteriormente, diversos autores formularam propostas litológicas e estratigráficas para essa sequência sedimentar (Plummer 1946, Brazil *et al.* 1948, Campbell 1949), incluindo-os nas formações Melancieiras, Motuca, Sambaíba ou Pedra de Fogo, consideradas de idade mesozoica. Mesner & Wooldridge (1962) analisaram os pelitos e arenitos que afloram no Riacho Pedra de Fogo, sul da cidade de Pastos Bons, Estado do Maranhão, elevando, assim, essa sucessão à posição de “Formação Pastos Bons”, posicionando-a no Triássico Superior.

Aguiar (1969) agrupou a Formação Pastos Bons ao Grupo Mearim (Triássico Superior), discordantemente sobreposta às formações Motuca, Pedra de Fogo, Piauí e Poti, do Oeste para o Leste da Bacia do Parnaíba. A formação possui contato concordante e gradacional com a Formação Corda e é sobreposta pela Formação Grajaú e cortada pelos basaltos da Formação Sardinha. Todavia, Cunha & Carneiro (1972) unificaram as formações Pastos Bons e Corda, situadas no Jurássico (Sistema Desértico-fluvial-lacustre Corda-Pastos Bons).

Lima *et al.* (1978, 1979) consideram os depósitos estudados por Lisboa (1914) como Formação Pastos Bons, no mesmo sentido estratigráfico proposto por Aguiar (1969), porém data-se do Jurássico médio a superior, sobreposta concordantemente pela Formação Corda. Os autores propõem que essa unidade se depositou em ambientes lacustres, assentados em paleodepressões causando descontinuidades expositivas, com espessura média de 60 metros. Segundo o mapeamento realizado pelos autores, essa unidade aflora na região centro-oeste da bacia, nos municípios do estado do Maranhão, à leste da cidade de Floriano-PI e no noroeste do Piauí.

Por outro lado, devido às complexidades litológicas, fossilíferas e estratigráficas da Formação Pastos Bons, Caldasso (1978a, 1978b) propôs o abandono do termo “Pastos Bons”, pois destaca que esse termo estava sendo utilizado para se referir a diferentes unidades estratigráficas da bacia do Parnaíba.

Contudo, Caputo (1984) subdividiu a Formação Pastos Bons em três partes: 1) a base constituída por arenitos brancos com variações esverdeadas-amareladas, compostos por grãos de granulometria fina a média, subarredondados e, comumente, com estratificação plano-paralela e, pontualmente, lentes de calcário; 2) parte intermediária representada por siltitos, folhelhos/argilitos cinza-esverdeados, com intercalações de arenitos; e 3) o topo da unidade

contém arenitos vermelhos/rosados, de granulometria fina, que gradam para siltitos, com alguns níveis de folhelho.

A partir da década de 1990, foram realizados novos esforços para a caracterização desses depósitos de maneira regional, a partir de dados de subsuperfície. Hasui *et al.* (1991) sugerem que a deposição da Formação Pastos Bons ocorreu ao longo da Estrutura de Xambioá, que se comportou como um baixo deposicional durante o Mesozoico.

Góes *et al.* (1990) e Góes & Feijó (1994) relacionam a Formação Pastos Bons à sequência Jurássica, correspondente ao Grupo Mearim. Entretanto, Vaz *et al.* (2007) sugerem que esta formação é a única representante da sequência Jurássica, depositada em paleodepressões continentais, lacustres, com alguma contribuição fluvial, em clima árido a semiárido. A subsidência que possibilitou a acomodação dos sedimentos dessa unidade foi causada pela distensão crustal e magmatismo relacionados à abertura do oceano Atlântico Equatorial (Góes *et al.* 1990, Góes & Feijó 1994, Vaz *et al.* 2007).

Atualmente, a fim de sanar essas dúvidas quanto à natureza, ao sistema deposicional e à distribuição espacial, esta unidade tem sido estudada em detalhes, a partir de análise de fácies sedimentares, estratigrafia de sequências em ambientes lacustres, tipos de bacias lacustres e possíveis fases de sedimentação (Romero Ballen 2012, Cardoso *et al.* 2017, 2019a, 2019b, 2020).

A Formação Pastos Bons representa uma sequência lacustre, na qual a base é constituída por folhelhos fossilíferos denominado de “Folhelhos Muzinho”, depositado em climas áridos a semiáridos em lagos rasos e fechados, do tipo *underfilled lake basin* que predominam evaporitos e folhelhos (Cardoso *et al.* 2019a, 2020). A porção superior corresponde a lagos rasos, relativamente mais espessos e largos, do tipo *overfilled lake basin* com deposição predominantemente siliciclástica constituída basicamente por arenitos e pelitos, influenciados por canais fluviais efêmeros que formam localmente *sheet like-delta fronts* (Cardoso *et al.* 2017, 2019a).

### **1.3.4 Folhelhos Muzinho**

A porção basal da Formação Pastos Bons denominada informalmente de “Folhelhos Muzinho”, engloba o registro fossilífero da unidade conhecido atualmente (Cardoso *et al.* 2020). O principal afloramento ocorre na Fazenda Muzinho, localizada a cerca de 16 km a nordeste de Floriano-PI (Santos 1953, Petra & Gallo 2012), porém alguns depósitos correlatos são encontrados no leste do Maranhão (Montefeltro *et al.* 2013).

Esse depósito apresenta cerca de 10 metros de espessura, alternância de folhelhos negros, fossilíferos com calcita fibrosa, que substituíram cristais de gipso, organizados em ciclos milimétricos a centimétricos de raseamento/salinização ascendente, gradando para uma espessa camada de folhelhos para o topo da sucessão. Cardoso *et al.* (2019a) sugerem que esses depósitos foram formados em um lago de hidrologia fechada, em clima árido a semiárido, de alta salinidade e com baixo suprimento de água e sedimentos.

Essa sucessão exhibe o gênero *Lepidotes piauhyensis*, cuja idade sugerida inicialmente foi Cretáceo Superior (Roxo & Löefgren 1936). Entretanto, o registro dos gêneros *Pholidophoridae*, *Lepidotes* e *Semionotus* conduziu Santos (1953) a recomendar que estas camadas fossem posicionadas no Triássico Médio-Jurássico Superior.

Em seguida, Beurlen (1954) adotou idade triássica superior a partir da análise do gênero *Macrolimnadiopsis*. Enquanto Santos (1974) sugeriu idade jurássica média, a partir de Pleurophoídeos e Macrosemiídeos. Pinto & Purper (1974) estudaram os ostracodes que ocorrem nesse depósito, identificaram os gêneros de conchostráceos *Lioestheria*, *Macrolimnadiopsis* e *Pseudestheria* e propuseram idade entre o Jurássico Superior ao Cretáceo Superior.

Os estudos palinológicos de Lima & Campos (1980) no Folhelho Muzinho indicaram idade eocretácea (Barremiano). Gallo (2005), em reavaliação do trabalho de Roxo e Löefgren (1936), atestou idade entre o Jurássico Superior-Cretáceo Inferior para a Formação Pastos Bons.

Petra (2006), Petra & Gallo (2012), Cardoso *et al.* (2019a, 2020) com base na descrição de peixes e de estudos faciográficos, respectivamente, sugerem idade similar. Em outra abordagem, Bernardes-de-Oliveira *et al.* (2007) identificaram palinóforos mesofíticos, possivelmente correlatos ao Andar Dom João, uma unidade fluvial-lacustre-eólica que ocorre nas bacias do nordeste brasileiro (Kuchle *et al.* 2011).

Mais recentemente, Montefeltro *et al.* (2013) identificaram nesta unidade o registro de uma nova espécie de crocodiliano (*Batrachomimus pastosbonensis*), pertencente ao Jurássico Superior, único representante dos Paralligatoridae, grupo anteriormente reconhecido apenas na Ásia.



## 1.4 MATERIAIS E MÉTODOS

### 1.4.1 Análise de Fácies

O modelamento de fácies sedimentares, proposto por Walker (1992), consiste em: 1) individualização e descrição de fácies sedimentares, utilizando a identificação mineralógica, textural e de aspectos geométricos, bem como estruturas sedimentares, conteúdo fossilífero e sentidos de paleocorrente; 2) domínio dos processos sedimentares formadores das fácies e 3) sugerir associações de fácies, fundamentado em conjuntos de fácies contemporâneos e cogenéticos que permitem a definição de diferentes ambientes sedimentares e sistemas deposicionais. Esse método foi utilizado durante a etapa de campo, auxiliado por perfis colunares confeccionados em afloramentos.

Foram utilizados os modelos de fácies para ambientes lacustres abordados em Talbot & Allen (1996), Nichols (2009) e Renaut & Gierlowski-Kordesch (2010). Esses trabalhos indicam a distribuição da sedimentação química e clástica (Fig. 1.3), principalmente nas margens dos lagos (*shoreline*, *shoreface*, *nearshore*, *lakeshore* ou *coastal zone*) ou zonas litorais, e em porções mais profundas ou centrais do lago (*offshore*).

As áreas marginais dos lagos concentram fácies sedimentares formadas por processos trativos gerados por ação de correntes que registram e descarga fluvial para dentro da bacia lacustre, logo, ocorrem arenitos com estratificações cruzadas que formam os sistemas deltaicos lacustres (*Delta lake*). Em áreas adjacentes à desembocadura dos rios, ocorre retrabalhamento dos sedimentos da linha de costa por ações de ondas e frequente estruturas que revelam exposição subaérea (gretas de contração), evaporitos e carbonatos (Renaut & Gierlowski-Kordesch 2010). Além disso, as zonas de litoral são as áreas relativamente mais oxigenadas e, conseqüentemente, acumulam o registro de estruturas biogênicas (e.g. estromatólitos e icnofósseis) (Buatois & Mángano 2007, Renaut & Gierlowski-Kordesch 2010).

As porções centrais dos lagos registram geralmente dois tipos de sedimentação: plumas de sedimentos em suspensão, que se depositam por decantação, e correntes fluviais densas que, por meio de processos trativos, se depositam nas porções mais profundas do lago (Talbot & Allen 1996, Nichols 2009).

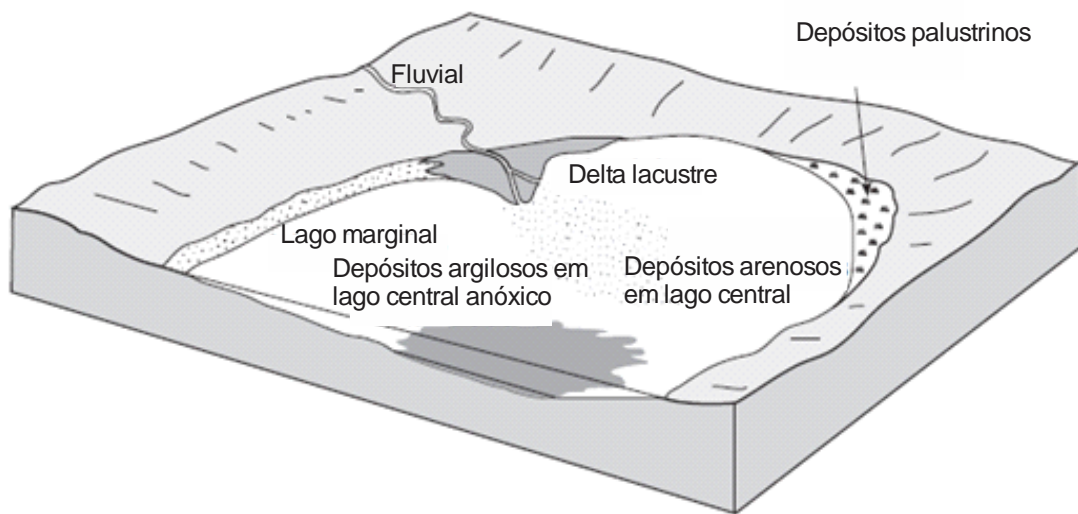


Figura 1.3 – Bloco diagrama que apresenta a distribuição dos ambientes de sedimentação em contextos lacustres. Fonte: Nichols (2009).

#### 1.4.2 Estratigrafia de seqüências em ambientes lacustres

A aplicação do estudo dos modelos de fácies sedimentares consiste na delimitação de padrões de empilhamento e ciclos deposicionais, que são definidos como alternâncias em pelo menos duas litologias, de maneira regular e recorrentes. Assim, os ciclos são interpretados como combinações rítmicas entre processos de sedimentação clástica, química ou orgânica (Talbot & Allen 1996, Nichols 2009), principalmente em ambientes de sedimentação marinhos para descrever mudanças relativas no nível do mar (e.g. regressões e transgressões) (Catuneanu *et al.* 2009, 2019).

Entretanto, a cicloestratigrafia tem sido aplicada para descrever padrões de empilhamento e relativas mudanças no nível da água também em ambientes lacustres (e.g. Bohacs *et al.* 2000, Keighley *et al.*, 2003, Cardoso *et al.* 2019, Abrantes Jr *et al.* 2019); um dos exemplos está exposto na Fig. 1.4, que descrevem os tipos de sedimentação nas diferentes estações do ano. Os ciclos não-glaciais estão representados pela intercalação de sedimentos depositados em períodos úmidos, onde predominam influxo sedimentar proveniente dos sistemas fluviáis alimentadores; e os períodos de seca, onde domina a sedimentação química de evaporitos e carbonatos (Talbot & Allen 1996, Renaut & Gierlowski-Kordesch 2010). Para isso, foram identificados ciclos de caráter progradacionais, retrogradacionais e agradacionais (Nichols 2009), de raseamento ascendente, aprofundamento ascendente, salinidade ascendente e granocrescência ascendente, limitados por superfícies de inundação.

Dessa forma, os ciclos deposicionais compõem de forma satisfatória o estudo baseado em estratigrafia de seqüências de bacias lacustres, pois seu foco é integrar observações sobre o ambiente de sedimentação em escalas locais e regionais (Carroll & Bohacs 1999, Bohacs *et al.* 2000), com adaptações conduzidas, principalmente, pelas diferenças intrínsecas entre lagos e oceanos (e.g. tempo de estabilidade ambiental, taxa de sedimentação, quantidade de água, frequência de avanço e recuo de costas).

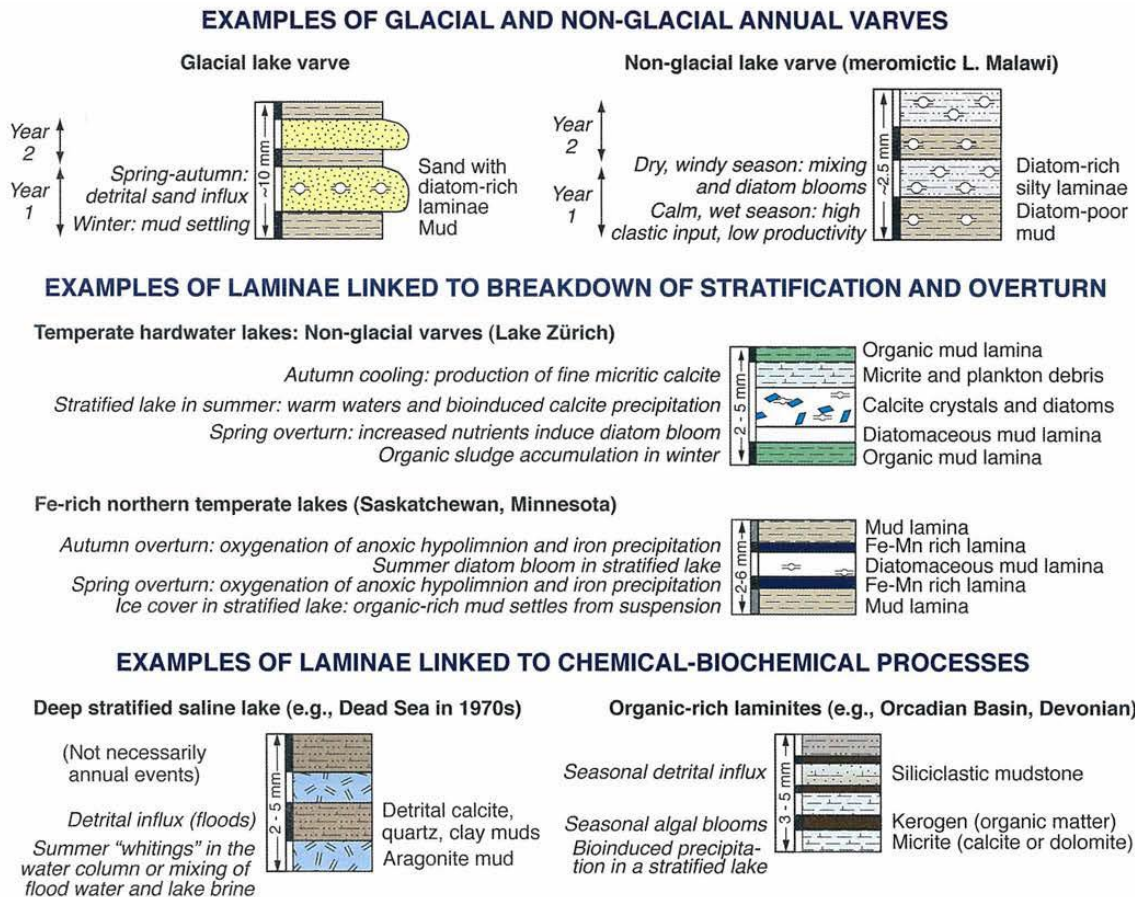


Figura 1.4 – Exemplos de ciclos deposicionais recorrentes em lagos atuais. Fonte: Renaut & Gierlowski-Kordesch (2010).

Para Carroll & Bohacs (1999) e Bohacs *et al.* (2000), o relativo balanço entre as taxas de influxo sedimentar e água ( $S_s$ ) e o potencial de acomodação ( $A_p$ ) são os fatores fundamentais que controlam a natureza, distribuição e a evolução dos sistemas deposicionais em bacias lacustres. Portanto, a partir do estudo de padrões de empilhamento, esses autores observaram três principais associações de fácies (*fluvial-lacustrine*; *fluctuating-profunda*; *evaporative*) que delimitam os três tipos de bacias lacustres, adotados nesse trabalho, respectivamente: *overfilled* ( $A_p < S_s$ ), *balanced-fill* ( $A_p \sim S_s$ ) e *underfilled* ( $A_p > S_s$ ) lake basins (Fig. 1.5).

Cada tipo de bacia lacustre apresenta padrões específicos de empilhamento estratal (Fig. 1.5); dessa forma, as bacias do tipo *overfilled* apresentam padrões ciclos deposicionais de

progradação; as do tipo *balanced-fill* podem apresentar variações entre ciclos que descrevem progradação, agradação e retrogradação; e, por fim, os lagos do tipo *underfilled* exibem padrões de agradação e retrogradação (Carroll & Bohacs 1999, Bohacs *et al.* 2000).

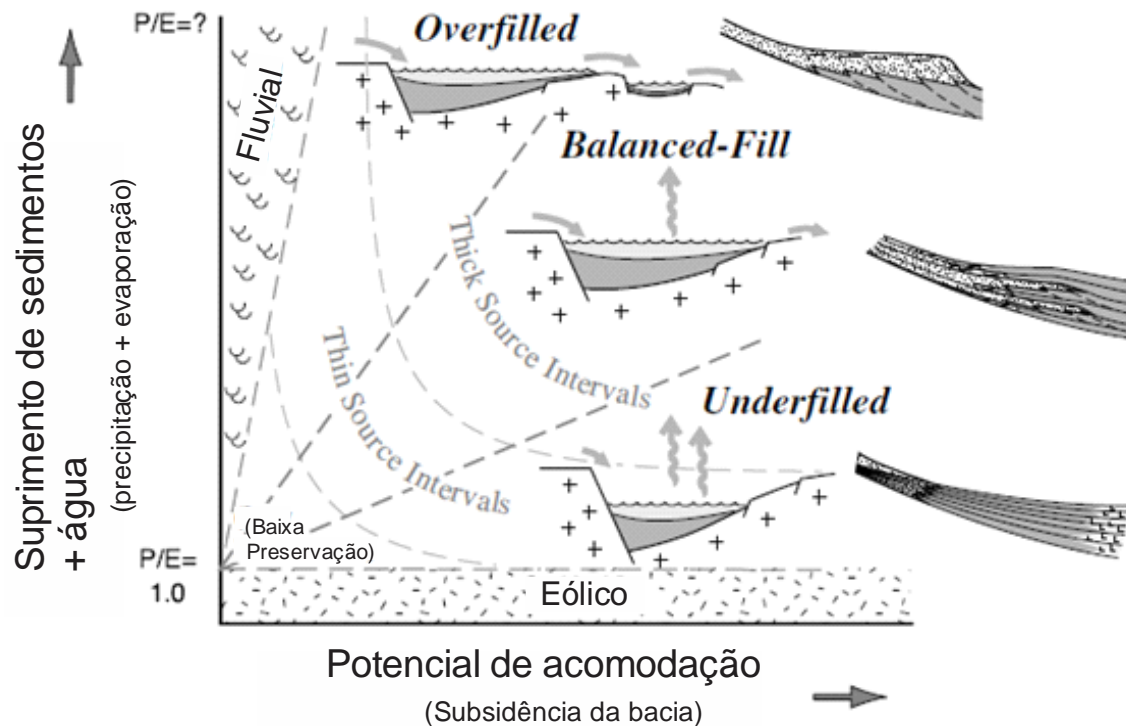


Figura 1.5 – Diagrama que sumariza as características estratigráficas e ambientais dos três tipos de bacias lacustres, *overfilled* ( $A_p < S_s$ ), *balanced-fill* ( $A_p \approx S_s$ ) e *underfilled* ( $A_p > S_s$ ) *lake basins*, segundo Carroll & Bohacs (1999) e Bohacs *et al.* (2000). Fonte: Bohacs *et al.* (2000).

### 1.4.3 Icnologia

Icnologia é o estudo de estruturas sedimentares biogênicas preservadas no substrato, sendo assim os principais objetos de estudo de análise paleoicnológica (Bromley 1996), servindo como uma ferramenta complementar para a reconstituição paleoambiental dos depósitos sedimentares. Em relação à classificação dos icnofósseis, podem ser aplicadas três metodologias distintas, sendo elas: 1) icnotaxonômica; 2) estratinômica; 3) etológica.

#### 1.4.3.1 Classificação icnotaxonômica

Essa classificação leva em consideração a morfologia dos icnofósseis. A determinação de um icnotáxon é baseada nas diretrizes dos procedimentos da sistemática Linneana que comporta duas categorias icnotaxonômicas: icnogênero e icnoespécie. Esses termos são

geralmente abreviados como ichnogen. e ichnosp. ou igen. e isp. (Bromley 1996, Buatois & Mángano 2011) com o intuito de diferenciar os icnofósseis de fósseis corporais. Bromley (1996) propôs o uso de características morfológicas, denominadas de icnotaxobases, para a determinação e diferenciação entre os diferentes espécimes de icnofósseis (Fig. 1.6). Baseado nas icnotaxobases de Bromley (1996), Knaust (2012) elaborou chaves de identificação de icnogêneros que foram utilizadas neste trabalho.

ICNOTAXOBASES					
FORMA GERAL	LIMITE DA ESTRUTURA		RAMIFICAÇÃO	PREENCHIMENTO	TRILHAS
Aspecto Morfológico	Sem Lineação		Verdadeira	Passivo	
Orientação no estrato	Com Lineação	Filme Pelitico	Falsa	Ativo	Compactado
		Parede delimitada			Peletado
		Parede construída	Interseção		Rastejamento
		Parede c/ preenchimento zonado			Nado
		Parede / Limite ornamentada(o)			
		Halo diagenético		Meniscado	

Figura 1.6 – Icnotaxobases utilizadas para classificação morfológica dos icnofósseis. Fonte: Bromley (1996).

#### 1.4.3.2 Classificação estratinômica

A classificação de Seilacher (1953, 1964) propõe duas subdivisões principais para os icnofósseis de acordo com seu posicionamento em relação ao estrato, sendo elas relevo completo e semirrelevo (positivo ou negativo). A classificação de Martinsson (1970) introduziu quatro termos principais: epichnia (topo do estrato), hipichnia (base do estrato), endichnia (dentro do estrato) e exichnia (fora do estrato arenoso) (Fig. 1.7).

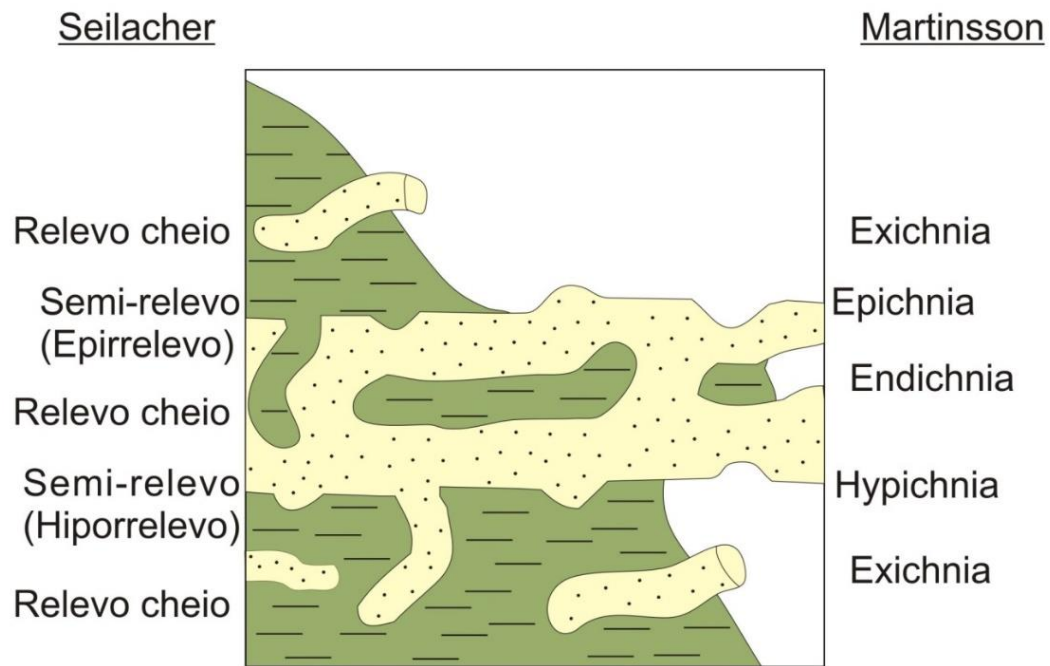


Figura 1.7 – Terminologia para classificação estratinômica de icnofósseis conforme seu modo de preservação segundo Seilacher (1964) e Martinsson (1970). Fonte: Ekdale *et al.* (1984).

#### 1.4.3.3 Classificação etológica

Essa classificação deriva do estudo do comportamento do organismo produtor do traço fóssil, as estruturas se enquadram em diferentes categorias de comportamento. Atualmente 14 grupos foram propostos por Buatois & Mángano (2011): agrichnia (cultivo), repichnia (locomoção), cubichnia (repouso), fodinichnia (alimentação), domichnia (habitação), fugichnia (escape), pascichnia (pastagem), equilibrichnia (equilíbrio), praedichnia (predação), calichnia (reprodução), pupichnia (pupação), fixichnia (fixação), impedichnia (bioclausturação), mortichnia (traços mortos).

#### 1.4.4 Icnofácies

O conceito de icnofácies seilacherianas (*Seilacherian or archetypal ichnofacies*), consiste na identificação de características-chave compartilhadas por icnocenoses recorrentes, no espaço e tempo, formadas sob um conjunto de condições ambientais semelhantes (Seilacher 1964, 1967, Bromley 1996, MacEachern *et al.* 2007, 2012, Buatois & Mángano 2011).

As bacias lacustres apresentam três principais icnofácies recorrentes no espaço e no tempo: *Mermia*, *Scoyenia* e *Skolithos* (Buatois & Mángano 1995, 1998, 2004, 2007, 2009, 2011,

Scott *et al.* 2012), conforme os principais icnogêneros constituintes (Buatois & Mángano 2004, 2007, 2011, Scott *et al.* 2012).

A icnofácies *Mermia*, proposta por Buatois & Mángano (1995, 1998), é composta por escavações horizontais simples e rasas (*shallow tier*), trilhas de insetos e estruturas bilobadas (Fig. 1.8), associadas com ambientes permanentemente subaquosos, bem oxigenados, com baixa energia em lagos de água doce (Scott *et al.* 2012). As estruturas biogênicas são geralmente associadas a laminações e estratificações plano-paralelas, laminações cruzadas formadas por correntes ou por ondas (Buatois & Mángano 1995, 1998, 2004, 2007).

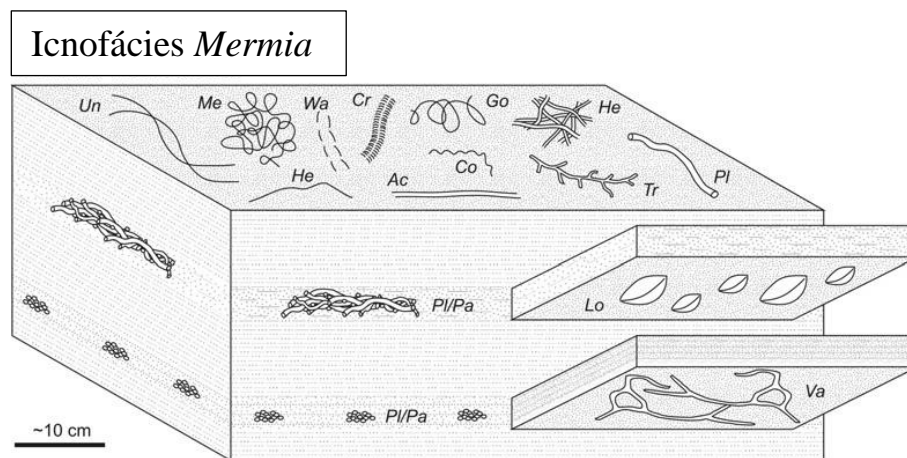


Figura 1.8 – Bloco diagrama com os principais icnogêneros que compõem a icnofácies *Mermia*. Me, *Mermia*; He, *Helminthoidichnites*; Go, *Gordia*; Co, *Cochlichnus*; Ac, *Archaeonassa*; Wa, *Warvichnium*; Cr, *Cruziana*; Pl, *Planolites*; Pa, *Palaeophycus*; Tr, *Treptichnus*; Va, *Vagorichnus*; Lo, *Lockeia*; Un, *Undichna*. Fonte: Scott *et al.* (2012).

A icnofácies *Scoyenia*, proposta inicialmente por Seilacher (1963, 1967) e adaptado por Frey *et al.* (1984), Frey & Pemberton (1987) e Buatois & Mángano (1995, 1998, 2004, 2007, 2011), é composta por escavações horizontais curvadas a sinuosas, bilobadas, meniscados, escavações verticais simples, cilíndricas, além de pistas e trilhas de artrópodes e pegadas de vertebrados (Fig. 1.9) (Buatois & Mángano 1995, 1998, 2004, 2007, 2011, Scott *et al.* 2012). São associadas com ambientes de baixa energia com substratos que experimentam inundação e exposição subaérea sazonalmente, sendo frequentemente utilizadas para delimitar margens de lagos (Buatois & Mángano, 1995, 1998, 2004, 2007, 2011, Scott *et al.* 2012). As estruturas biogênicas são geralmente correlacionadas a gretas de contração e outras estruturas de exposição subaérea e diminuição da espessura da coluna d'água (Buatois & Mángano, 1995, 1998, 2004, 2007).

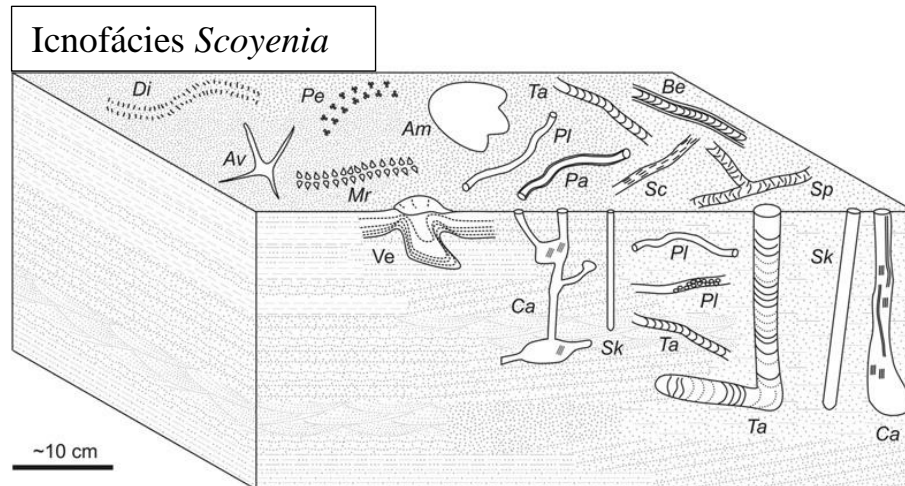


Figura 1.9 – Bloco diagrama com os principais icnogêneros que compõem a icnofácies *Scoyenia*. Av, *Avipeda*; Am, *Amblydactylus*; Be, *Beaconites*; Ca, *Camborygma*; Di, *Diplichnites*; Mr, *Merostomichnites*; Pa, *Palaeophycus*; Pe, *Paleohelcura*; Ta, *Taenidium*; Pl, *Planolites*; Sc, *Scoyenia*; Sk, *Skolithos*; Sp, *Spongeliomorpha*; Ta, *Taenidium*; Ve, pegadas de vertebrados;. . Fonte: Scott *et al.* (2012).

A icnofácies *Skolithos* continental, proposta por Buatois & Mángano (2004, 2007), é composta por escavações verticais simples, em forma de “U” ou de “Y” (Fig. 1.10), associadas a arenitos, estratificações e laminações cruzadas em condições de energia moderada a alta, nas porções mais energéticas do lago, em margens de lagos dominadas por ondas ou em áreas de desembocadura dos rios (Buatois & Mángano 2004, 2007, 2009, 2011; Scott *et al.* 2012).

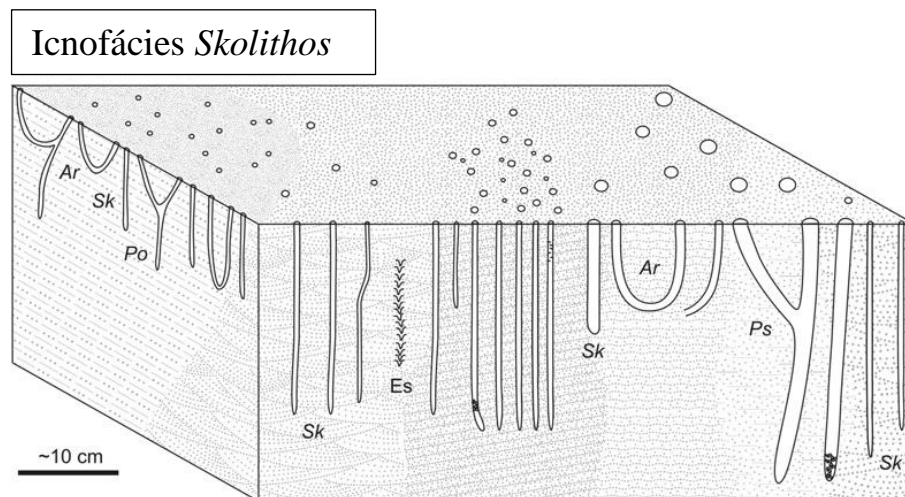


Figura 1.10 – Bloco diagrama com os principais icnogêneros que compõem a icnofácies *Skolithos*. Ar, *Arenicolites*; Es, estruturas de escape; Po, *Polykladichnus*; Ps, *Pylonichnus*; Sk, *Skolithos*. Fonte: Scott *et al.* (2012).

A partir da aplicação desse conjunto de métodos, buscou-se relacionar os padrões de sedimentação e os modelos de icnofácies (Buatois e Mángano 2007, 2009, Scott *et al.* 2012) para identificar os tipos de bacias lacustres registrados na sequência sedimentar estudada (*overfilled*, *underfilled* e *balanced fill*), seguindo as propostas de Carroll & Bohacs (1999) e Bohacs *et al.* (2000) e suas distribuições paleogeográficas (Fig. 1.11).



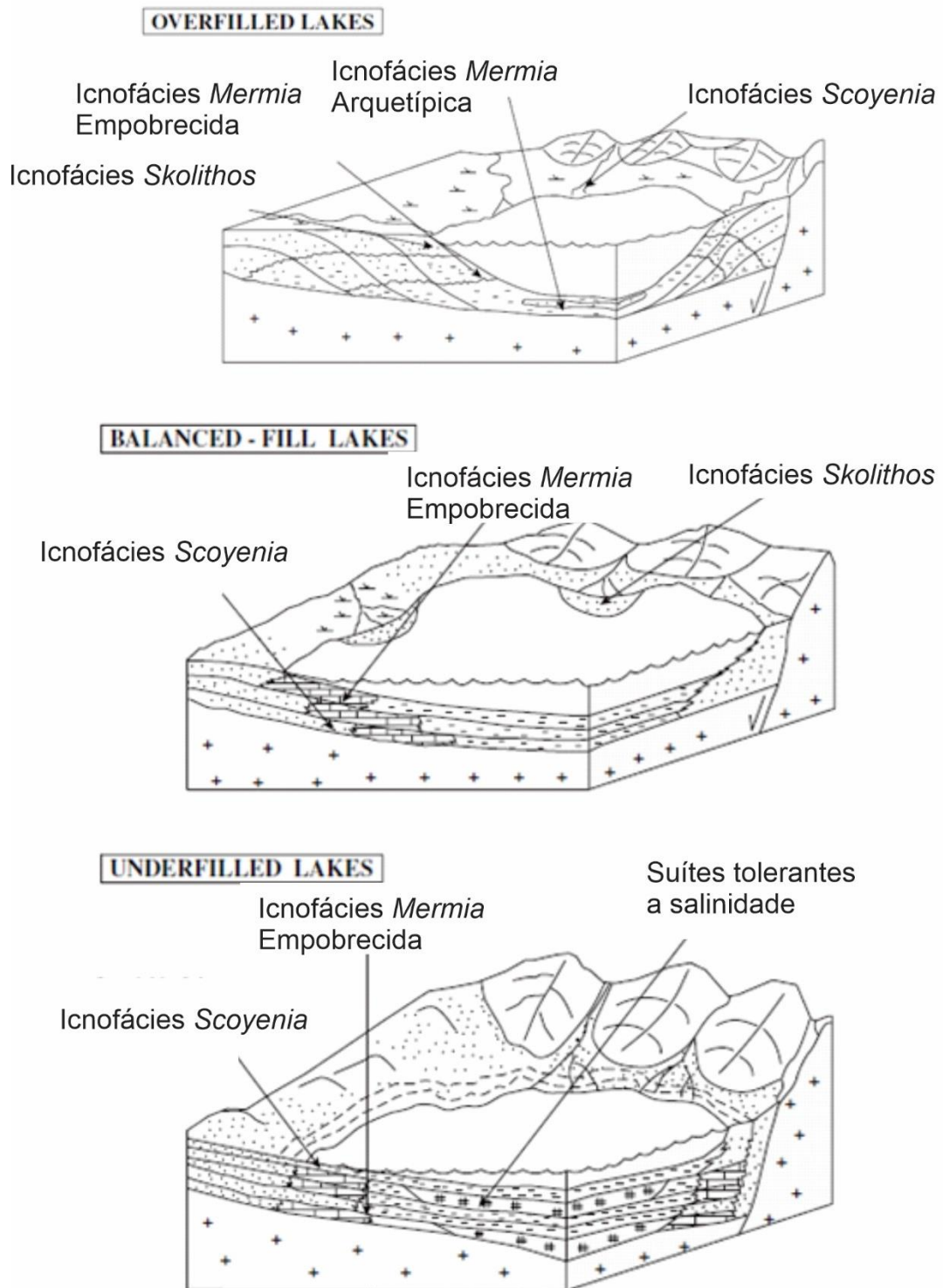


Figura 1.11 – Modelo de icnofácies para a estratigrafia de seqüência de ambientes lacustres, conforme a classificação de bacias lacustres postulada por Bohacs *et al.* (2000). Fonte: Buatois & Mángano (2007).

## **2 THE EARLY CRETACEOUS LACUSTRINE FACIES AND ICHNOFOSSILS OF THE PARNAÍBA BASIN, BRAZIL: A record of bioactivity in response to post-CAMP thermal subsidence in West Gondwana.**

Argel de Assis Nunes Sodré<sup>1</sup>; Joelson Lima Soares<sup>1</sup>; Afonso César Rodrigues Nogueira<sup>1</sup>; Alexandre Ribeiro Cardoso<sup>2</sup>; Renan Fernandes dos Santos<sup>1</sup>

(1) Universidade Federal do Pará - Instituto de Geociências.

(2) Universidade Estadual de Campinas.

### ABSTRACT

After the voluminous lava eruption related to the Central Atlantic Magmatic Province (CAMP), in the Triassic–Jurassic (~200 Ma), a large subsiding area formed in West Gondwana, allowing the Upper Jurassic–Lower Cretaceous lacustrine system of the Pastos Bons Formation in the Parnaíba Basin to form. Despite recent studies on this system, these deposits still need to be investigated in detail with palaeoenvironmental mapping based on the ichnological content, facies analysis and lacustrine sequence stratigraphy. Outcrop-based facies analysis allowed the identification of four palaeoenvironments: central lake, lakeshore, braided fluvial, and delta front. The ichnological content is concentrated in the lakeshore deposits and includes of eight ichnofossils, organized in three ichnofacies: *Mermia* (*Cochlichnus anguineus* and *Lockeia siliquaria*), *Scoyenia* (*Agrichnium* isp., *Gyrochorte comosa*, *Palaeophycus tubularis*, *Planolites berkeleyensis*, and *Rusophycus* isp.), and *Skolithos* (*Skolithos linearis*). This lacustrine succession is organized in five millimeter- to meter-scale depositional cycles bounded by erosive surfaces or flooding surfaces. Four cycles define a retrogradational and aggradational stratal stacking pattern composing the transgressive systems tract, and one cycle indicates the progradational stratal stacking pattern constituting the highstand systems tract. The sequence stratigraphy suggests that post-CAMP thermal subsidence and responsible for creating the accommodation space, controlling the sedimentary supply and water inflow/outflow, and the proportional relationship between them. At the base of this system, an underfilled lacustrine basin characterized by body fossil and ichnofossil-bearing layers and thick mudstones predominated, and after the maximum subsidence, an overfilled lacustrine basin characterized by cross-laminated sandstone of the fluvio-deltaic system was established.

Keywords: lacustrine stratigraphy; lacustrine ichnofacies, Jurassic-Cretaceous, post-CAMP subsidence.

## 2.1 INTRODUCTION

After the voluminous Triassic–Jurassic (~200 Ma) lava eruption, large areas of West Gondwana subsided (Klöcking *et al.* 2018). This event is related to the intrusion of the Central Atlantic Magmatic Province (CAMP), an important Large Igneous Province (LIP) that covered approximately 10 million km<sup>2</sup> of North and South America, Europe, and Africa and that was linked to the Pangea supercontinent's breakup and opening of the central Atlantic Ocean (Marzulli *et al.* 1999, McHone 2000).

The record of the post-CAMP isostatic signature is poorly documented in the sedimentary basins of West Gondwana. While subvolcanic rocks have been described by geophysical, outcrop, and drill core analyses, the distribution of extrusive volcanic rocks is restricted in some places, such as in the Parnaíba Basin, north-eastern Brazil, whereas sediment-lava interactions have been documented there (Rabelo *et al.* 2019, Nogueira *et al.* 2021).

Therefore, the post-CAMP subsidence in the basins has never been addressed in detail, mainly, how the localized uplifting and thermal subsidence influenced the reorganization of the depocenters and the evolution of the depositional systems. The fluvial-lacustrine system related to the Upper Jurassic–Lower Cretaceous Pastos Bons Formation has been considered a record of the post-CAMP subsidence phase in the Parnaíba Basin (Cardoso *et al.* 2017, 2019a) (Fig. 2.1).

Despite recent palaeontological and local stratigraphic and facies analyses (Petra 200, Bernardes-de-Oliveira *et al.* 2007, Petra & Gallo 2012, Montefeltro *et al.* 2013, Cardoso *et al.* 2017, 2019a, 2019b, 2020), these deposits need to be investigated in detail based on palaeoenvironmental mapping to verify the real extension of these processes in the Parnaíba Basin. Here, the ichnological content associated with the local stratigraphy and sedimentology is interpreted, improving the palaeoenvironmental interpretation of these deposits and contributing to the understanding of the post-CAMP conditions in West Gondwana.

## 2.2 GEOLOGICAL SETTING

The Palaeozoic intracratonic Parnaíba Basin is situated in north-eastern Brazil, covers an area of 600,000 km<sup>2</sup>, and reaches approximately 3.5 km thick in the depocenter. This basin shows shallow marine to continental sediments and long subsidence histories (Góes & Feijó 1994, Vaz *et al.* 2007, Daly *et al.* 2014). The Mearim Group comprises post-CAMP fluvial-lacustrine deposits that unconformably overlie Palaeozoic successions of the Poti, Piauí, Pedra

de Fogo, and Motuca formations from east to west (Lima & Leite 1978). The contact with the overlying Grajaú Formation is erosional (Rabelo & Nogueira 2015, Cardoso *et al.* 2019a).

The Pastos Bons Formation comprises mudstone, sandstone, and lenses of carbonate rocks related to the fluvial-lacustrine system and local presence of deltas (Cardoso *et al.* 2017, 2019a). This sedimentary succession was deposited in lacustrine basins, developed by post-CAMP thermal subsidence, with a fluvial contribution in arid to semiarid climates (Cardoso *et al.* 2017, 2019a, 2020) (Fig. 2.1).

The fossil content is composed of *Lepidotes piauhyensis*, *Semionotus*, *Pholidophoridae*, *Macrosemiideos*, and *Gondwanapleuropholis longimaxillaris* fish fossils (Roxo & Löfgren 1936, Brito & Gallo 2002, Gallo 2005, Petra & Gallo 2012, Cardoso *et al.* 2019a, 2020), ostracods (*Macrolimnadiopsis*) and *Batrachomimus pastosbonensis* crocodiles (Montefeltro *et al.* 2013), as well as palynomorphs, which are correlated to the Upper Jurassic–Lower Cretaceous (~152–145 Ma) Dom João stage (Bernardes-de-Oliveira *et al.* 2007).

Furthermore, numerous invertebrate ichnological studies since the 1990s have focused on lacustrine environments worldwide (Buatois & Mángano 2007 and references therein). Recently, the ichnofacies model has expanded to the lacustrine system (e.g., Buatois & Mángano 1995, 1998, 2004, 2007, 2009, Scott *et al.* 2012). However, papers focused on lacustrine system invertebrate ichnology are rare in Brazilian basins (Buatois *et al.* 2006, Guimarães Netto *et al.* 2009, Guimarães Netto *et al.* 2012). In Brazilian Mesozoic lacustrine deposits, authors have frequently mentioned the occurrence of ichnofossils, nevertheless underusing their palaeoenvironmental proxy, e.g., the Cretaceous of the Parecis Basin (Rubert *et al.* 2017, 2019) and the Upper Jurassic–Lower Cretaceous of the Araripe Basin (Fambrini *et al.* 2013), Northern Brazil.

### 2.3 METHODS

The Pastos Bons Formation was investigated in an area of the central eastern portion of the Parnaíba Basin, along a SW-NE 50 km-long zone near the cities of Floriano and Nazaré do Piauí, Piauí State (Fig. 2.1). Outcrops were studied to determine the sedimentary facies, as proposed by Walker (1992). The steps are as follows: identification and description of sedimentary facies; determination of the sedimentary processes; and suggestion of the facies associations based on sets of contemporary and cogenetic facies emphasized in the lacustrine facies model proposed by Talbot & Allen (1996), Nichols (2009) and Renalt & Gierlowski-Kordesch (2010).

Three different methodologies were used to analyse the ichnofossil assemblage: 1) ichnotaxonomy classification (Bromley 1996, Buatois & Mángano 2011); 2) stratigraphic analysis (Seilacher 1953, 1967, Martinsson 1970); and 3) ethological analysis (Buatois & Mángano 2011). Ichnofacies analyses are based on the archetypal ichnofacies models proposed by Seilacher (1964, 1967), Bromley (1996), MacEachern *et al.* (2007, 2010), and Buatois & Mángano (2011); here, we focus on the lacustrine ichnofacies model suggested by Buatois & Mángano (1998, 2004, 2007), and Scott *et al.* (2012). Miller & Small (1997) proposed the semiquantitative field method for evaluating bioturbation on bedding planes (with bioturbation index denoted BI) utilized in this paper for ichnofabric analysis.

The identification and delimitation of meter-scale cycles as fourth- and fifth-order processes, such as the parasequence definition, corresponds to genetically related sedimentary successions bounded by flooding surfaces (Spence & Tucker 2007, Catuneanu *et al.* 2009). In this paper, we apply the facies model and ichnofacies model associated with cyclostratigraphy and sequence stratigraphy to define the lacustrine basin type and the evolution of the lacustrine system (Carroll & Bohacs 1999, Bohacs *et al.* 2000, Buatois & Mángano 2004, 2007, 2009, Scott & Smith 2015).

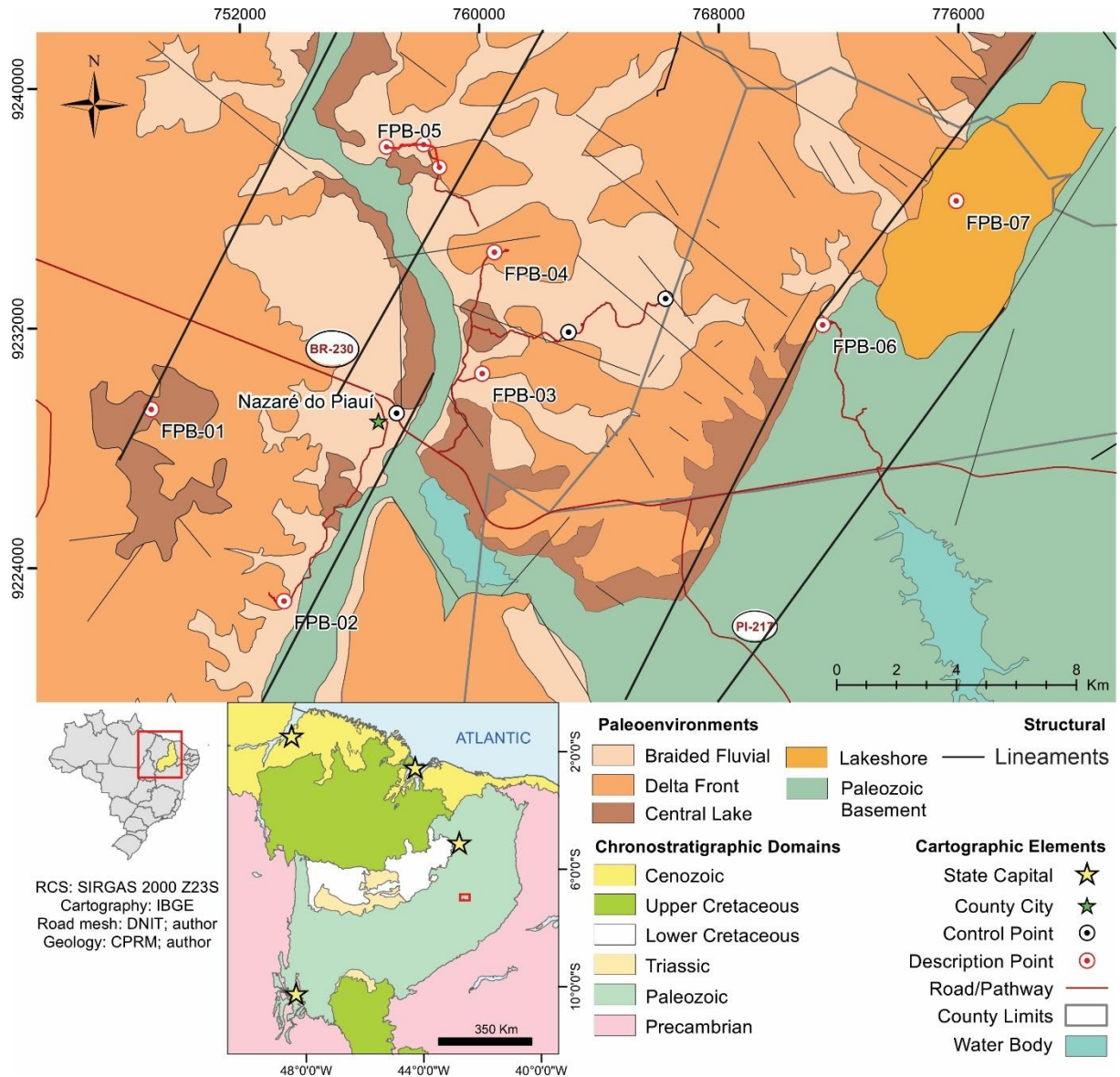


Figure 2.1 – Location map of the study area. A. Geographic map of Brazil, with Piauí State marked in yellow. B. Parnaíba Basin, north-eastern Brazil, and geological mapping of the local sedimentary supersequences; the red rectangle delimits the study area (modified from Santos and Carvalho, 2004). C. Palaeoenvironmental map of the study area, south-eastern Parnaíba Basin.

## 2.4 FACIES ASSOCIATION

The 60 m-thick siliciclastic succession is best exposed in residual hills and intermittent drainages composed of primary sandstone and mudstone, with less limestone, conglomerate, and evaporite beds (Tab. 2.1). The sandstone and mudstone facies are organized in centimeter-scale coarsening and fining-upward cycles. Iron oxides/hydroxides are the most common cement of clastic rocks, resulting in a reddish to yellowish colour. Fifteen sedimentary facies were grouped in four associations (FA) representative of a fluvial to lacustrine setting: the FA1 central lake, FA2 lakeshore, FA3 braided fluvial, and FA4 delta front associations (Fig. 2.2).

This succession unconformably overlies the Upper Devonian and Lower Carboniferous rocks and is truncated by NE-trending Cretaceous dikes and fault zones coincident with NW-SE and NE-SW lineaments forming a multi-scale graben-horst structure, causing offsets up to 50 m (Fig. 2.2).

Table 2.1 – Facies, facies associations and depositional processes of Upper Jurassic – Lower Cretaceous lacustrine succession Pastos Bons Formation, of the Parnaíba Basin, Northeastern Brazil.

(continua)

Facies	Description	Depositional process
Laminated limestone (L1)	Fibrous calcite crystals form up to 5 cm-thick tabular beds.	Lake waters drop, increase of evaporation rate (outflow) associated with minimum riverine discharge. The primary gypsum was replaced by fibrous calcite pseudomorphs.
Fossiliferous shale (Sf)	Grey-colored shale with even-parallel lamination showing <i>Lepidotes piauhyensis</i> throughout the up to 10 cm-thick tabular beds.	Deposition through fall-out in shallow water, high organic matter preservation in anoxic environment and with low sedimentary supply.
Laminated mudstone (M1)	Red, green, to gray-colored mudstone with even-parallel lamination to structureless forming 0.5–12 m-thick tabular beds.	Transportation through suspension and deposition by fall-out with subordinated traction in calm water environments.
Mudstone with desiccation cracks (Mc)	Red and gray-colored mudstone with even-parallel lamination to structureless with desiccation cracks forming up to 1 m-thick tabular beds.	Transportation through suspension and deposition by fall-out with subordinated traction, in calm waters environments with posterior subaerial exposure in semiarid/arid climate.
Massive sandstone (Sm)	Yellow-colored sandstone showing incipient cross-laminated to structureless forming up to 5 cm-thick tabular beds.	Rapid deposition by traction forming underflows in the lake bottom, with consequent liquefaction.

(continuação)

Sandstone with sigmoidal cross-stratification (Ssg)	Yellow to red-colored, medium-grained sandstone with medium-scale sigmoidal cross-stratification forming 1 – 10 m-thick lobate beds. The foresets dip directions indicate 330° – 360° Az, average 320° Az. Ichnoassemblage: <i>Agrichnium</i> isp.	Migration of bedforms under the unidirectional flow of high sand supply, high-energy homopycnal/hyperpycnal flows with rapid deceleration.
Sandstone with supercritical climbing ripples cross-lamination (Scr)	Yellow to red-colored, fine to medium-grained sandstone with supercritical climbing ripples cross-lamination forming up to 1m-thick tabular beds. The foresets dip to NW (320° Az) and exhibits angle of climbing > stoss side angle.	Migration of small-scale bedforms by unidirectional and lower flow regime with a high rate of suspension.
Sandstone with current ripples (Sr)	Yellow to red-colored, fine to medium-grained, sandstone with 2D and 3D crests current ripples forming up to 50 cm-thick tabular beds. The crests are rounded, up to 4 cm-height, up to 8 cm-wavelength, 6 cm stoss side-length, and 2 cm lee side-length. Ichnoassemblage: <i>Cochlichnus anguineus</i> , and <i>Lockeia siliquaria</i> .	Migration of small-scale bedforms by unidirectional and lower flow regime.
Sandstone with trough cross-stratification (St)	Yellow to red-colored, coarse- to very coarse-grained sandstone with medium-scale trough cross-stratification locally shows rip-up clasts forming 2-9 m-thick tabular beds. The foresets dip directions indicate 330° – 40° Az, average 315° Az.	Transportation by traction and migration of bedforms with sinuous crests and predominance of lower flow regime. Rip-up clasts generated after substrate reworking.
Sandstone with tabular cross-stratification (Sta)	Yellow-colored, coarse- to very coarse- grained sandstone with medium-scale tabular cross-stratification forming 1-2 m-thick tabular beds. The foresets dips indicate 330° – 350° Az, average 320° Az.	Transportation by traction and migration of bedforms with 2D crest and predominance of lower flow regime.
Massive conglomerate (Cm)	Red-colored, clast-supported conglomerate with granules and pebbles of polycrystalline quartz dispersed in coarse-grained matrix forming 1-meter-thick lenticular beds.	Rapid sedimentation by ephemeral inflows with the predominance of unidirectional bed-load currents.



Intraformational conglomerate (Ci)	Red-colored, clast-supported conglomerate with subangular to subrounded granules and pebbles of mudstone and minor quartz dispersed in coarse-grained matrix forming 1-meter-thick lenticular beds.	Rapid sedimentation (conclusão) inflows with the predominance of unidirectional bed-load currents in a mudstone substrate.
Bioturbated sandstone (Sb)	Yellow-colored, medium-grained sandstone with vertical burrows of <i>Skolithos</i> ichnogenus (BI 4-5), ripple marks and desiccation crack up to 50 cm-thick tabular beds.	Migration of small-scale bedforms by unidirectional and lower flow regime; Colonization by infaunal communities generating bioturbation structures that obliterate the primary sedimentary structures; and posterior subaerial exposure in semiarid/arid climate.
Sandstone with wave ripples (Sw)	Red-colored, fine- to medium-grained sandstone with symmetric wave ripples forming up to 30 cm-thick tabular beds. Present rounded base and peaked crest, up to 4 cm-height, up to 8 cm-wavelength. Ichnoassemblage: <i>Gyrochorte comosa</i> , <i>Planolites beverleyensis</i> , <i>Palaeophycus tubularis</i> , and <i>Rusophycus</i> isp.	The wave ripples are formed by a decrease in water level, causing the bedforms reworking by waves, and colonization by infaunal communities generating bioturbation structures.
Massive limestone with intraclast (Lm)	Coarse-grained, with intraclasts and some detrital grains in a micritic matrix limestone with tepee-like and cone-in-cone structures forming up to 10 cm-thick lenticular beds.	Saturation and biochemical precipitation of CaCO <sub>3</sub> in shallow waters and reworking for waves and posterior subaerial exposure in semiarid/arid climate.

#### 2.4.1 FA1- Central Lake

**Description:** FA1 is composed of laminated limestone (Ll), fossiliferous shale (Sf), laminated mudstone (Ml), and massive sandstone (Sm), subdivided into two phases. The first phase is organized in centimeter-scale shallowing/salinization upward cycles (Fig. 2.3A). The Ll facies displays fibrous calcite crystals composing tabular layers interbedded with grey shale with parallel lamination with abundant *Lepidotes piauhyensis* fish fossils of adult and young specimens (Fig. 2.3B and C) of different sizes. The second phase exhibits structureless to parallel laminated meter-scale mudstone beds interbedded with structureless to incipient cross-laminated centimeter-scale sandstone beds organized in coarsening-upward cycles (Fig. 2.3D and E), unconformably overlying FA2, FA3, and FA4.

**Interpretation:** The Sf facies indicates lower energy deposition by sediment fall-out in moderately deep to shallow water, with partial anoxia that allowed high organic matter preservation. Low sedimentary supply dominated the deepest portions (offshore) of the lake,

protected from oxygen accumulation (Cardoso *et al.* 2019a, 2020). The L1 facies indicates the lake contraction increasing evaporation rate (outflow) associated with minimum riverine discharge. The primary gypsum was replaced by fibrous calcite pseudomorphs (Cardoso *et al.* 2019a). The well-preserved *Lepidotes piauhyensis* corroborates the low-energy environment of a closed underfilled lacustrine basin exemplified by the classic fossiliferous Muzinho Shale (Cardoso *et al.* 2019a, 2020).

The fine- to very fine-grained suspended sediments (overflows) accumulated due to fall-out in calm water environments, and higher density sediments were washed over the lake margins and transported by density currents (underflows) through tractive processes towards the lake centre (Sm facies). These mechanisms caused the deposition of sand-grained sediments on the lake floor, creating tabular and laterally extensive sandy layers under oxic conditions (e.g., Scherer *et al.* 2007, Andrade *et al.* 2014, Cardoso *et al.* 2017, 2019a, Abrantes Jr. *et al.* 2019).

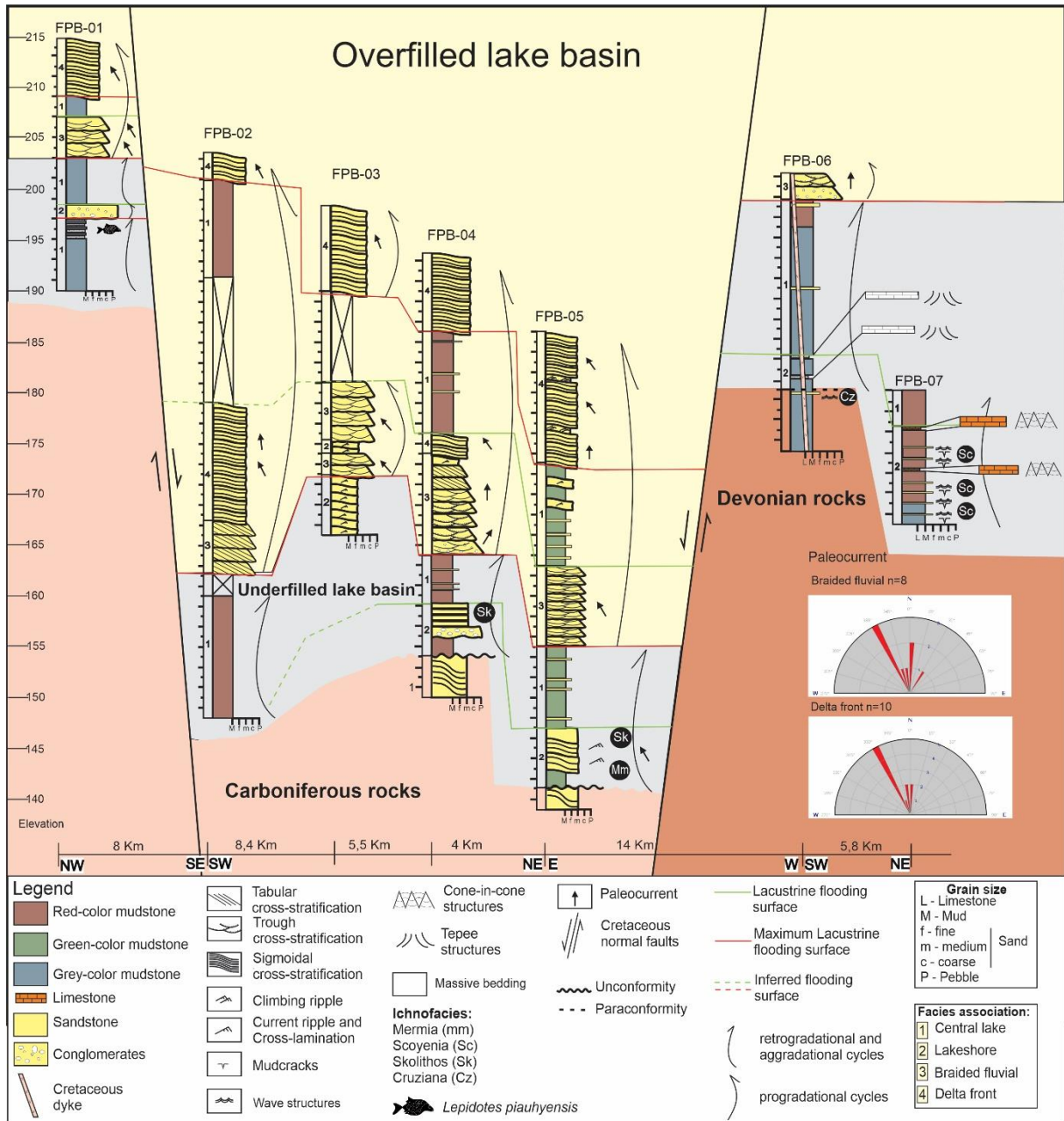


Figure 2.2 – The stratigraphic context of measured sections of the Upper Jurassic–Lower Cretaceous Pastos Bons Formation in the eastern Parnaíba Basin, Brazil.

2.4.2 FA2 – Lakeshore

**Description:** This facies association is composed of mudstone with desiccation cracks (Mdc), massive limestone with intraclasts (Lm), sandstone with sigmoidal cross-stratification (Ssg), bioturbated sandstone (Sb), sandstone with current ripples (Sr), sandstone with wave ripples (Sw) and massive conglomerate (Cm). The meter-scale beds of structureless to parallel laminated mudstone with desiccation cracks (Fig. 2.3F) are interbedded with clast-supported centimeter-scale limestone beds with tepee-like and cone-in-cone structures and symmetric

wave ripple centimeter-scale sandstone beds (Fig. 2.4A) with *Gyrochorte comosa*, *Planolites beverleyensis*, *Palaeophycus tubularis*, and *Rusophycus* isp. and BI = 1 (1–5%). The facies sandstone with sigmoidal cross-stratification presents in meter-scale lobed beds with foresets dipping NW and grades toward the top to cross-lamination capped by clay films, and asymmetrical wave ripples can be observed in both 2D and 3D in the centimeter-scale sandstone beds (Fig. 2.4B, C) with horizontal ichnofossils *Agrichnium* isp., *Cochlichnus anguineus*, and *Lockeia siliquaria* and BI = 2 (10–15%). The Sb facies exhibits *Skolithos linearis* with BI = 4–5 (60–100%) in tabular bioturbated beds, obliterating other sedimentary structures (Fig. 2.4D, E, F). The Cm are up to 1 m thick lenticular beds of closed-framework polimitic conglomerate beds, with subrounded pebble clasts of mudstone and sandstone.

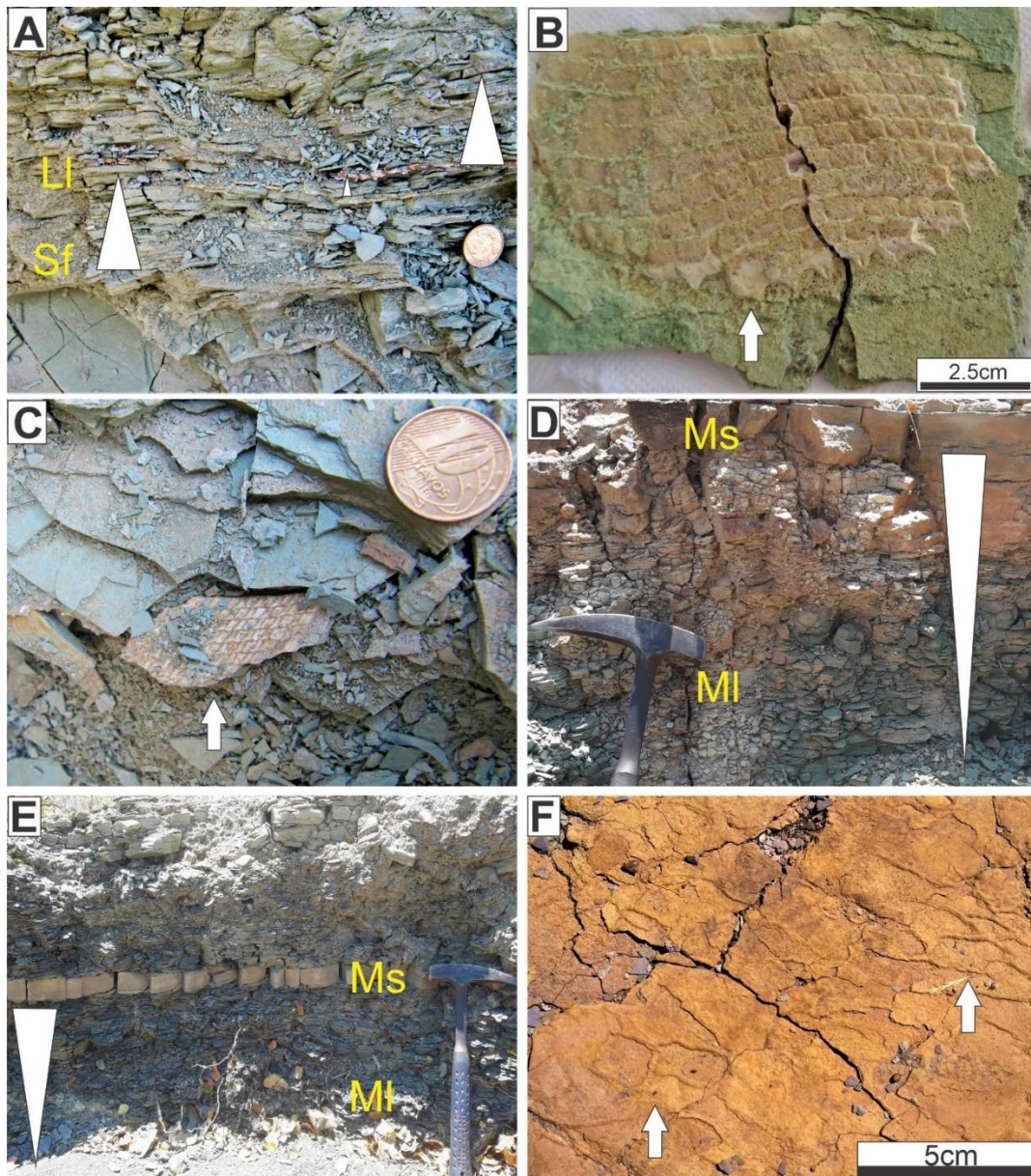


Figure 2.3 – Sedimentary facies. A. Central lake. Grey mudstone interbedded with laminated limestone, forming millimeter- to centimeter-thick shallowing/salinization-upward cycles (white triangles). B and

C. Fragments of *Lepidotes piauhyensis* (white arrows). D and E. Central lake (FA1). Grey to green laminated mudstone (Ml), grading to grey to red massive sandstone (Ms), arranged in coarsening-upward cycles (white triangles). F. Lakeshore (FA2). Mudstone with complete, nonorthogonal, and nonoriented desiccation cracks (white arrows).

**Interpretation:** The mudstone beds suggest the deposition of fine-grained sediments by the fall-out process, and the limestone beds denote the seasonal reduction in clastic sediment input and drop in lake water level, enhancing biochemical precipitation of  $\text{CaCO}_3$  in a shallow lake setting. Tepee-like and desiccation crack structures indicate posterior subaerial exposure in semiarid/arid climates (e.g., Paik and Kim, 1998; Zaleha, 1997). The reworked-wave deposits indicate a decrease in the water table and consequent reworking by fair-weather wave action in subaqueous conditions (e.g., Melchor, 2004; Ilgar and Nemec, 2005). Thus, the wave structures and *Scoyenia* ichnofacies occurrence indicate the development of wave-dominated shorelines (Buatois and Mángano, 1998, 2004, 2007).

The complex sigmoidal lobe geometry is related to the shallow lake conditions (e.g., Ambrosetti et al. 2017); therefore, the Sr facies indicates that the sedimentary build-up by sigmoidal lobes caused infilling of the shallow lake zones, allowing the migration of smaller-scale bedforms related to the *Mermia* ichnofacies occurrence (Buatois and Mángano, 1998, 2004, 2007). The Cm was formed under upper-energy flow regime rapid and ephemeral unidirectional current and the presence of the mudstone and sandstone clasts are evidence of lacustrine margin substrate current reworking. Thus, the *Skolithos* ichnofacies occurrence indicate the development of ephemeral current-influenced shorelines (Buatois and Mángano, 1998, 2004, 2007).

The wave activity and the current inflow allow the optimization of the distribution of oxygen, salinity, and temperature, causing the proliferation of benthic organisms in the lake margins and marking the nondepositional stages (Savdra, 2007; Buatois and Mángano, 2009).

This association represents a low-gradient, wave-dominated deposition, with a subordinate unidirectional current in the marginal zone, periodically exposed to subaerial conditions in a shallow lacustrine setting. This area experienced variable energy regimes during deposition, although the presence of fair-weather wave structures and the dominance of mudstone and carbonate rocks reflect that low-energy environments predominated (Talbot and Allen, 1996; Buatois and Mángano, 2004; Nichols, 2009; Renaut and Gierlowski-Kordesch, 2010).

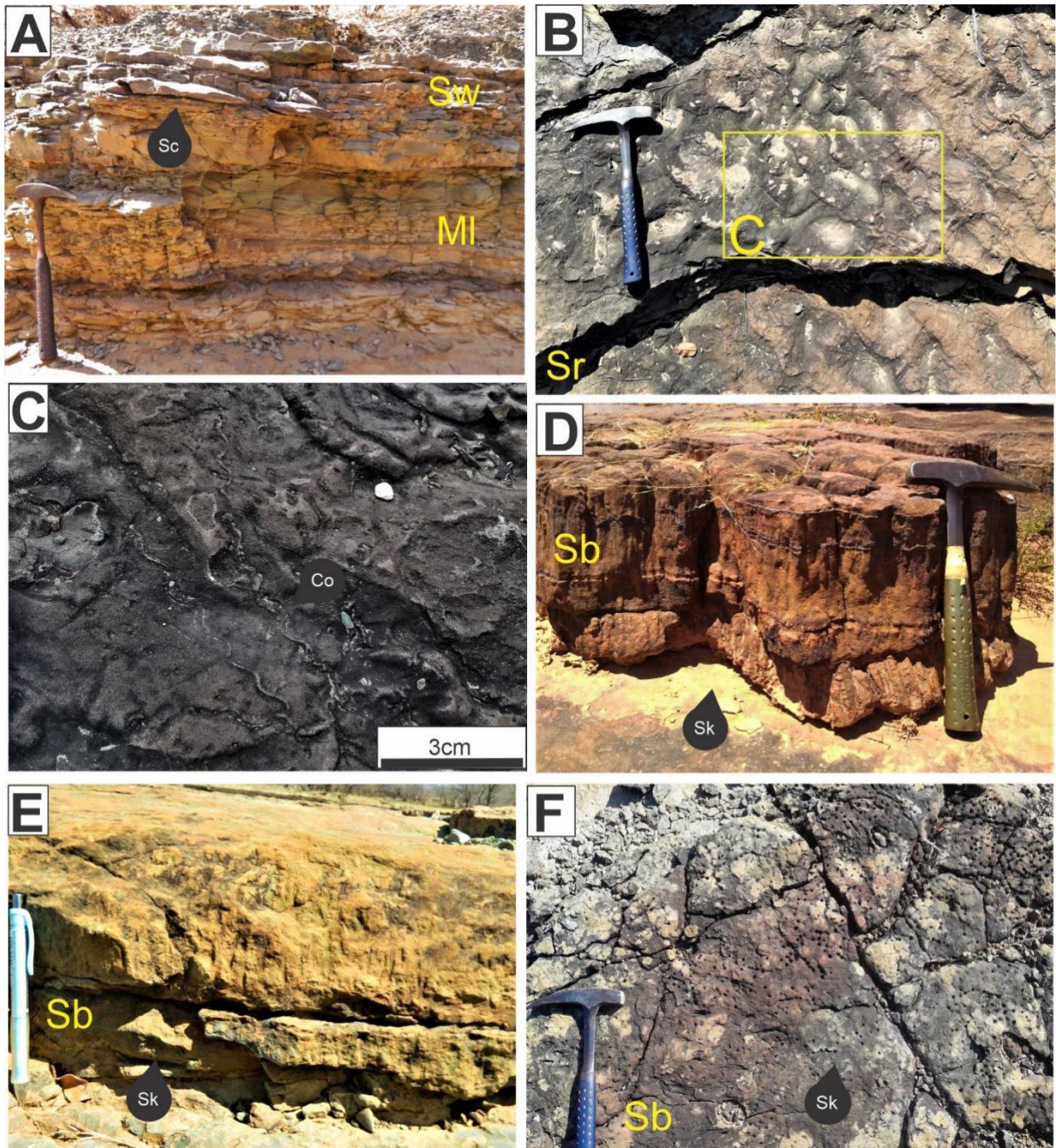


Figure 2.4 – Ichnofossils in outcrops. A. At the base, red to green laminated mudstone is overlain by red sandstone with bioturbated wave ripples (0–5%) and trace fossils of *Scoyenia* ichnofacies. B. and C. Sandstone with 3D current crest ripples with horizontal trace fossils (*Cochlichnus anguineus*) B2 (10–15%). D. and E. Bioturbated sandstone (Sb). Red to yellow sandstone with vertical bioturbation (*Skolithos linearis*); B3-B4 (40–50%). F. Bioturbated sandstone (Sb). Red to yellow sandstone with vertical bioturbation (*Skolithos linearis*), in plant visualization, B3-B4 (40–50%).

### 2.4.3 FA3 – Braided fluvial

**Description:** FA3 comprises sandstone with trough cross-stratification (St), sandstone with tabular cross-stratification (Sta), massive conglomerate (Cm), and intraformational conglomerate (Ci). This association forms amalgamated sandy tabular beds up to 10 m thick that are laterally continuous for dozens of meters and show a sharp contact with FA1 and FA4. The medium-scale trough and tabular cross-stratification sandstone beds with foresets dipping to the NW/N/NE (Fig. 2.5A and B); and the clast-supported conglomerate presents structureless to incipient parallel stratification and locally presents rip-up clasts composed of pebble-sized angular clasts of mudstone (Fig. 2.5C and D). The grain size varies from coarse sand to pebble, forming centimeter-scale fining-upward cycles and normal grading.

**Interpretation:** The cross-bedded sandstone tabular beds and closed-framework conglomeratic lenses suggest high-energy subaqueous processes; thus, these are the evidence of unidirectional flow that suggests that the fluvial currents formed sandy and gravel bars during channel migration. This stacking pattern likely reflects rapid sedimentation inflows with unidirectional bedload currents. The presence of rip-up clasts corresponds to muddy substrate reworking. The transition from Cm to St and Sta facies corresponds to a slight decrease in unidirectional current energy, causing transportation by traction and the migration of bedforms with 2D and 3D crests and a predominance of a lower-energy flow regime (Miall 1977a, 1977b, 2014, Collinson & Reading 1996, Nichols 2009). The migration of sandy to gravelly bedforms with straight (Sta) and sinuous crests (St) under unidirectional currents towards N/NW/NE indicates that a bedload braided fluvial system fed into areas of this endorheic basin, typical of a continental lacustrine setting (e.g., Nichols 2004, 2007, 2012; Fisher *et al.* 2007, Fisher & Nichols 2013).

### 2.4.4 FA4 – Delta front

**Description:** FA4 comprises sandstone with sigmoidal cross-stratification (Ssg) and sandstone with supercritical climbing ripple cross-lamination (Scr). This association produces lobate- to tabular-shaped beds up to 10 m thick and laterally continuous for dozens of meters, forming amalgamated sandstone beds, generally on top of the succession. The sandstone shows medium-scale sigmoidal cross-stratification with foresets dipping to the NW (Fig. 2.5E, F, G and H) with sharp contact to the facies M1 – FA1 (Fig. 2.5E) and gradual contact with

supercritical climbing ripple cross-lamination (Scr), in which foresets dip to the NW (Fig. 2.5I), forming coarsening-upward cycles.

**Interpretation:** The sandstone with sigmoidal cross-stratification suggests tractive, subaqueous, unconfined, and homopycnal/hyperpycnal flows that underwent abrupt deceleration when debouching into the large and calm water body of the lacustrine setting (e.g., Abrantes Jr *et al.* 2019). The subordinated beds indicate that the sedimentary build-up by sigmoidal lobes caused infilling of the shallow lake zones, allowing the migration of smaller scale bedforms. The migration of sandy bedforms under unidirectional currents towards the N/NW indicates that during highstand periods, the perennial braided fluvial system (FA3) flowed into the shallow lacustrine basin, forming a series of deltaic lobes (FA4) and shoal water-delta deposits (Postma 1990, Collinson & Reading 1996, Ilgar & Nemec 2005, Fisher *et al.* 2007, Nichols 2009, Renaut & Gierlowski-Kordesch 2010, Fisher & Nichols 2013).



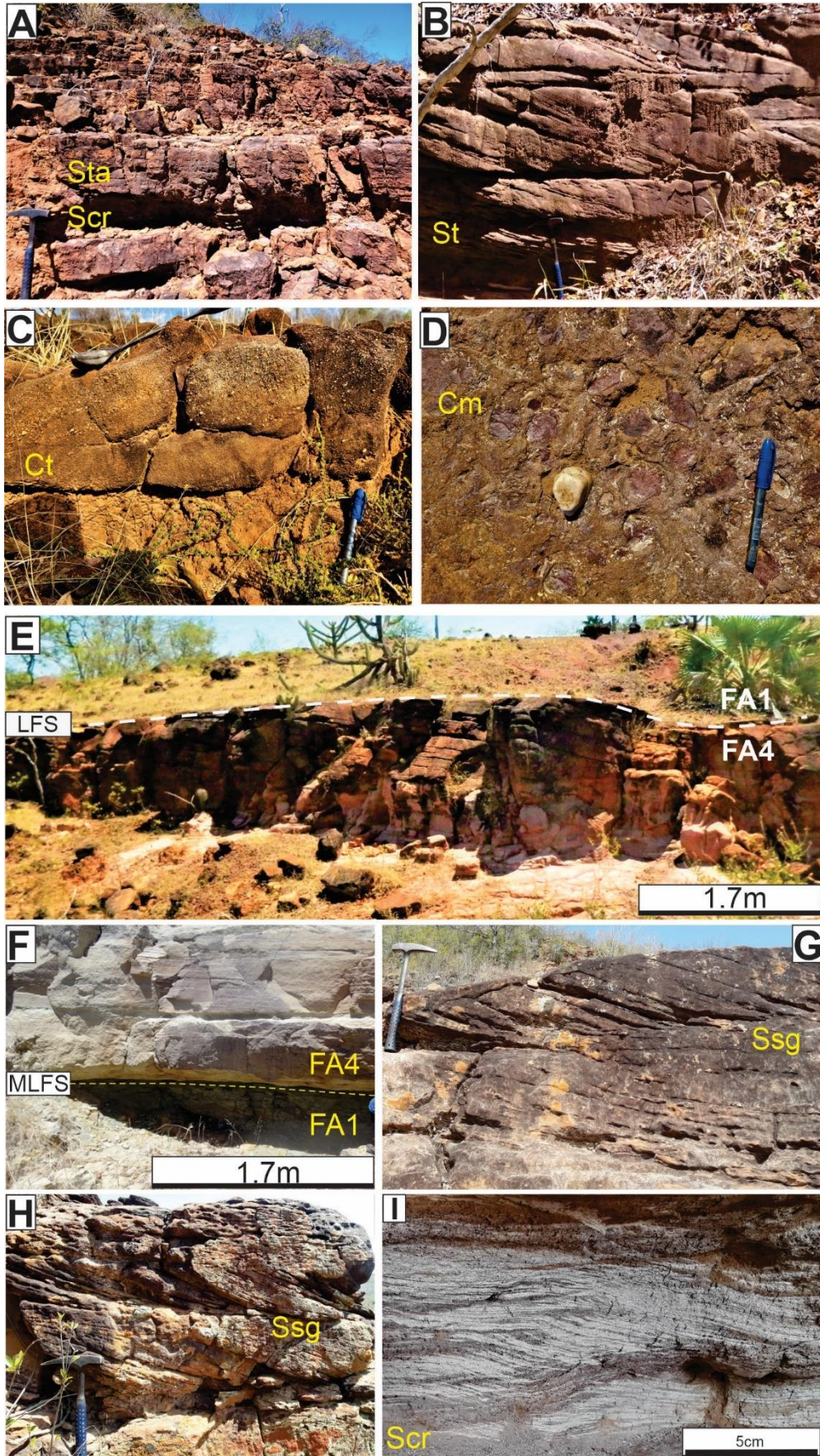


Figure 2.5 – Sedimentary facies. A. FA3 braided fluvial system. Thinning-upward of set of the Sandstone with tabular cross-stratification (Sta.) B. Detail of the sandstone with trough cross-stratification (St). C. Conglomerate with trough cross-stratification (Ct). D. Structureless conglomerate with subrounded mudstone and quartz clasts (Ci). E. Grey sandstone with sigmoidal cross-stratification (Ssg-FA4) overlain by grey laminated mudstone (MI-FA1). This transition of FA4 to FA1 marks the Lacustrine Flooding Surface (LFS), characterizing the retrogradational pattern (C4). F. Sandstone with sigmoidal cross-stratification (Ssg), overlying laminated mudstone (MI). The transition of MI-FA1 to Ssg-FA4 marks the Maximum Lacustrine Flooding Surface (MLFS), characterizing the progradational pattern (C5). G and H. G and H. FA4 delta front. Sandstone with sigmoidal cross-stratification (Ssg). I. FA4 delta front. Grey to red sandstone showing supercritical climbing ripple cross-lamination (Scr).

## 2.5 ICHNOLOGY

The sedimentary succession records eight ichnogenera and six ichnospecies, a total of 288 specimens were described in this paper, 200 in situ and 88 in samples (Tab. 2.2). The ichnofossils occur in the Sr, Sw, and Sb facies (base and top of bedding planes), included in the lakeshore associations - FA2 (Tab. 2.3), demonstrating different degrees of preservation and abundance (bioturbation index). These ichnotaxa are listed alphabetically.

### 2.5.1 *Agrichnium* Pfeiffer, 1968 – *Agrichnium* isp.

**Description:** Sinuous burrows, horizontal, unbranched, and unornamented, preserved as negative epirelief (Fig. 2.6A and B). Smooth wall and typical V-shape in cross-section (Fig. 2.6A). Diameters range from 0.3 to 1 cm; length is variable up to 22 cm.

**Interpretation:** Bivalve mollusks originate graze traces (pascichnia) *Agrichnium*-like (Baldwin 1974, Chamberlain 1975, Boeira & Guimarães Netto 1987). This ichnofossil has been generally associated with the marine *Cruziana* ichnofacies (e.g., Bayet-Goll *et al.* 2015). Nevertheless, Goldring *et al.* (2005), in the lakeshore of Cretaceous deposits of southern England and Baldwin (1974), Chamberlain (1975), and White & Miller (2008) in modern lakes, have described similar structures (horizontal burrows with V-shaped cross-sections) in lacustrine settings associated with continental *Scoyenia* ichnofacies.

Table 2.2 – Ichnospecies, number total of specimens described *in situ* and in samples of the ichnofossils of Upper Jurassic – Lower Cretaceous lacustrine succession Pastos Bons Formation, of the Parnaíba Basin, Northeastern Brazil.

Ichnospecies	number of specimens described		Total
	<i>In situ</i>	Samples	
<i>Agrichnium</i> isp.	1	1	2
<i>Cochlichnus anguineus</i>	50	5	55
<i>Gyrochorte comosa</i>	0	1	1
<i>Lockeia siliquaria</i>	0	13	13
<i>Palaeophycus tubulares</i>	0	4	4
<i>Planolites berkeleyensis</i>	0	2	2
<i>Rusophycus</i> isp.	0	1	1
<i>Skolithos linearis</i>	150	60	210
<b>Total</b>	<b>200</b>	<b>88</b>	<b>288</b>

### 2.5.2 *Cochlichnus* Hitchcock, 1848 – *Cochlichnus anguineus*, Hitchcock, 1858

**Description:** Simple meandering burrows, horizontal to subhorizontal orientation, smooth-walled, and cylindrical form (Fig. 2.6C). Branched, with bifurcation and slight to accentuated curves (Fig. 2.6D), preserved as positive epirelief. Diameters range from 0.2 to 0.7 cm; length is variable up to 19 cm; amplitude varies from 0.3 to 0.5 cm, and wavelength ranges from 1.4 to 4 cm.

**Interpretation:** Nematode, annelid, and Ceratopogonidae larvae generate this locomotion (repichnia) or graze traces (pascichnia) (Buatois & Mángano 1998, 2007). Nevertheless, the sinusoidal form of *Cochlichnus* derives from the locomotory principle of nematode worms on the substrate (Neibur & Erdös 1991, Seilacher 2007). *Cochlichnus* has been observed in continental and marine deposits (Pemberton & Frey 1984, Gluszek 1995). *Cochlichnus* specimens are usually larger in marine and brackish settings than continental specimens (Stanley & Pickerill 1998, Uchman *et al.* 2004). *Cochlichnus* in lacustrine settings is typical of *Mermia* ichnofacies and has been reported from the upper Carboniferous turbiditic glacial lacustrine sediments of northwest Argentina (Buatois & Mángano 1993); the Upper Pennsylvanian fluvial-lacustrine (Carboniferous) sediments of Sardinia, Italy (Marchetti *et al.* 2017); the Lower Triassic deltaic-lacustrine sediments of northwest Argentina (Melchor 2003,

2004); the Upper Triassic playa-lake system of Coastal Meseta, Morocco (Hminna *et al.* 2020); the Upper Jurassic lacustrine littoral sediments of the Rocky Mountain region, USA (Hasiotis 2004); the Cretaceous lacustrine marginal sediments of southern coast of Korea (Kim & Pickerill 2003, Kim *et al.* 2005); and the recent marginal lacustrine system of Germany (Hminna *et al.* 2020). The slight to accentuated curves are probably related to different producers or changes in substrate conditions (e.g., Uchman *et al.* 2004, Hminna *et al.* 2020). Buatois & Mángano (2011) interpreted the bifurcation as a “false branching”, which is the second successive branching that results from an animal revisiting a previously formed structure.

### 2.5.3 *Gyrochorte* Heer, 1865 – *Gyrochorte comosa* Heer, 1865

**Description:** Bilobate, curved, and horizontal burrows composed of two convex ridges separated by a median groove (Fig. 2.6E). These burrows exhibit an almond-shaped to heart-shaped cross-section. *Gyrochorte* presents transverse biserially arranged pads, and the median groove is straight. The trace diameter ranges from 0.4 to 0.6 cm; the length is variable up to 10 cm. The ridges show 0.1 to 0.2 cm-diameter and discontinuity planes. Exhibition of epirelief preservation and absence of hyporelief and 3D patterns.

**Interpretation:** Elongated organisms moving obliquely through the sediment (Heinberg 1973), probably a detritus-feeding worms (fodinichnia and pascichnia), most likely annelids, produce this ichnofossil (Weiss 1941, Heinberg 1973, Stanley & Pickerill 1998, Gibert & Benner 2002). *Gyrochorte* is not an ichnofossil typical of nonmarine environments; nevertheless, Savage (1971) and Lima *et al.* (2015) report similar structures in late Carboniferous freshwater periglacial lakes of South Africa and south-eastern Brazil, respectively. In this paper, they belong to nonmarine *Scoyenia* ichnofacies. From the Early Ordovician to Pliocene, *Gyrochorte* is particularly abundant in the Jurassic and Cretaceous rocks (Gibert & Benner 2002).

### 2.5.4 *Lockeia* James, 1879 – *Lockeia siliquaria* James, 1879

**Description:** Small horizontal trace, seed-like or almond-shaped, oblong, horizontal bodies, rounding and tapering to sharp or obtuse points, frequently symmetrical (Fig. 2.6F). They sometimes exhibit a slight longitudinal depression. The length varies from 0.5–1.5 cm

(average of approximately 1 cm), and the average width is 0.7 mm. Preserved in positive hyporelief.

**Interpretation:** Isolated *Lockeia siliquaria* represents resting traces (cubichnia) produced by bivalves (Osgood 1970, Seilacher & Seilacher 1994), while small crustaceans (e.g., Conchostracans) may have also produced such traces in freshwater settings (Bromley & Asgaard 1979). *Lockeia* in nonmarine environments is found in fluvial environments (Gluszek 1995, Goldring *et al.* 2005, Lawfield & Pickerill 2006) and has been reported in the Upper Triassic lacustrine systems of marginal lacustrine settings in Germany (Schlirf *et al.* 2001); the Lower Cretaceous marginal lacustrine settings in southern England (Radley *et al.* 1998, Goldring *et al.* 2005); the Late Permian to Middle Triassic fluvial-lacustrine system in North China (Guo *et al.* 2019); and the Late Miocene lacustrine setting of south-eastern Iceland (Pokorný *et al.* 2017).

#### **2.5.5 *Palaeophycus* Hall, 1847 – *Palaeophycus tubularis* Hall, 1847**

**Description:** Straight to slightly curved burrows, subhorizontal, sometimes branched, bifurcated, and unornamented (Fig. 2.6G). The fills exhibit the same lithology and texture as the host stratum. The walls are smooth. Diameters range from 0.5 to 1.5 cm; length is variable up to 7 cm. They are preserved as positive epirelief or, less commonly, positive hyporelief.

**Interpretation:** Vermiform organisms produced these dwelling (domichnia) or feeding traces (fodinichnia) (Pemberton & Frey 1982, Knaust 2017). *Palaeophycus* is typical of *Scoyenia* ichnofacies in nonmarine settings and has been reported in Late Carboniferous turbiditic glacial lake sediments in northwest Argentina (Buatois & Mángano 1993); the Late Permian to Middle Triassic fluvial-lacustrine system in North China (Guo *et al.* 2019); the Middle Triassic sandflat of playa lake in Argentina (Mancuso *et al.* 2020); the Late Triassic playa lake in Morocco (Hminna *et al.* 2020); the Upper Jurassic lacustrine littoral environments in the Rocky Mountain region, USA (Hasiotis 2004); and the Cretaceous lacustrine marginal environment along the southern coast of South Korea (Kim & Pickerill 2003, Kim *et al.* 2005).

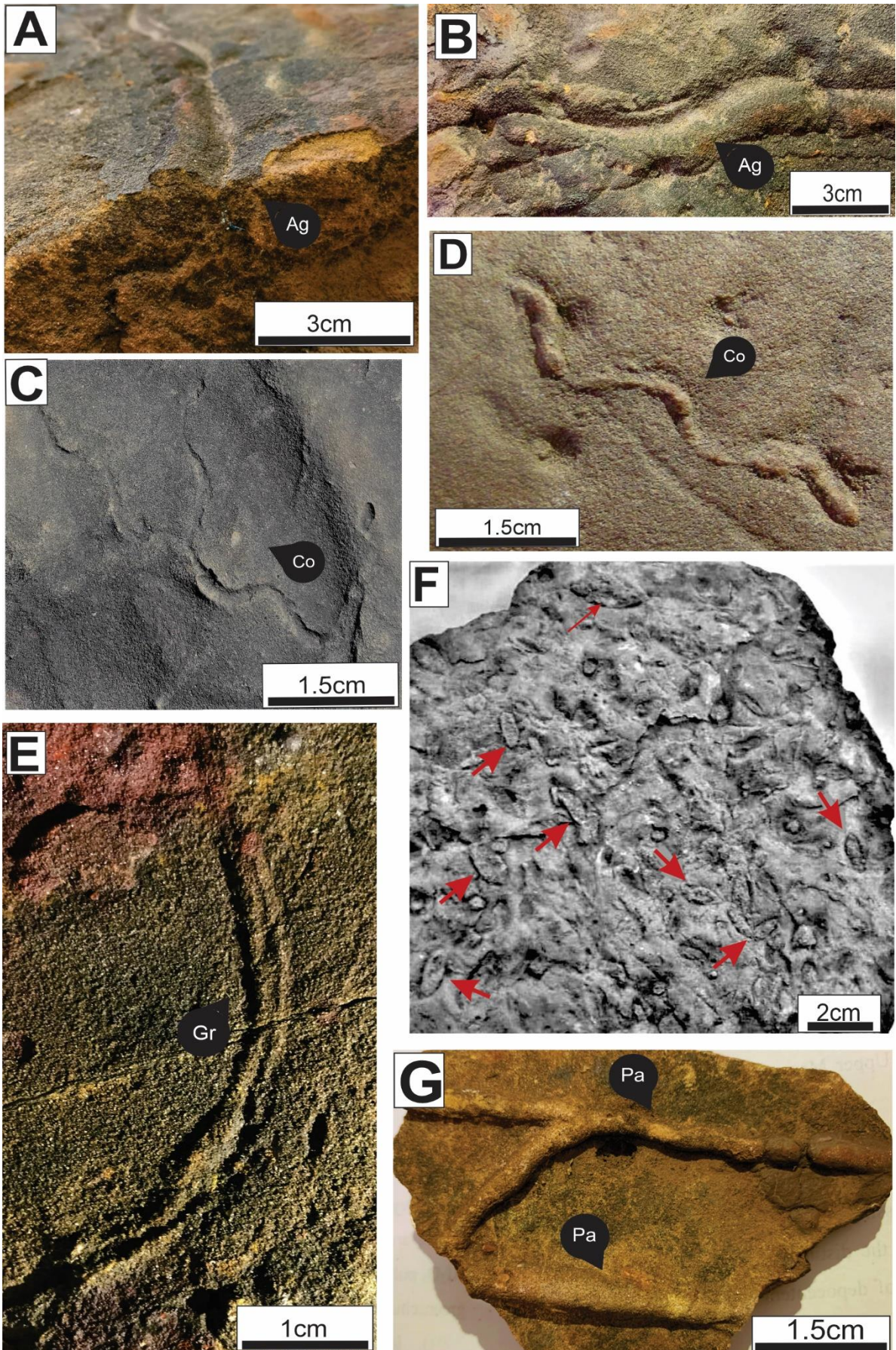


Figure 2.6 – Ichnofossils of the Pastos Bons Formation. A. *Agrichnium* isp. (Ag) showing V-shaped, in cross-sections, preserved as negative epirelief. B. *Agrichnium* isp. showing sinuous shaped, in

longitudinal sections. C. and D. *Cochlichnus anguineus* (Co), simple meandering burrows, preserved as positive epirelief (E. showing bifurcation). E. *Gyrochorte comosa* (Gr) curved and horizontal burrow, preserved as positive epirelief. F. *Lockeia siliquaria* (red arrows), small horizontal trace, seed-like or almond-shaped, preserved as positive epirelief. G. *Palaeophycus tubularis* (Pa), subhorizontal and bifurcated burrows, preserved as a positive epirelief.

### 2.5.6 *Planolites* Nicholson, 1873 – *Planolites beverleyensis* Billings, 1862

**Description:** Straight to slightly curved burrows, horizontal to inclined, sometimes bifurcated, unornamented, and smooth walls. The sediment fill is finer than the host rock fill (Fig. 2.7A). Diameters range from 1 to 1.5 cm; length is variable up to 10 cm. Present epirelief preservation.

**Interpretation:** Vermiform organisms or mollusks bivalves formed these feeding traces (fodinichnia) (Pemberton & Frey 1982, Knaust 2017). *Planolites* are typical of *Scoyenia* ichnofacies in nonmarine settings and have been observed in the Early Permian playa lake rock in Texas, USA (Minter *et al.* 2007); the Late Permian to Middle Triassic fluvial-lacustrine system in North China (Guo *et al.* 2019); the Cretaceous lacustrine marginal environment along the southern coast of Korea (Kim & Pickerill 2003, Kim *et al.* 2005); and the Eocene lake basins in Wyoming, USA (Bohacs *et al.* 2007).

### 2.5.7 *Rusophycus* Hall, 1852 – *Rusophycus isp.*

**Description:** Horizontal, oval, and slightly elongated and bilobated burrow. One specimen was 5 cm long and 3 cm wide, and each lobe was 1.5 cm wide (Fig. 2.7B). The burrow is sculptured with oblique striae, bilaterally symmetrical, and preserved as positive hyporelief.

**Interpretation:** Notostraca brachiopods produced these resting traces (cubichnia) in continental environments (Minter *et al.* 2007, Fillmore *et al.* 2019). In lacustrine settings, *Rusophycus* is typical of *Scoyenia* ichnofacies and has been reported from the late Carboniferous turbiditic glacial lake in northwest Argentina (Buatois & Mángano 1993); the Early Permian playa lake deposits in Texas, USA (Minter *et al.* 2007); the Early Triassic deltaic-lacustrine deposits in northwest Argentina (Melchor *et al.* 2003); the Upper Triassic marginal lacustrine environment in Germany (Schlirf *et al.* 2001); and the Upper Triassic playa-lake system of Coastal Meseta, Morocco (Hminna *et al.* 2020).

Table 2.3 – Palaeoenvironments; trace fossil assemblage; ethology; ichnofacies; and bioturbation index (BI) of the Upper Jurassic–Lower Cretaceous lacustrine succession in the Pastos Bons Formation of the Parnaíba Basin, north-eastern Brazil.

Paleoenvironments	Ichnofossils assemblage	Ethology	Ichnofacies	Bioturbation Index (BI)
	<i>Skolithos</i>	Domichnia/Fodinichnia	<i>Skolithos</i>	B4-B5
	<i>Cochlichnus</i>	Repichnia		
	<i>Lockeia</i>	Cubichnia	<i>Mermia</i>	B2
Lakeshore				
	<i>Agrichnium</i>	Pascichnia		
	<i>Gyrochorte</i>	Fodinichnia/Repichnia		
	<i>Palaeophycus</i>	Domichnia/ Fodinichnia	<i>Scoyenia</i>	B1
	<i>Planolites</i>	Fodinichnia		
	<i>Rusophycus</i>	Cubichnia		

### 2.5.8 *Skolithos* Haldemann, 1840 – *Skolithos linearis* Haldemann, 1840

**Description:** Vertical to subvertical burrows. In the transverse section, burrows are circular to subcircular with a diameter ranging from 0.3 to 3 cm (Fig. 2.7C and D). The burrows are funnel-like in the first centimeter, changing to a cylindrical shape to the longitudinal section base (Fig. 2.7E and F). The burrows present a maximum length of 30 cm, are commonly straight, and are only sometimes curved. These traces present clay-grained, grey to green sediment in the walls, and they exhibit the same lithology of the host rock (sandy) in the core, with incipient concentric lamination.

**Interpretation:** The activity of many different organisms in various phyla, including polychaetas, phoronids, priapulids, anthozoans, crustaceans, holothurians, insects, spiders, and even plant roots, formed these dwellings (domichnia) or feeding traces (fodinichnia) (Chamberlain 1975, Fitzgerald & Barrett 1986, Droser 1991, Gregory *et al.* 2006, Knaust *et al.* 2018). In continental settings, this ichnofossil is typical of *Skolithos* ichnofacies and has been reported from mainly the Lower Triassic deltaic-lacustrine deposits of northwest Argentina



(Melchor *et al.* 2003, Melchor 2004); the Middle Triassic sandflat of playa lake in Argentina (Mancuso *et al.* 2020); the Upper Triassic marginal lacustrine environment in Germany (Schlirf *et al.* 2001); the Upper Triassic lacustrine systems in New Mexico, USA (Gillette *et al.* 2003, Lucas & Lerner 2006); the Upper Jurassic lacustrine littoral environments in the Rocky Mountain region, USA (Hasiotis 2004); the Cretaceous lacustrine marginal environments along the southern coast of Korea (Kim & Pickerill 2003, Kim *et al.* 2005); and the Upper Cretaceous fluvial-lacustrine system in south-western China (Wang *et al.* 2015).

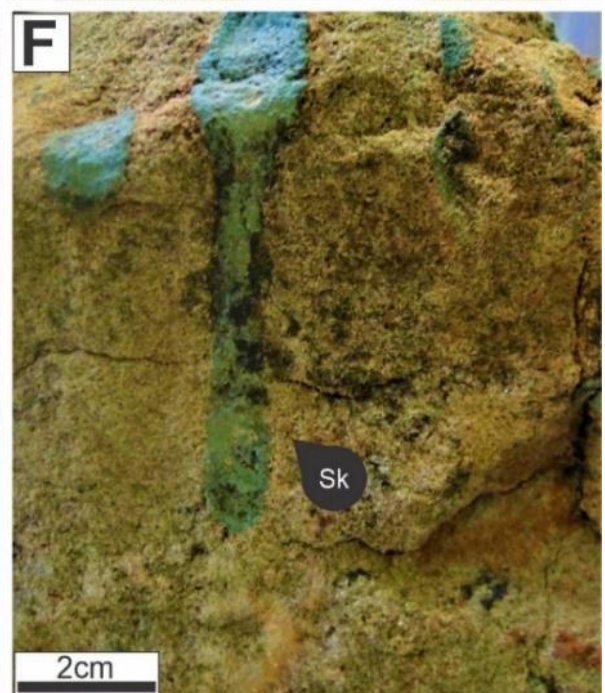
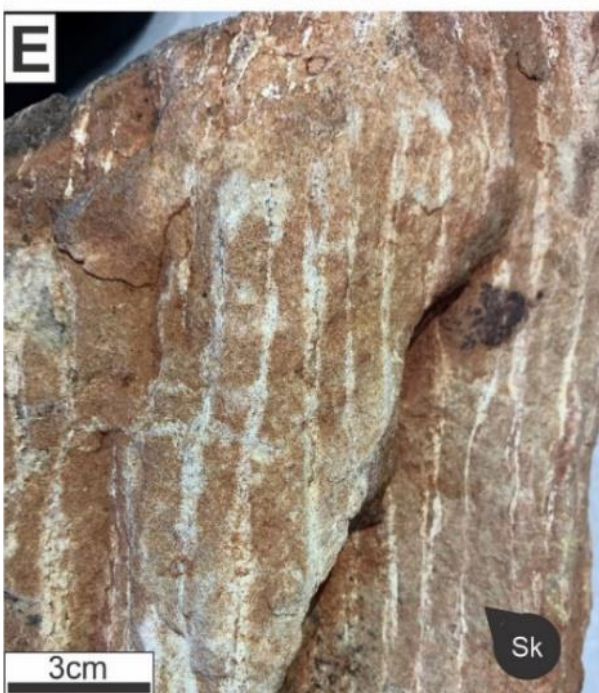
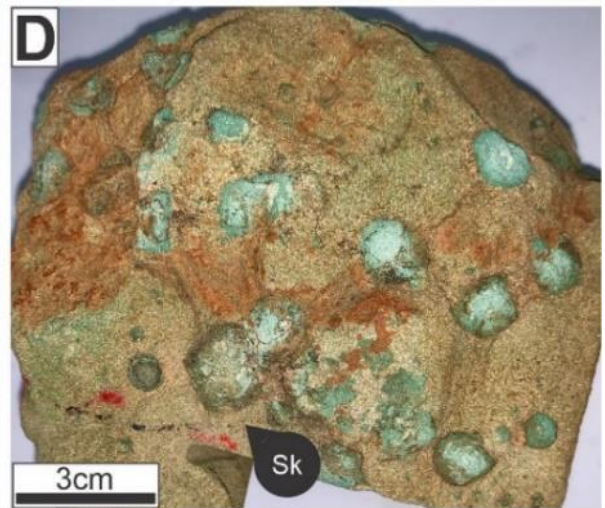
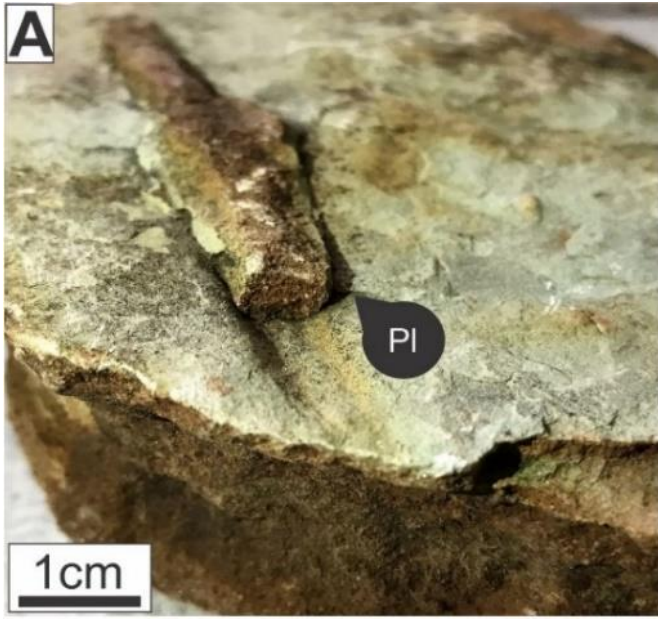


Figure 2.7 – Ichnofossils of Pastos Bons Formation. A. *Planolites beverleyensis* (Pl), subhorizontal, straight burrows with active fill, preserved as positive hyporelief. B. *Rusophycus* isp. (Rs), horizontal, oval, and slightly elongate and bilobate burrow, preserved as positive hyporelief. C. and D. The *Skolithos linearis* show a circular to subcircular structure, in the transverse section, and a grey to green clay wall. E. and F. The *Skolithos linearis* show funnel-shaped apertures grading to a cylindrical shape towards the base, the longitudinal section, and grey to green clay walls.

## 2.6 LACUSTRINE DEPOSITIONAL CYCLES

The lacustrine depositional cycles correspond to cyclic episodes of expansion and contraction of the lacustrine basin. Small-scale shallowing, shallowing/salinization, and coarsening-upward cycles bounded by flooding surfaces are observed in this lacustrine deposit. These cycles are detailed below, according to their facies associations (Fig. 2.8).

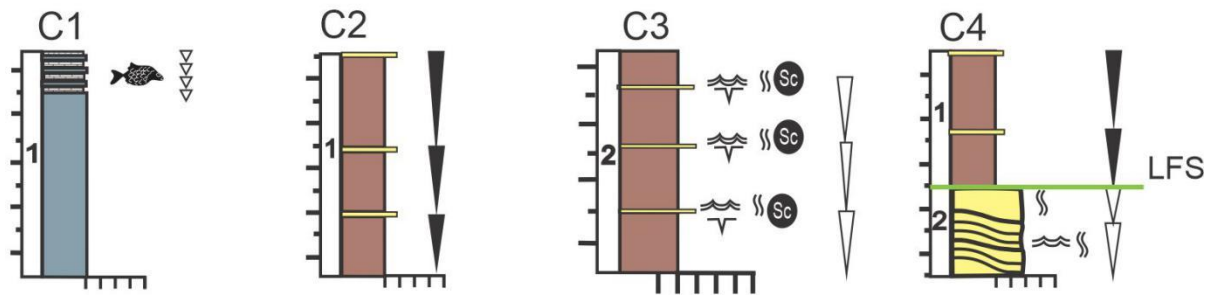
### 2.6.1 Retrogradational-aggradational cycles

Cycle Type 1 (C1) comprises the aggradational shallowing/salinization upward cycles defined by the limestone beds, symmetrically repeated exclusively in FA1. Cycle Type 2 (C2) comprises asymmetrical coarsening-upward cycles composed of meter-scale mudstone and centimeter-scale sandstone beds and exhibits an aggradational pattern exclusively in FA1, extending to lacustrine flooding surface (LFS) and bounded by the maximum flooding surface (MLFS). Cycle Type 3 (C3) is composed of shallowing-upward cycles delimited by meter-scale mudstone with mud cracks, a centimeter-scale limestone with a tepee structure, and a centimeter ichnofossil-bearing sandstone asymmetrically repeated exclusively of FA2, generating an aggradational pattern. Cycle Type 4 (C4) marks the deposition over the LFS, describing coarsening-upward cycles composed of FA1 overlying FA2, FA3, and FA4, forming a retrogradational pattern.

### 2.6.2 Progradational cycles

Cycle Type 5 (C5) marks that the deposition over the Maximum Lacustrine Flooding Surface (MLFS) is composed of meter-scale cross-bedded sandstones of FA3 and FA4 overlying the mudstone beds, forming progradational patterns.

## Retrogradational-aggradational cycles



## Progradational cycles

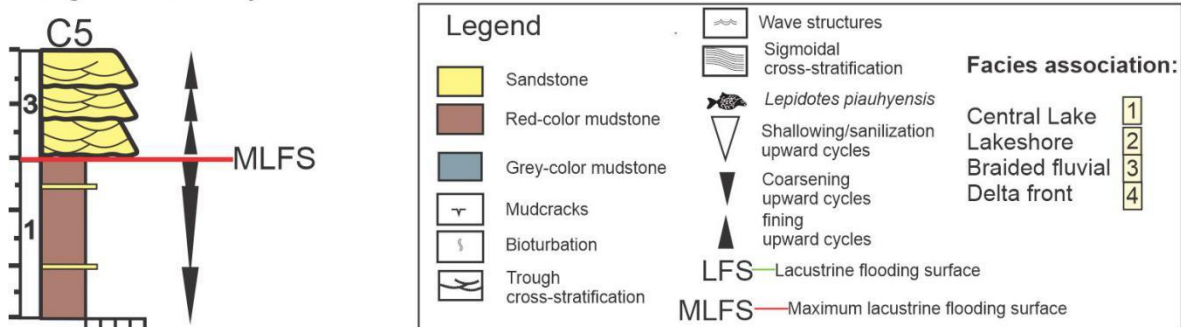


Figure 2.8 – High-frequency lacustrine cycles. Retrogradational-aggradational cycles: Cycle Type 1 and Cycle Type 2 – central lake; Cycle Type 3 – lakeshore and Cycle Type 4 – transition of FA2 (base) and FA1 (top). Progradational cycles; Cycle Type 5 – fluvial and delta front deposition.

## 2.7 PALAEOENVIRONMENTAL RECONSTRUCTION

The facies associations correspond to shallow lacustrine systems, including saline lakes and fluvial-influenced lakes. The fossiliferous shale indicates lower-energy deposition via sediment fall-out in moderately deep to shallow water, with partial anoxia that allowed high organic matter preservation. This horizon sandwiched by nonfossiliferous beds indicates a mass mortality event that may have been influenced by the water column stratification (Cardoso *et al.* 2020). The limestone beds with fibrous calcite mark the lake contraction, which increased the evaporation rate associated with minimum riverine discharge, and the primary gypsum was replaced by fibrous calcite pseudomorphs (Cardoso *et al.* 2019a). Therefore, the high concentration of complete *Lepidotes piauhyensis*, the absence of wave or current marks, and the high preservation grade suggest that the hypolimnion of this lake presented low energy and temperature equal to or lower than 16 °C in a closed, underfilled lacustrine basin (Cardoso *et al.* 2019a, 2020).

The tabular mudstone beds intercalated with sandstone beds correspond to lake expansion, which increased the accommodation potential and was characterized by deposition in the distal portions of the lacustrine basin (Talbot & Allen 1996, Nichols 2009, Renaut & Gierlowski-Kordesch 2010). The lack of fossil and organic-bearing beds suggests that fluvial

discharge generates density currents that oxygenate lake bottoms, therefore, allowed the infaunal organisms colonization and bioturbation preservation (e.g., Melchor 2004).

At this time, the low clastic sediment supply favoured mudstone and limestone formation, and the decrease in the water table allowed reworking of the shoreline sandy sediments by waves and posterior subaerial exposure. This environment corresponds to a low-gradient, wave-dominated environment with subordinate unidirectional currents in the marginal zone of a shallow lacustrine setting in an arid/semiarid climate (Talbot & Allen 1996, Buatois & Mángano 2004, Nichols 2009, Renaut & Gierlowski-Kordesch 2010).

The braided fluvial system was marked by high-energy currents forming gravel bars during channel migration grading to the unidirectional current and the migration of sandy bedforms with sinuous and straight crests under a lower flow regime (Nichols 2009, Miall 2010, 2014). The palaeocurrents indicate migration towards N/NW/NE, characterizing endorheic drainage (e.g., Nichols 2007).

The sigmoidal cross-stratification expresses tractive, subaqueous, unconfined, and homopycnal/hyperpycnal flows that underwent abrupt deceleration when they entered the vast and calm water body of the lacustrine setting (Talbot & Allen 1996, Nichols 2009, Renaut & Gierlowski-Kordesch 2010). The migration of sandy bedforms under unidirectional currents towards N/NW/NE characterizes a delta front connected to a perennial braided fluvial system, which was the feeder of this lacustrine system. The channels of the braided fluvial systems (FA3) flowed into a low-gradient shallow lake, forming a series of deltaic lobes (FA4) (e.g., Ilgar & Nemeč 2005, Fisher *et al.* 2007, Fisher & Nichols 2013, Marensi *et al.* 2020).

### **2.7.1 Underfilled lake ichnofacies model**

The *Mermia* ichnofacies exhibits low ichnodiversity and low-density of traces (B2), records horizontal to subhorizontal locomotion traces produced by annelids (*Cochlichnus anguineus*), and resting traces produced by bivalves (*Lockeia siliquaria*). This ichnofacies presents fine-grained sediments in well-oxygenated, low energy, and permanently subaqueous marginal zones of freshwater lacustrine systems, generally associated with parallel lamination and stratification, ripple cross-lamination, normal grading, tool, flute marks, and soft-sediment deformation structures (Buatois & Mángano 1995, 1998, 2004, Scott *et al.* 2012). Examples of the *Mermia* ichnofacies range from Carboniferous to Recent (Buatois & Mángano 1998 and references therein). In shallow overfilled lacustrine basins, the *Mermia* ichnofacies occurs mainly under delta-fed underflow currents and in fall-out deposits (Buatois & Mángano 2009).

The *Scoyenia* ichnofacies comprises low ichnodiversity of traces and bioturbation index B1 (1–5%). It records horizontal to subhorizontal burrows of mobile detritus feeders (*Gyrochorte comosa* and *Planolites beverleyensis*), dwelling (*Palaeophycus tubularis*), grazing (*Agrichnium* isp.), and resting traces (*Rusophycus* isp.) produced by annelids, arthropods, bivalves, and vermiform organisms. These ichnofossils are related to FA2, which delimits the lake's marginal areas, and was associated with the decreased water table and reworking of substrate by fair-weather waves. The *Scoyenia* ichnofacies has been recorded in protected lake margins, in low-energy zones, that experimented the subaerial exposure, periodically, useful to delineate marginal lacustrine facies in sedimentologic studies (Seilacher 1963, 1967, Frey & Pemberton 1984, 1987, Buatois & Mángano 1995, 1998, 2004, 2007, 2009).

The continental *Skolithos* ichnofacies occurs under conditions to the well-oxygenate and higher-energy lake margins, such as wave or current-dominated shorelines (Melchor et al. 2003; Buatois and Mángano, 1995; 1998, 2004, 2007, 2009; Scott et al. 2012; Mancuso et al. 2020). This ichnofacies displays low ichnodiversity and a higher abundance of traces B4-B5 (60–100%) comprising records simple vertical burrows of detritus-feeders or dwelling tubes likely produced by annelids, arthropods, or vermiform organisms (*Skolithos linearis*). The bioturbation index (B4-B5) obliterated other sedimentary structures originating the Sb facies, which delimits the high energy lake's marginal areas (FA2), and was associated with the current-influenced shorelines, caused by the ephemeral fluvial inflows (Cm facies).

## 2.7.2 Interpretation of the staking pattern

The Transgressive System Tract (TST) comprises retrogradational and aggradational cycles (Fig. 2.9A) and represents the record of the pulse of thermal subsidence and creation of accommodation space for lacustrine deposition. C1 corresponds to the autogenic cycles defined by fibrous calcite that suggest lake contraction, a high evaporation rate, a low siliciclastic supply, and low energy in the deepest portions of the lake. C3 reflects the autogenic cycle of a decrease in the water table and subsequent reworking by waves and subaerial exposure in the lake margins. The lake margin is a typical environment of well-developed soft-ground ichnofossils that are useful to delineate the brief periods of nondeposition (Buatois & Mángano 2004, 2007, 2009). A lacustrine flooding surface (C4) marks when a thermal subsidence pulse expanded the lake during periods of increase of the water table and corresponds to C2 deposition overlying the lakeshore deposits (Fig. 2.9C). This depositional cycle can explain the

rise in the water table of a lake, and the expansion of lake margins is mainly provoked by a subsidence rate.

The Highstand System Tract (HST) comprises the progradational cycle (Fig. 2.9B) and represents the record of sedimentation during the lake's maximum expansion (e.g., Bohacs *et al.* 2000). Under HST conditions, the thermal subsidence pulse ceased, and braided fluvial channels (FA3) flowed into the low-gradient shallow lake, forming a series of deltaic lobes (FA4) (e.g., Ilgar & Nemeč 2005, Fisher *et al.* 2007, Fisher & Nichols 2013, Marensi *et al.* 2020) over the MLFS. This depositional cycle can explain the lowering of the water table, and the contraction of lake margins is mainly provoked by increased fluvial sediment discharge into the lacustrine basin.

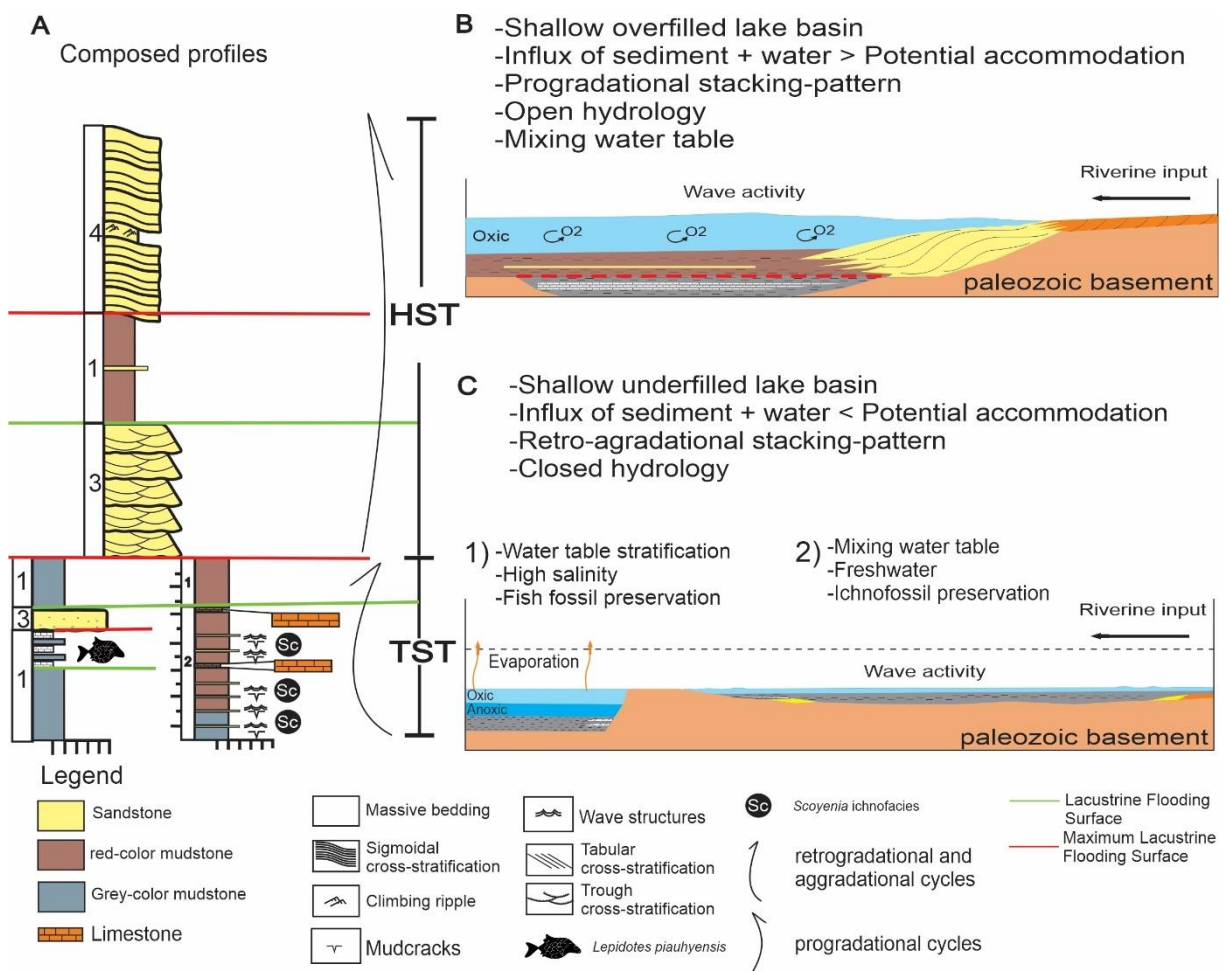


Figure 2.9 – A. Composite profile, sequence stratigraphic stages of the lacustrine system, and the depositional cycles, retrogradational and aggradational cycles, compose the TST; and the progradational cycles compose the HST. B. Overfilled Lake phase. C. Underfilled lake phase.

### 2.7.3 Lacustrine basin evolution

A thermal subsidence stage affected a great part of the Parnaíba Basin during the Jurassic–Cretaceous. This event resulted from the drawdown of isotherms after cooling of the voluminous subsurface basaltic magma intrusions related to the CAMP (fig. 2.10A), which induced crustal loading and flexural effects (Klößing *et al.* 2018, Cardoso *et al.* 2019a). The thermal subsidence pulse, related to the post-CAMP phase, was responsible for the formation and evolution of this Upper Jurassic–Lower Cretaceous lake system in north-eastern Brazil (Cardoso *et al.* 2017, 2019a).

During the TST, many closed lake basins were created along the Parnaíba Basin, separated by palaeotopography. These were underfilled lacustrine basins characterized by accommodation rates exceeding the sediment input (e.g., Carrol & Bohacs 1999, Bohacs *et al.* 2000, 2007) (Fig. 2.10B). In C1, the lack of unidirectional and wave sedimentary structures and the presence of well-preserved *Lepidotes piauhyensis* suggest low-energy anoxic conditions related to the deepest portions of the lake under an arid/semiarid climate, correlated with the fossiliferous Muzinho shales (Cardoso *et al.* 2019a, 2020).

However, the adjacent subsiding areas allowed the deposition of C3, reflecting well-oxygenated lakes and the formation of the NW-trending drainage and consequent riverine discharge and wave activity in the lakeshore, generating a retrogradational-aggradational stacking pattern and forming a freshwater lacustrine basin. This freshwater lake was less stressed, allowing epifaunal and infaunal communities, evidenced by the ichnofossil-bearing beds. The *Scoyenia* ichnofacies develops in low-energy lake margin areas, the *Mermia* ichnofacies is present in permanent subaqueous lacustrine zones on distal sigmoidal lobes, the *Skolithos* ichnofacies represents sediments deposited in relatively high-energy lacustrine environments, such as unidirectional current-influenced shorelines (Fig. 2.10B) (Buatois and Mángano, 2004, 2007, 2009; Scott *et al.* 2012).

The progression of thermal subsidence caused the expansion of the lake during periods of transgression (TST) marked by the lacustrine flooding surface (C4) that is overlain by C2 in the central lake, forming a retrogradational stacking pattern. The end of thermal subsidence is represented by the MLFS (C5). This event promoted an increase in riverine discharge (sediment plus water) exceeding the potential accommodation, leading to overfilled lake deposits in the HST (e.g., Carrol & Bohacs 1999, Bohacs *et al.* 2000, 2007) (Fig. 2.10C). Therefore, the coarsening-upward trend shows decreased accommodation potential and increased fluvial



sediment input, typically associated with a fluvial-dominated lacustrine system (e.g., Carrol & Bohacs 1999, Bohacs *et al.* 2000, 2007).

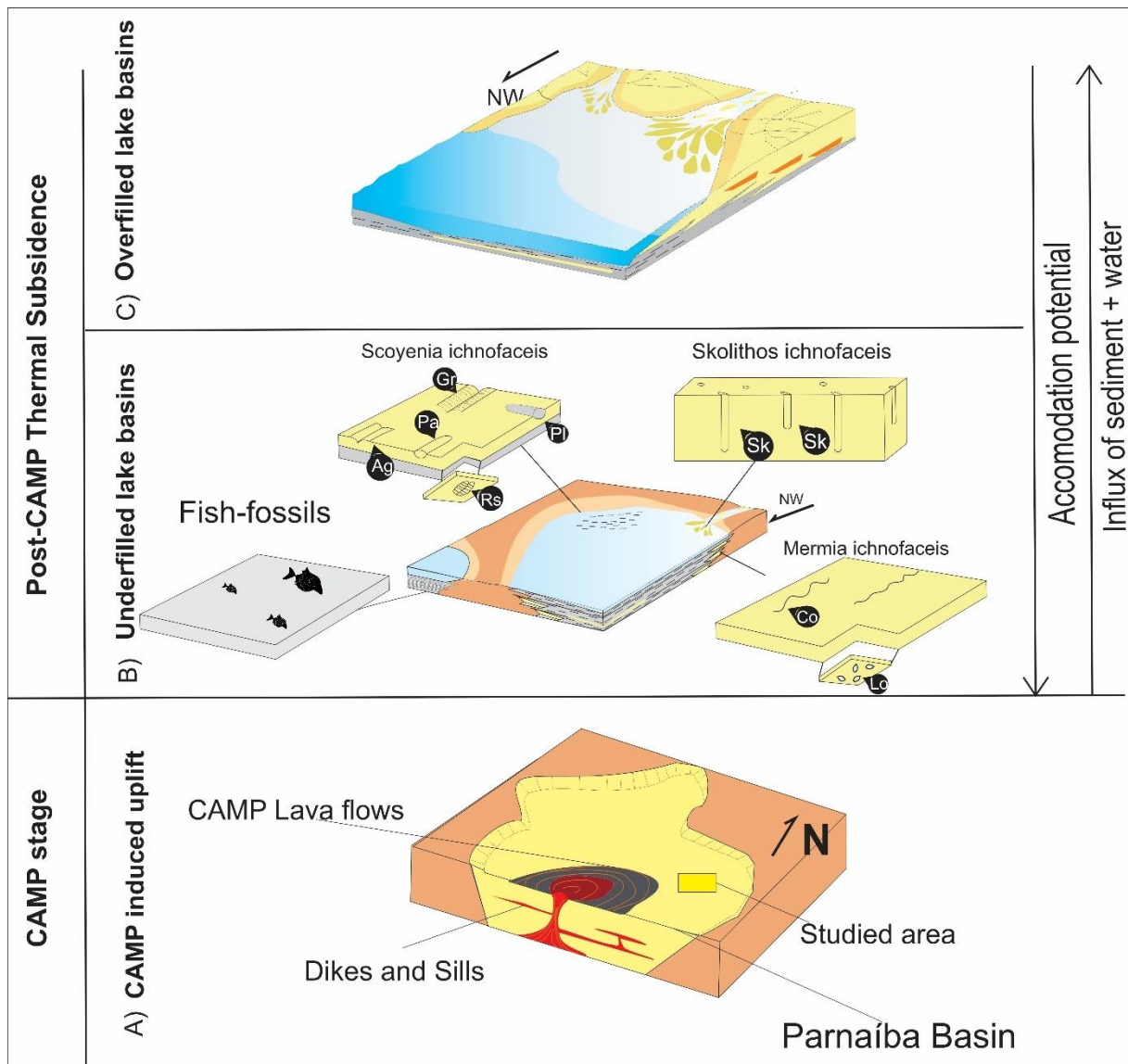


Figure 2.10 – A. CAMP deposition dikes and sills extension in Parnaíba Basin, causing the CAMP induced uplift; adapted from Nogueira *et al.* 2021; B. Underfilled Lacustrine basins with retrogradational stacking pattern. Ichnofacies model. *Mermia* ichnofacies: Co: *Cochlichnus anguineus*. Lo: *Lockeia siliquaria*. *Scoyenia* ichnofacies: Ag: *Agrichnium* isp. Gr: *Gyrochorte comosa*; Pa: *Palaeophycus tubularis*; Pl: *Planolites beverleyensis*; Rs: *Rusophycus* isp.; *Skolithos* ichnofacies: Sk: *Skolithos linearis*. Fish-fossils of *Lepidotes piauhyensis*. C. Overfilled lacustrine basin phase with a progradational stacking pattern.

## 2.8 CONCLUSIONS

The Post-CAMP thermal subsidence stage in the Parnaíba Basin during the Jurassic – Cretaceous resulted of the voluminous subsurface intrusions in the northern South American Platform during Jurassic times induced crustal loading and flexural effects probably affected a

great part of the Parnaíba Basin. This geological history is better indicated by the Upper Jurassic - Lower Cretaceous lacustrine succession of the Pastos Bons Formation. This stratigraphic unit consists in central lake (FA1), lakeshore (FA2), braided fluvial (FA3) and delta front (FA4) deposits. In this shallow fluvio-lacustrine environment, the lakeshore concentrates the ichnological content. The *Scoyenia* ichnofacies develops in low-energy lake-margin areas; the *Mermia* ichnofacies is present in permanent subaqueous lacustrine zones on distal sigmoidal lobes, and the *Skolithos* ichnofacies represents the sediments deposited in relatively high-energy lacustrine environments, such as the wave or current-dominated shorelines. In the base of this succession, four cycles define a retrogradational and aggradational stratal stacking pattern composing the TST, therefore forming the underfilled lake basin characterized by fossiliferous lake center (FA1) and lake margin ichnofossil-bearing beds (FA2); on the top, over the maximum lacustrine flooding surface, one cycle indicate the progradational stratal stacking pattern, constituting the HST, setting up the overfilled lake basin characterized by cross-laminated sandstone of the fluvio-deltaic system (FA3 and FA4).

### 3 CONCLUSÕES

A transição Triássico-Jurássico é marcada pela fragmentação do supercontinente Gondwana e consequente abertura do Oceano Atlântico. Esse evento foi acompanhado por um intenso magmatismo, denominado como Província Magmática do Atlântico Central (CAMP), uma das mais significativas LIPs (Grande Província Ígnea). Os registros do CAMP são geralmente basaltos toleíticos que afloram na América do Norte, Europa, África e na América. No Brasil, o CAMP é registrado nas bacias sedimentares do Solimões e Amazonas; na Bacia do Parecis; na Bacia Lavras da Mangabeira e na Bacia do Parnaíba.

Na Bacia do Parnaíba, esse evento é registrado pela Formação Mosquito, que apresenta rochas vulcanossedimentares, evidenciando fluxo de lava em superfície. Entretanto, uma grande quantidade de magma basáltico se instalou também em subsuperfície causando entumescimento da crosta continental e consequentes soerguimentos. O estágio pós-CAMP na Bacia do Parnaíba estende-se pelo Jurássico – Cretáceo e é caracterizado por amplas áreas que passaram por subsidência térmica, resultado do resfriamento do magma basáltico e diminuição das isotermas, que foi capaz de induzir efeitos de flexão na crosta que afetaram uma extensa área da Bacia do Parnaíba.

A história geológica do estágio pós-CAMP é representada pela sucessão lacustre do Jurássico Superior - Cretáceo Inferior da Formação Pastos Bons. Esta unidade estratigráfica consiste em depósitos de lago central (AF1), margem do lago (AF2), fluvial entrelaçado (AF3) e frente delta (AF4). Nesse ambiente flúvio-lacustre raso, a margem do lago (AF2) concentra o conteúdo icnológico.

A icnofácies *Scoyenia* se desenvolve em áreas de baixa energia nas margens do lago que experimentam rebaixamento periódico da espessura da coluna d'água e posterior exposição subaérea; a icnofácies *Mermia* está presente em zonas lacustres subaquáticas permanentes em lobos sigmoidais distais; e a icnofácies *Skolithos* representam os sedimentos depositados em ambientes lacustres de energia relativamente alta, como linhas de costa dominadas por ondas ou frentes deltaicas.

Na porção inferior da sucessão, quatro ciclos deposicionais foram identificados; eles apresentam padrão de empilhamento estratal retrogradacional e agradacional e compõem o trato do sistema transgressivo (TST), formando bacias lacustres do tipo *underfilled* que apresentam as principais ocorrências de conteúdo fossilífero (AF1) e icnofossilífero (AF2). Na porção intermediária e superior, a subsidência térmica atinge seu nível máximo, representado pela superfície de inundação máxima lacustre (MLFS), e um ciclo deposicional se estabelece

indicando o padrão de empilhamento estratal progradacional, engendrando o trato do sistema de máxima inundação (HST), configurando a bacia lacustre do tipo *overfilled*, caracterizado pelo domínio de arenito com estratificações cruzadas que constituem o sistema flúvio-deltaico (AF3 e AF4).

## REFERÊNCIAS

- Abrantes Jr. F. R., Nogueira A. C. R., Andrade L. S., Bandeira J., Soares J. L., Medeiros R. S. P. 2019. Register of increasing continentalization and paleoenvironmental changes in the west-central Pangaea during the Permian-Triassic, Parnaíba Basin, Northern Brazil. *Journal of South American Earth Sciences*, **93**: 294–312. Disponível em: <https://www.sciencedirect.com/science/article/abs/pii/S0895981118304127?via%3Dihub>. Acesso em: 27 jul. 2021.
- Aguiar G. A. 1969. *Bacia do Maranhão*: geologia e possibilidades de petróleo. Belém, Petrobrás. p. 55–106. (Relatório Técnico, n. 371).
- Ambrosetti E., Martini I., Sandrelli F. 2017. Shoal-water deltas in high-accommodation settings: Insights from the lacustrine Valimi Formation (Gulf of Corinth, Greece). *Sedimentology*, **64**(2): 425–452. Disponível em: <https://onlinelibrary.wiley.com/doi/abs/10.1111/sed.12309>. Acesso em: 02 ago. 2021.
- Andrade L. S., Nogueira A. C. R., Silva Jr J. B. C. 2014. Evolução de um sistema lacustre árido permiano, parte superior da Formação Pedra de Fogo, borda oeste da Bacia do Parnaíba. *Geologia USP: Série Científica*, **14**(4): 39–60. Disponível em: <https://www.revistas.usp.br/guspsc/article/view/95920>. Acesso em: 28 jul. 2021.
- Baldwin C. T. 1974. The control of mud crack patterns by small gastropod trails. *Journal of Sedimentary Research*, **44**(3): 695–697. Disponível em: <https://pubs.geoscienceworld.org/sepm/jsedres/article-abstract/44/3/695/96759/The-control-of-mud-crack-patterns-by-small>. Acesso em: 31 jul. 2021.
- Bayet-Goll A., Carvalho C. N. de, Mahmudy-Gharaei M. H., Nadaf R. 2015. Ichnology and sedimentology of a shallow marine Upper Cretaceous depositional system (Neyzar Formation, Kopet-Dagh, Iran): Palaeoceanographic influence on ichnodiversity. *Cretaceous Research*, **56**: 628–646. Disponível em: <https://www.sciencedirect.com/science/article/abs/pii/S0195667115300318>. Acesso em: 28 jul. 2021.
- Bernardes-de-Oliveira M. E. C., Mohr B., Dino R., Guerra-Sommer M., Garcia M. J., Sucerquia P. A. 2007. *As flores mesofíticas brasileiras no cenário paleoflorístico mundial*. Rio de Janeiro, Editora Interciência, 40p.
- Boeira J. B. & Guimarães Netto R. 1987. Novas considerações sobre os icnofósseis da Formação Rio Bonito, Cachoeira do Sul, RS. *Acta Geologica Leopoldensia*, **11**: 105–140.
- Bohacs K. M. 1999. Sequence stratigraphy of lake basins; unraveling the influence of climate and tectonics. *American Association of Petroleum Geologists Bulletin*, **83**: 1878–1898.
- Bohacs K. M., Carroll A. R., Neal J. E., Mankiewicz P. J. 2000. Lake-basin type, source potential, and hydrocarbon character: an integrated sequence stratigraphic – geochemical framework. In: Gierlowski-Kordesch E., Kelts K. (Eds.). *Lake Basins Through Space and Time*, Oklahoma, AAPG, p. 3–37. (American Association of Petroleum Geologists Studies in Geology, 46)

Bohacs K. M., Carroll A. R., Neal J. E. 2003. Lessons from large lake systems – thresholds, nonlinearity, and strange attractors. *In: Chan M. A. & Archer A. W. (eds.). Extreme Depositional Environments: Mega End Members in Geologic Time.* Boulder, Geological Society of America, p. 75–90. (Special Paper, v. 370).

Bohacs K. M., Hasiotis S., Demko T. 2007. Continental ichnofossils of the Green River and Wasatch formations, Eocene, Wyoming: a preliminary survey, proposed relation to lake-basin type, and application to integrated paleoenvironmental interpretation. *The Mountain Geologist*, **44**(2): 79–108.

Brazil J. J. 1948. *Zona Sul da Bacia do Maranhão.* Rio de Janeiro, Conselho Nacional de Petróleo, p. 71–78 (Relatório Interno).

Buatois L. A. & Mángano M. G. 2009. Applications of ichnology in lacustrine sequence stratigraphy: potential and limitations. *Palaeogeography, Palaeoclimatology, Palaeoecology*, **272**(3–4): 127–142. Disponível em: <https://www.sciencedirect.com/science/article/abs/pii/S0031018208005828?via%3Dihub>. Acesso em: 28 jul. 2021.

Buatois L. A. & Mángano M. G. 2016. Ediacaran ecosystems and the dawn of animals. *In: Buatois L. A. & Mángano M. G. The trace-fossil record of major evolutionary events.* Springer, Dordrecht, Springer, p. 27–72.

Buatois L. A. & Mángano M. G. 2004. Ichnology of fluvio-lacustrine environments: animal substrate interactions in freshwater ecosystems. *In: McIlroy D. (ed.). The application of ichnology to palaeoenvironmental and stratigraphic analysis.* London, Geological Society London, p. 311–333. (Special Publication n. 228).

Buatois L. A. & Mángano M. G. 2011. *Ichnology: organism–substrate interactions in space and time.* Cambridge, Cambridge University Press.

Buatois L. A. & Mángano M. G. 2007. Invertebrate ichnology of continental freshwater environments. *In: Miller III W. (ed.). Trace fossils: concepts, problems, prospects.* Amsterdam, Elsevier, p. 285–323.

Buatois L. A. & Mángano M. G. 1995. The paleoenvironmental and paleoecological significance of the lacustrine Mermia ichnofacies: an archetypical subaqueous nonmarine trace fossil assemblage. *Ichnos*, **4**: 151–161. Disponível em: <https://www.tandfonline.com/doi/abs/10.1080/10420949509380122>. Acesso em: 28 jul. 2021.

Buatois L. A. & Mángano M. G. 1998. Trace fossil analysis of lacustrine facies and basins. *Palaeogeography, Palaeoclimatology, Palaeoecology*, **140**(1–4): 367–382. Disponível em: <https://www.sciencedirect.com/science/article/abs/pii/S0031018298000200?via%3Dihub>. Acesso em: 28 jul. 2021.

Buatois L. A. & Mángano M. G. 2002. Trace fossils from Carboniferous floodplain deposits in western Argentina: implications for ichnofacies models of continental environments. *Palaeogeography, Palaeoclimatology, Palaeoecology*, **183**(1–2): 71–86. Disponível em: <https://www.sciencedirect.com/science/article/abs/pii/S003101820100459X?via%3Dihub>. Acesso em: 28 jul. 2021.

- Buatois L. A., Guimarães Netto R., Mángano M. G., Balistieri P. R. M. N. 2006. Extreme freshwater release during the late Paleozoic Gondwana deglaciation and its impact on coastal ecosystems. *Geology*, **34**(12): 1021–1024. Disponível em: <https://pubs.geoscienceworld.org/gsa/geology/article-abstract/34/12/1021/129424/Extreme-freshwater-release-during-the-late?redirectedFrom=fulltext>. Acesso em: 31 jul. 2021.
- Beurlen K. 1954. Um novo gênero de conchostráceo da família Limnadiidae. *Notas Preliminares e Estudos*. Rio de Janeiro, Departamento Nacional de Produção Mineral DNPM, n. 83, p. 23–28.
- Bromley R. & Asgaard U. 1979. Triassic freshwater ichnocoenose from Carlsberg fjord, East Greenland. *Palaeogeography, Palaeoclimatology, Palaeoecology*, **28**: 39–80. Disponível em: <https://www.sciencedirect.com/science/article/abs/pii/0031018279901123>. Acesso em: 05 ago. 2021.
- Bromley R. G. 1996. *Trace fossils*. Biology, taphonomy and applications. 2nd ed. London, Glasgow, Weinheim, New York, Tokyo, Melbourne, Madras, Chapman & Hall. 361 p.
- Caldasso A. L. S. 1978. *O problema Pastos Bons na estratigrafia da Bacia do Parnaíba*. Recife, Companhia de Pesquisa de Recursos Minerais. Não paginado (Relatório Interno).
- Caldasso A. D. S. 1978. *A sedimentação mesozóica e seu relacionamento com a evolução geomorfológica da bacia do Parnaíba*. Recife, CPRM.
- Campbell D. F. 1949. *Bacia do Maranhão*. Rio de Janeiro, Conselho Nacional de Petróleo, p. 68–74. (Relatório Interno 153).
- Caputo M. V. 1984. *Stratigraphy, tectonics, paleoclimatology and paleogeography of Northern Basins of Brazil*. PhD Thesis, University of California, Santa Barbara, USA, 583 p.
- Capriolo M., Marzoli A., Aradi L. E., Callegaro S., Dal Corso J., Newton R. J., Mills B. J. W., Bartoli O., Baker D. R., Youbi N., Remusat L., Spiess R., Szabó C. 2020. Deep CO<sub>2</sub> in the end-Triassic Central Atlantic Magmatic Province. *Nature communications*, **11**(1): 1–11. Disponível em: <https://www.nature.com/articles/s41467-020-15325-6>. Acesso em: 02 ago. 2021.
- Cardoso A. R., Nogueira A. C. R., Rabelo C. E. N. 2019a. Lake cyclicality as response to thermal subsidence: a post-CAMP scenario in the Parnaíba Basin, NE Brazil. *Sedimentary Geology*, **385**: 96–109. Disponível em: <https://www.sciencedirect.com/science/article/abs/pii/S0037073819300703?via%3Dihub>. Acesso em: 28 jul. 2021.
- Cardoso A. R., Nogueira A. C. R., Abrantes Jr. F. R. A., Rabelo C. E. N. 2017. Mesozoic lacustrine system in the Parnaíba Basin, northeastern Brazil: paleogeographic implications for West Gondwana. *Journal of South American Earth Sciences*, **74**: 41–53. Disponível em: <https://www.sciencedirect.com/science/article/abs/pii/S0895981116301882?via%3Dihub>. Acesso em: 28 jul. 2021.

Cardoso A. R., Nogueira A. C. R., Rabelo C. E. N., Soares J. L., Góes A. M. 2019b. Multi-approach provenance in stratigraphy: implications for the Upper Mesozoic evolution of the Parnaíba Basin, NE Brazil. *Journal of South American Earth Sciences*, **96**: 102386.

Disponível em:

<https://www.sciencedirect.com/science/article/abs/pii/S0895981119302780?via%3Dihub>.

Acesso em: 28 jul. 2021.

Cardoso A. R., Romero G. R., Osés G. L., Nogueira A. C. R. 2020. Taphonomy of lacustrine fish fossils of the Parnaíba Basin, northeastern Brazil: Spatial and causative relations of Konservat Lagerstätten in West Gondwana during Jurassic-Cretaceous. *Palaeogeography, Palaeoclimatology, Palaeoecology*, **542**: 109602. Disponível em:

<https://www.sciencedirect.com/science/article/abs/pii/S0031018219309009?via%3Dihub>.

Acesso em: 28 jul. 2021.

Carroll A. R., Bohacs K. M. 1999. Stratigraphic classification of ancient lakes: balancing tectonic and climatic controls. *Geology*, **27**: 99–102. Disponível em:

<https://pubs.geoscienceworld.org/gsa/geology/article-abstract/27/2/99/207139/Stratigraphic-classification-of-ancient-lakes?redirectedFrom=fulltext>. Acesso em: 28 jul. 2021.

Catuneanu O., Abreu V., Battacharya J. P., Blum M. D., Dalrymple R. J., Eriksson P. G., Fielding C. R., Fisher W. L., Galloway W. E., Gibling M. R., Giles K. A., Holbrook J. M., Jordan R., Kendall C. G. S. C., Macurda B., Martinsen O. J., Miall A. D., Neal J. E., Nummedal J., Pomar L., Posamentier H. W., Pratt B. R., Sarg J. F., Sharley K.W., Steel R. J., Strasser A., Tucker M. E., Winker C. 2009. Towards the standardization of sequence stratigraphy. *Earth-Science Reviews*, **92** (1–2): 1–33. Disponível em:

<https://www.sciencedirect.com/science/article/abs/pii/S0012825208001104?via%3Dihub>.

Acesso em: 28 jul. 2021.

Catuneanu O. 2019. Scale in sequence stratigraphy. *Marine and Petroleum Geology*, **106**: 128–159. Disponível em:

<https://www.sciencedirect.com/science/article/abs/pii/S026481721930176X>. Acesso em: 02 ago. 2021.

Chamberlain C. K. 1975. Recent lebensspuren in nonmarine aquatic environments. In: Frey R. W. *The study of trace fossils*. Berlin, Springer, p. 431–458.

Collinson J. D. & Reading H. G. 1996. *Sedimentary environments: Processes, facies and stratigraphy*. Alluvial Sediments. Oxford, Blackwell Scientific Publications, p. 37–82.

Cunha F. B. & Carneiro R. G. 1972. Interpretação fotogeológica do centro-oeste da Bacia do Maranhão. In: SBG, 26º Congresso Brasileiro de Geologia. *Anais[...]*, Belém, v. 3, p. 64–80.

Daly M. C., Andrade V., Barousse C. A., Costa R., Mcdowell K., Piggott N., Poole A. J., 2014. Brasileiro crustal structure and the tectonic setting of the Parnaíba basin of NE Brazil: results of a deep seismic reflection profile. *Tectonics*, **33** (11): 1–19. Disponível em:

<https://agupubs.onlinelibrary.wiley.com/doi/10.1002/2014TC003632>. Acesso em: 28 jul. 2021.



Daly M. C., Fuck R. A., Julià J., Macdonald D. I. M., Watts A. B. 2018. *Cratonic basin formation: a case study of the Parnaíba Basin of Brazil*. London, Geological Society of London, p. 1–15. Disponível em:

<https://pubs.geoscienceworld.org/books/book/2149/chapter/120159933/Cratonic-basin-formation-a-case-study-of-the>. Acesso em: 28 jul. 2021. (Special Publications, 472)

Droser M. L. 1991. Ichnofabric of the Paleozoic Skolithos ichnofacies and the nature and distribution of Skolithos piperock. *Palaios*, **6**(3): 316–325. Disponível em:

<https://pubs.geoscienceworld.org/sepm/palaios/article-abstract/6/3/316/100257/Ichnofabric-of-the-Paleozoic-Skolithos-ichnofacies?redirectedFrom=fulltext>. Acesso em: 05 ago. 2021.

Ekdale A. A., Bromley R. G., Pemberton S. G. 1984. *Ichnology: trace fossils in sedimentology and stratigraphy*. Houston, Soc. Econ. Paleontologists & Mineralogists, 317 p. (SEPM Short Course Notes 15)

Fambrini G. L., Neumann V. H. M. L., Barros C. L. B., Silva S. M. O. A., Galm P. C., Menezes Filho J. A. B. 2013. Stratigraphic analysis of Brejo Santo Formation, Araripe Basin, Northeast Brazil: paleogeographic implications. *Geologia USP: série científica*, São Paulo, **13**(4): 3–28. Disponível em: <https://www.revistas.usp.br/guspssc/article/view/78912>. Acesso em: 28 jul. 2021.

Fisher J. A. & Nichols G. J. 2013. Interpreting the stratigraphic architecture of fluvial systems in internally drained basins. *Journal of the Geological Society*, **170**(1): 57–65. Disponível em: <https://pubs.geoscienceworld.org/jgs/article-abstract/170/1/57/144650/Interpreting-the-stratigraphic-architecture-of?redirectedFrom=fulltext>. Acesso em: 31 jul. 2021.

Fisher J. A., Nichols G. J., Waltham D. A. 2007. Unconfined flow deposits in distal sectors of fluvial distributary systems: examples from the Miocene Luna and Huesca Systems, northern Spain. *Sedimentary Geology*, **195**(1–2): 55–73. Disponível em:

<https://www.sciencedirect.com/science/article/abs/pii/S0037073806002065?via%3Dihub>. Acesso em: 28 jul. 2021.

Fitzgerald P. G. & Barrett P. J. 1986. Skolithos in a Permian braided river deposit, southern Victoria Land, Antarctica. *Palaeogeography, Palaeoclimatology, Palaeoecology*, **52**(3–4): 237–247. Disponível em:

<https://www.sciencedirect.com/science/article/abs/pii/0031018286900490>. Acesso em: 05 ago. 2021.

Frey R. W., Pemberton S. G., Fagerstrom J. A. 1984. Morphological, ethological, and environmental significance of the ichnogenera *Scoyenia* and *Ancorichnus*. *Journal of Paleontology*, **58**(2): 511–528. Disponível em:

<https://pubs.geoscienceworld.org/jpaleontol/article/58/2/511/81803/Morphological-ethological-and-environmental>. Acesso em: 02 ago. 2021.

Frey R. W. & Pemberton S. G. 1987. The *Psilonichnus* ichnocoenose, and its relationship to adjacent marine and nonmarine ichnocoenoses along the Georgia coast. *Bulletin of Canadian Petroleum Geology*, **35**(3): 333–357. Disponível em:

<https://pubs.geoscienceworld.org/cspg/bcpbg/article-abstract/35/3/333/57447/THE-PSILONICHNUS-ICHNOCOENOSE-AND-ITS-RELATIONSHIP?redirectedFrom=PDF>. Acesso em: 02 ago. 2021.

- Gallo V. 2005. Redescription of *Lepidotes Piauhyensis* Roxo and Löefgren, 1936 (Neopterygil, Seminotiformes, Semionotidae) from the Late Jurassic-Early Cretaceous of Brazil. *Journal of Vertebrate Paleontology*, **25**(4): 757-769. Disponível em: <https://www.jstor.org/stable/4524504>. Acesso em: 02 ago. 2021.
- Gierlowski-Kordesch E. H. 2010. Lacustrine carbonates. *Developments in Sedimentology*, **61**: 1–101. Disponível em: <https://www.sciencedirect.com/science/article/pii/S0070457109061019?via%3Dihub>. Acesso em: 28 jul. 2021.
- Gierlowski-Kordesch E. H. & Park L. E. 2004. Comparing species diversity in the modern and fossil record of lakes. *The Journal of Geology*, **112**(6): 703–717. Disponível em: <https://www.journals.uchicago.edu/doi/abs/10.1086/424578>. Acesso em: 28 jul. 2021.
- Gibert J. M. & Benner J. S. 2002. The trace fossil "Gyrochorte": ethology and paleoecology. *Revista Espanola de Paleontologia*, **17**(1): 1–12.
- Gillette L., Pemberton S. G., Sarjeant W. 2003. A Late Triassic invertebrate ichnofauna from Ghost Ranch, New Mexico. *Ichnos*, **10**(2–4): 141–151. Disponível em: <https://www.tandfonline.com/doi/abs/10.1080/10420940390255493>. Acesso em: 28 jul. 2021.
- Gluszek A. 1995. Invertebrate trace fossils in the continental deposits of an Upper Carboniferous coal-bearing succession, Upper Silesia, Poland. *Studia Geologica Polonica*, **108**: 171–202.
- Góes A. M. O., Souza J. M. P., Teixeira, L. B. 1990. Estágio exploratório e perspectivas petrolíferas da Bacia do Parnaíba. *Boletim de Geociências da Petrobras*, **4**(1): 55–64.
- Góes A. M. O. & Feijó F. J. 1994. A Bacia do Parnaíba. *Boletim de Geociências da Petrobras*, **15**(2): 57–67.
- Goldring R., Pollard J. E., Radley J. D. 2005. Trace fossils and pseudofossils from the Wealden strata (non-marine Lower Cretaceous) of southern England. *Cretaceous Research*, **26**(4): 665–685. Disponível em: <https://www.sciencedirect.com/science/article/abs/pii/S0195667105000686>. Acesso em: 31 jul. 2021.
- Gregory M. R., Campbell K. A., Zuraida R., Martin A. J. 2006. Plant traces resembling *Skolithos*. *Ichnos*, **13**(4): 205–216. Disponível em: <https://www.tandfonline.com/doi/abs/10.1080/10420940600843617>. Acesso em: 05 ago. 2021.
- Guimarães Netto R., Balistieri P. R. M. N., Lavina E. L., Silveira D. M. 2009. Ichnological signatures of shallow freshwater lakes in the glacial Itarare Group (Mafra Formation, Upper Carboniferous e Lower Permian of Parana Basin, S Brazil). *Palaeogeography, Palaeoclimatology, Palaeoecology*, **272**(3–4): 240–255. Disponível em: <https://www.sciencedirect.com/science/article/abs/pii/S0031018208006135?via%3Dihub>. Acesso em: 28 jul. 2021.

Guimarães Netto R., Tognoli F. M. W., Gandini R., Lima J. H. D., Gibert J. M. 2012. Ichnology of the Phanerozoic deposits of southern Brazil: Synthetic review. *In: Guimarães Netto R., Carmona N. B., Tognoli, F. M. W. (eds.). Ichnology of Latin America (Selected Papers)*, Monografias da Sociedade Brasileira de Paleontologia, 2, Porto Alegre, SBP, p. 37–68.

Guo W., Tong J., Tian L., Chu D., Bottjer D. J., Shu W., Ji K. 2019. Secular variations of ichnofossils from the terrestrial Late Permian–Middle Triassic succession at the Shichuanhe section in Shaanxi Province, North China. *Global and Planetary Change*, **181**: 102978. Disponível em: <https://www.sciencedirect.com/science/article/abs/pii/S0921818119301961>. Acesso em: 28 jul. 2021.

Hasiotis S. T. 2004. Reconnaissance of Upper Jurassic Morrison Formation ichnofossils, Rocky Mountain Region, USA: paleoenvironmental, stratigraphic, and paleoclimatic significance of terrestrial and freshwater ichnocoenoses. *Sedimentary Geology*, **167**(3–4): 177–268. Disponível em: <https://www.sciencedirect.com/science/article/abs/pii/S0037073804000090>. Acesso em: 28 jul. 2021.

Hasiotis S. T. 2007. Continental Ichnology: fundamental processes and controls on trace fossil distribution. *In: Miller III W. (ed.). Trace fossils. concepts, problems, prospects.* Amsterdam, Elsevier, p. 268–284.

Hasui Y., Costa J. B. S., Borges M. S., Assis J. F. P., Pinheiro R. V. L., Bartorelli A., Pires Neto A. G., Mioto J. A. 1991. A borda sul da Bacia do Parnaíba no Mesozóico. *In: SBG, 3º Simpósio Nacional de Estudos Tectônicos, Rio Claro. Boletim de resumos.* p. 93–98.

Heinberg C. 1973. The internal structure of the trace fossils Gyrochorte and Curvolithus. *Lethaia*, **6**(3): 227–238. Disponível em: <https://onlinelibrary.wiley.com/doi/10.1111/j.1502-3931.1973.tb01196.x>. Acesso em: 28 jul. 2021.

Hminna A., Lagnaoui A., Zouheir T., Saber H., Schneider J. W. 2020. Late Triassic ichnoassemblage from a playa-lake system of the Coastal Meseta, Morocco: Palaeoenvironmental and palaeoecological implications. *Journal of African Earth Sciences*, **172**: 103995. Disponível em: <https://www.sciencedirect.com/science/article/abs/pii/S1464343X20302466?via%3Dihub>. Acesso em: 28 jul. 2021.

Holz M. 2015. Mesozoic paleogeography and paleoclimate – a discussion of the diverse greenhouse and hothouse conditions of an alien world. *Journal of South American Earth Sciences*, **61**: 91–107. Disponível em: <https://www.sciencedirect.com/science/article/abs/pii/S0895981115000024?via%3Dihub>. Acesso em: 28 jul. 2021.

Ilgar A. & Nemeç W. 2005. Early Miocene lacustrine deposits and sequence stratigraphy of the Ermenek Basin, Central Taurides, Turkey. *Sedimentary Geology*, **173**(1–4): 233–275. Disponível em: <https://www.sciencedirect.com/science/article/abs/pii/S0037073804002994?via%3Dihub>. Acesso em: 28 jul. 2021.

- Keighley D., Flint S., Howell J., Moscariello A. 2003. Sequence stratigraphy in lacustrine basins: a model for part of the Green River Formation (Eocene), southwest Uinta Basin, Utah, U.S.A. *Journal of Sedimentary Research*, **73**(6): 987–1006. Disponível em: <https://pubs.geoscienceworld.org/sepm/jsedres/article-abstract/73/6/987/99351/Sequence-Stratigraphy-in-Lacustrine-Basins-A-Model?redirectedFrom=fulltext>. Acesso em: 28 jul. 2021.
- Kim J. Y. & Pickerill R. 2003. Cretaceous Nonmarine Trace Fossils from the Hasandong and Jinju Formations of the Namhae Area, Kyongsangnamdo, Southeast Korea, *Ichnos*, **9**(1–2): 41–60. Disponível em: <https://www.tandfonline.com/doi/abs/10.1080/10420940190034076>. Acesso em: 28 jul. 2021.
- Kim J. Y., Keighley D. G., Pickerill R. K., Hwanga W., Kim K. 2005. Trace fossils from marginal lacustrine deposits of the Cretaceous Jinju Formation, southern coast of Korea. *Palaeogeography, Palaeoclimatology, Palaeoecology*, **218**(1–2): 105–124. Disponível em: <https://www.sciencedirect.com/science/article/abs/pii/S0031018204006315?via%3Dihub>. Acesso em: 28 jul. 2021.
- Klöcking M., White N., MacLennan J. 2018. Role of basaltic magmatism within the Parnaíba cratonic basin, NE Brazil. In: Daly M. C., Fuck R. A., Julià J., Macdonald D. I. M., Watts A. B. (eds.). *Cratonic basin Formation: a case study of the Parnaíba basin of Brazil*. London, Geological Society of London, p. 309–319. Disponível em: <https://pubs.geoscienceworld.org/books/book/2149/chapter/120161222/Role-of-basaltic-magmatism-within-the-Parnaiba>. Acesso em: 28 jul. 2021. (Special Publications 472)
- Knaust D. 2012. Trace-fossil systematics. *Developments in Sedimentology*, **64**: 79–101. Disponível em: <https://www.sciencedirect.com/science/article/pii/B9780444538130000034>. Acesso em: 02 ago. 2021.
- Knaust D. 2017. *Atlas of trace fossils in well core: appearance, taxonomy and interpretation*. New York, Springer, 209 p.
- Knaust D., Thomas R. D., Curran H. A. 2018. *Skolithos linearis* Haldeman, 1840 at its early Cambrian type locality, Chickies Rock, Pennsylvania: analysis and designation of a neotype. *Earth-Science Reviews*, **185**: 15–31. Disponível em: <https://www.sciencedirect.com/science/article/abs/pii/S0012825218300540?via%3Dihub>. Acesso em: 28 jul. 2021.
- Kuchle J. 2011. A contribution to regional stratigraphic correlations of the Afro-Brazilian depression – The Dom João Stage (Brotas Group and equivalent units–Late Jurassic) in Northeastern Brazilian sedimentary basins. *Journal of South American Earth Sciences*, **31**(4): 358–371. Disponível em: <https://www.sciencedirect.com/science/article/abs/pii/S0895981111000150?via%3Dihub>. Acesso em: 28 jul. 2021.
- Lawfield A. M. W. & Pickerill R. K. 2006. A novel contemporary fluvial ichnocoenose: unionid bivalves and the *Scoyenia-Mermia* ichnofacies transition. *Palaios*, **21**(4): 391–396. Disponível em: <https://pubs.geoscienceworld.org/sepm/palaios/article-abstract/21/4/391/145837/A-NOVEL-CONTEMPORARY-FLUVIAL-ICHNOCOENOSE-UNIONID>. Acesso em: 28 jul. 2021.

- Lima M. R. & Campos D. A. 1980. Palinologia dos folhelhos da fazenda Muzinho, Floriano, Piauí. *Boletim IG*, **11**: 149-154. Disponível em: <http://www.ppegeo.igc.usp.br/index.php/bigusp/article/view/2871>. Acesso em: 05 ago. 2021.
- Lima E. A. M. & Leite J. F. 1978. *Projeto de estudo global dos recursos minerais da Bacia Sedimentar do Parnaíba*. Integração Geológico-Metalogenética: Relatório Final da Etapa III. Recife, Companhia de Pesquisa de Recursos Minerais. 212p.
- Lima J. H. D., Guimarães Netto R., Corrêa C. G., Lavina E. L. C. 2015. Ichnology of deglaciation deposits from the Upper Carboniferous Rio do Sul Formation (Itarare Group, Parana Basin) at central-east Santa Catarina State (southern Brazil). *Journal of South American Earth Sciences*, **63**: 137–148. Disponível em: <https://www.sciencedirect.com/science/article/abs/pii/S0895981115300274?via%3Dihub>. Acesso em: 28 jul. 2021.
- Lisboa M. A. R. 1914. Permian geology of northern Brazil. *American Journal of Science*, **4**(221): 425-443. Disponível em: <https://www.ajsonline.org/content/s4-37/221/425>. Acesso em: 05 ago. 2021.
- Lucas S. G. & Lerner A. J. 2006. Invertebrate ichnofossil assemblages of the upper Triassic Redonda Formation at Mesa Redonda, east-central New Mexico. In: Harris J. D., Lucas S. G., Spielmann J. A., Lockley M. G., Milner A. R. C., Kirkland, J. I. (eds.). *The Triassic-Jurassic Terrestrial Transition*. Albuquerque: New Mexico Museum of Natural History, p. 122–127. (Bulletin 37)
- MacEachern J. A., Pemberton S. G., Gingras M. K., Bann K. L. 2007. The ichnofacies concept: a fifty-year retrospective. In: Miller III W. (ed.). *Trace fossils: concepts, problems, prospects*. Amsterdam, Elsevier, p. 50–75.
- MacEachern J. A., Pemberton S. G., Gingras M. K., Bann K. L. 2010. Ichnology and facies models. In: James N. P. & Dalrymple R. W. (eds.). *Facies models 4, GEOText 6*. Ottawa, Geological Association of Canada, p. 19–58.
- Mancuso A. C., Krapovickas V., Benavente C. A., Marsicano C. A. 2020. An integrative physical, mineralogical and ichnological approach to characterize underfilled lake-basins. *Sedimentology*, **67**(6): 3088–3118. Disponível em: <https://onlinelibrary.wiley.com/doi/abs/10.1111/sed.12736>. Acesso em: 03 ago. 2021.
- Mángano M. G. & Buatois L. A. 2014. Decoupling of body-plan diversification and ecological structuring during the Ediacaran–Cambrian transition: evolutionary and geobiological feedbacks. *Proceedings of the Royal Society B: Biological Sciences*, **281** (1780): 20140038. Disponível em: <https://royalsocietypublishing.org/doi/10.1098/rspb.2014.0038>. Acesso em: 28 jul. 2021.

Marchetti L., Petti F. M., Zoboli D., Pillola G. L. 2017. Vertebrate and invertebrate trace fossils in the Late Pennsylvanian (Carboniferous) fluvio-lacustrine San Giorgio Basin (South-West Sardinia): remarks on the oldest continental ichnoassociation of Italy. *Ichnos*, **25**(2–3): 94–105. Disponível em: <https://www.tandfonline.com/doi/abs/10.1080/10420940.2017.1337572>. Acesso em: 28 jul. 2021.

Marensi S. A., Limarino C. O., Schencman L. J., Ciccioli P. L. 2020. Tectonic and geomorphic controls on the lacustrine deposits of the Neogene Vinchina basin, northwestern Argentina. *Journal of Sedimentary Research*, **90**(2): 250–267. Disponível em: <https://pubs.geoscienceworld.org/sepm/jsedres/article-abstract/90/2/250/581952/Tectonic-and-geomorphic-controls-on-the-lacustrine?redirectedFrom=fulltext>. Acesso em: 28 jul. 2021.

Martinsson A. 1970. Toponymy of trace fossils. In: Crimes T. P. & Harper J. C. (eds.). *Trace fossils*. Liverpool, Seel House Press, p. 323–330. (Geological Journal Special Issue 3).

Marzoli A., Renne P. R., Piccirillo E. M., Ernesto M., Bellieni G., De Min, A. 1999. Extensive 200-million-year-old continental flood basalts of the Central Atlantic Magmatic Province. *Science*, **284**(5414): 616–618. Disponível em: <https://science.sciencemag.org/content/284/5414/616>. Acesso em: 03 ago. 2021.

McHone J. G. 2000. Non-plume magmatism and rifting during the opening of the central Atlantic Ocean. *Tectonophysics*, **316**(3–4): 287–296. Disponível em: <https://www.sciencedirect.com/science/article/abs/pii/S0040195199002607?via%3Dihub>. Acesso em: 28 jul. 2021.

Melchor R. N. 2003. Invertebrate and vertebrate trace fossils from a Triassic lacustrine delta: the Los Rastros Formation, Ischigualasto Provincial Park, San Juan, Argentina. *Publicación Electrónica de la Asociación Paleontológica Argentina*, **9**(1). Disponível em: <https://www.peapaleontologica.org.ar/index.php/peapa/article/view/17>. Acesso em: 28 jul. 2021.

Melchor R. N. 2004. Trace fossil distribution in lacustrine deltas: examples from the Triassic rift lakes of the Ischigualasto-Villa Unión basin, Argentina. In: McIlroy, D. (ed.). *The Application of Ichnology to Palaeoenvironmental and Stratigraphic Analysis*. London, Geological Society, p. 335–354. Disponível em: <https://pubs.geoscienceworld.org/books/book/1605/chapter/107393988/Trace-fossil-distribution-in-lacustrine>. Acesso em: 28 jul. 2021. (Special Publications, v. 228).

Mesner C. J. & Wooldridge C. P. 1964. Maranhão Paleozoic basin and Cretaceous coastal basin, north Brazil. *Bulletin of the American Association of Petroleum Geologists*, **48**(9):1475-1512. Disponível em: <https://pubs.geoscienceworld.org/aapgbull/article-abstract/48/9/1475/36296/Maranhao-Paleozoic-Basin-and-Cretaceous-Coastal?redirectedFrom=PDF>. Acesso em: 05 ago. 2021.

Miall A. D. 1977a. Lithofacies types and vertical profile models in braided river deposits: a summary. In: Miall A. D. (ed.). *Fluvial sedimentology*. Calgary, Geological Survey of Canada, p.597-604.

- Miall A. D. 1977b. A review of the braided-river depositional environment. *Earth-Science Reviews*, **13**(1): 1-62. Disponível em: <https://www.sciencedirect.com/science/article/abs/pii/0012825277900551>. Acesso em: 05 ago. 2021.
- Miall A. D. 2014. *Fluvial depositional systems*. Berlin, Springer International Publishing.
- Miller M. F. & Small S. E. 1997. A semiquantitative field method for evaluating bioturbation on bedding planes. *Palaios*, **12**(4): 391–396. Disponível em: <https://pubs.geoscienceworld.org/sepm/palaios/article-abstract/12/4/391/99663/A-semiquantitative-field-method-for-evaluating?redirectedFrom=fulltext>. Acesso em: 28 jul. 2021.
- Minter N. J., Krainer K., Lucas S. G., Braddy S. J., Hunt A. P. 2007. Palaeoecology of an Early Permian playa lake trace fossil assemblage from Castle Peak, Texas, USA. *Palaeogeography, Palaeoclimatology, Palaeoecology*, **246**(2–4): 390–423. Disponível em: <https://www.sciencedirect.com/science/article/abs/pii/S0031018206005864>. Acesso em: 31 jul. 2021.
- Montefeltro F. C., Larsson H. C. E., França M. A. G., Langer M. C. 2013. A new neosuchian with Asian affinities from the Jurassic of northeastern Brazil. *Naturwissenschaften*, **100**: 835–841. Disponível em: <https://link.springer.com/article/10.1007%2Fs00114-013-1083-9>. Acesso em: 28 jul. 2021.
- Silva P. H. M., Sá E. F. J., Souza Z. S., Córdoba V. C. 2020. Structural controls and stratigraphic setting of sills: Example of the Central Atlantic Magmatic Province in the Parnaíba Basin, Northeast Brazil. *Journal of South American Earth Sciences*, **101**:102606. Disponível em: <https://www.sciencedirect.com/science/article/abs/pii/S089598112030119X>. Acesso em: 04 ago. 2021.
- Neibur E. & Erdős P. 1991. Theory of the locomotion of nematodes. *Biophysical Journal*, **60**(5): 1132–1146. Disponível em: <https://www.sciencedirect.com/science/article/pii/S000634959182149X>. Acesso em: 05 ago. 2021.
- Nichols G. J. 2004. Sedimentation and base level in an endorheic basin: the early Miocene of the Ebro Basin, Spain. *Boletín Geológico y Minero*, **115**(3): 427–438.
- Nichols G. J. 2007. Features of fluvial systems in desiccating endorheic basins. In: Nichols G. J., Williams E. A., Paola C. (Eds.). *Sedimentary Processes, Environments and Basins: A Tribute to Peter Friend*. International Association of Sedimentologists, Oxford, Blackwell, p. 567–587. (Special Publication 38).
- Nichols G. J. 2009. *Sedimentary and stratigraphy*. 2nd ed. Chichester, Wiley-Blackwell, 432 p.
- Nichols G. J. 2012. Endorheic basins. In: Busby C. & Azor A. (eds.). *Tectonics of sedimentary basins: recent advances*. Oxford, Wiley, p. 621–632.

- Nogueira A. C. R., Rabelo C. E. N., Góes A. M., Cardoso A. R., Bandeira J., Rezende G. L., Santos R. F., Truckenbrodt W. 2021. Evolution of Jurassic intertrap deposits in the Parnaíba Basin, northern Brazil: The last sediment-lava interaction linked to the CAMP in West Gondwana. *Palaeogeography, Palaeoclimatology, Palaeoecology*, **572**: 110370. Disponível em: [https://www.sciencedirect.com/science/article/abs/pii/S0031018221001553?dgcid=rss\\_sd\\_all](https://www.sciencedirect.com/science/article/abs/pii/S0031018221001553?dgcid=rss_sd_all). Acesso em: 05 ago. 2021.
- Oliveira D. C. & Mohriak W. U. 2003. Jaibaras trough: an important element in the early tectonic evolution of the Parnaíba interior sag basin, Northern Brazil. *Marine and Petroleum Geology*, **20**(3–4), 351–383. Disponível em: <https://www.sciencedirect.com/science/article/abs/pii/S0264817203000448>. Acesso em: 05 ago. 2021.
- Osgood Jr R. G. 1970. Trace fossils of the Cincinnati area. *Palaeontographica Americana*, **6**(41): 281–444.
- Paik I. S. & Kim H. J. 1998. Subaerial lenticular cracks in Cretaceous lacustrine deposits, Korea. *Journal of Sedimentary Research*, **68**: 80–87.
- Pemberton S. G. & Frey R. W. 1982. Trace fossil nomenclature and the Planolites-Palaeophycus dilemma. *Journal of Paleontology*, **56**(4): 843–881.
- Pemberton S. G. & Frey R. W. 1984. Ichnology of storm-influenced shallow marine sequence: Cardium Formation (Upper Cretaceous) at Seebe, Alberta. In: Stott D. F., Glass D. J. *The Mesozoic of Middle North America: A Selection of Papers from the Symposium on the Mesozoic of Middle North America*, Calgary, Alberta, Canada. Alberta, Canadian Society of Petroleum Geologists. (Memoir 9)
- Pereira E., Carneiro C. D. R., Bergamaschi S., Almeida F. D. 2012. Evolução das sinéclises paleozoicas: províncias Solimões, Amazonas, Parnaíba e Paraná. In: Hasui Y., Carneiro D. R. C., Almeida F. F. M., Bartorelli A. (org.). *Geologia do Brasil*. São Paulo, Beca, p. 510–513. (v. 1)
- Petra M. S. 2006. *Paleoictiofauna da Formação Pastos Bons (Bacia do Parnaíba) – reconstituição paleoambiental e posicionamento cronoestratigráfico*. MS Dissertation. Programa de Pós-Graduação em Biociências, Universidade do Estado do Rio de Janeiro, Rio de Janeiro, 141 p.
- Petra R. & Gallo V. 2012. Tafonomia da paleoictiofauna do Jurássico da Bacia do Parnaíba e comparação bioestratinômica com as bacias da América do Sul e África. In: Gallo V., Silva H. M. A., Brito P. M., Figueiredo F. J. *Paleontologia de vertebrados: relações entre América do Sul e África*. Rio de Janeiro, Editora Interciência, p. 151–173.
- Plummer F. D. 1946. *Geossinclíneo do Parnaíba*. Rio de Janeiro, Conselho Nacional de Petróleo. (Relatório).
- Pinto I. D. & Purper Y. 1974. Observations on Mesozoic Conchostracea from the north of Brazil. In: SBG, 28º Congresso Brasileiro de Geologia, Porto Alegre. *Anais...* Porto Alegre, SBG, v. 2, p. 5–16.



Pollard J. E. & Hardy P. G. 1991. Trace fossils from the Westphalian D of Writhlington Geologica Nature Reserve nr. Radstock. *Avon Geologists' Association Proceedings*, **102**: 169–178.

Pokorný R., Krmíček L., Sudo M. 2017. An endemic ichnoassemblage from a late Miocene paleolake in SE Iceland. *Palaeogeography, Palaeoclimatology, Palaeoecology*, **485**: 761–773. Disponível em: <https://www.sciencedirect.com/science/article/abs/pii/S0031018217302110?via%3Dihub>. Acesso em: 31 jul. 2021.

Porto A., Daly M. C., La Terra E., Fontes S. 2018. The pre-Silurian Riachão Basin: a new perspective on the basement of the Parnaíba Basin, NE Brazil. In: Daly M. C., Fuck R. A., Julià J., Macdonald D. I. M., Watts A. B. (eds.). *Cratonic basin Formation: a case study of the Parnaíba basin of Brazil*. London, Geological Society of London, p. 127–145. Disponível em: <https://pubs.geoscienceworld.org/books/book/2149/chapter/120160511/The-pre-Silurian-Riachao-basin-a-new-perspective>. Acesso em: 31 jul. 2021. (Special Publications 472)

Postma G. 1990. An analysis of the variation in delta architecture. *Terra Nova*, **2**(2): 124–130.

Rabelo C. N. & Nogueira A. C. R. 2015. O sistema desértico úmido do Jurássico Superior da Bacia do Parnaíba, na região entre formosa da Serra Negra e Montes Altos, Estado do Maranhão, Brasil. *Geologia USP: Série Científica*, **15**(3–4): 3–21. Disponível em: <http://ppegeo.igc.usp.br/index.php/GUSPSC/article/view/4121>. Acesso em: 31 jul. 2021.

Rabelo C. E. N., Cardoso A. R., Nogueira A. C. R., Soares J. L., Góes A. M. 2019. Genesis of poikilotopic zeolite in aeolianites: an example from the Parnaíba Basin, NE Brazil. *Sedimentary Geology*, **385**: 61–78. Disponível em: <https://www.sciencedirect.com/science/article/abs/pii/S0037073819300685>. Acesso em: 05 ago. 2021.

Radley J. D., Barker M. J., Munt M. C. 1998. Bivalve trace fossils (*Lockeia*) from the Barnes High Sandstone (Wealden Group, Lower Cretaceous) of the Wessex Sub-basin, southern England. *Cretaceous Research*, **19**(3–4): 505–509. Disponível em: <https://www.sciencedirect.com/science/article/abs/pii/S0195667197901099?via%3Dihub>. Acesso em: 31 jul. 2021.

Renaut R. W., Gierlowski-Kordesch E. H., 2010. Lakes. In: Dalrymple R. & James N. (eds.) *Facies models*. 4th ed. Toronto, Geological Association of Canada, p. 541–575.

Rezende N. G. A. M. 1997. *Argilas Nobres e zeólitas da Bacia do Parnaíba*: relatório final de projeto. Belém, CPRM, p. 33–44. (Informe de Recursos Minerais, Série Diversos 2)

Rezende G. L., Martins C. M., Nogueira A. C., Domingos F. G., Ribeiro-Filho N. 2021. Evidence for the Central Atlantic magmatic province (CAMP) in Precambrian and Phanerozoic sedimentary basins of the southern Amazonian Craton, Brazil. *Journal of South American Earth Sciences*, **108**: 103216. Disponível em: <https://www.sciencedirect.com/science/article/abs/pii/S0895981121000638>. Acesso em: 05 ago. 2021.

Romero Ballén O. A. R. 2012. *As sucessões sedimentares interderrames da Formação Mosquito, exemplo de um sistema eólico úmido, Província Parnaíba*. MS Dissertation, Universidade de São Paulo, 85 f.

Romero Ballén O. A. R., Góes A. M., Negri F. A., Mazivieiro M. V., Teixeira V. Z. S. 2013. Sistema eólico úmido nas sucessões sedimentares interderrames da Formação Mosquito, Jurássico da Província Parnaíba. *Brazilian Journal of Geology*, **43**: 695–710. Disponível em: <http://www.ppegeo.igc.usp.br/index.php/bjg/article/view/7491>. Acesso em: 31 jul. 2021.

Roxo M. & Löfgren A. 1936. *Lepidotus piauhyensis, sp. nov.* Notas Preliminares e Estudos. Rio de Janeiro, Divisão de Geologia e Mineralogia/DNPM, p. 7–12.

Rubert R. R., Mizusaki A. M. P., Martinelli A. G. 2019. Mesozoic tectonic in the deposition and evolution of Cretaceous sedimentary packages of the Parecis Basin, centerwestern Brazil, *Journal of South American Earth Sciences* **93**: 140–154. Disponível em: <https://www.sciencedirect.com/science/article/abs/pii/S0895981118305066?via%3Dihub>. Acesso em: 31 jul. 2021.

Rubert R. R., Mizusaki A. M. P., Martinelli A. G., Urban C. 2017. Paleoenvironmental reconstruction and evolution of an Upper Cretaceous lacustrine-fluvial-deltaic sequence in the Parecis Basin, Brazil. *Journal of South American Earth Sciences*, **80**: 512–528. Disponível em: <https://www.sciencedirect.com/science/article/abs/pii/S0895981117302638?via%3Dihub>. Acesso em: 31 jul. 2021.

Santos R. S. 1953. Peixes triássicos dos folhelhos da Fazenda Muzinho, estado do Piauí. *Notas Preliminares e Estudos*, Rio de Janeiro, Departamento Nacional de Produção Mineral. DNPM, **82**:170-178.

Santos M. E. C. M. & Carvalho M. S. S. 2004. *Paleontologia das Bacias do Parnaíba, Grajaú e São Luís*. 2nd. ed. Rio de Janeiro, CPRM, 212p.

Santos H. P., Mángano M. G., Soares J. L., Nogueira A. C., Bandeira J., Rudnitzki I. D. 2017. Ichnologic evidence of a Cambrian age in the Southern Amazon Craton: Implications for the onset of the Western Gondwana history. *Journal of South American Earth Sciences*, **76**: 482–488. Disponível em: <https://www.sciencedirect.com/science/article/abs/pii/S0895981117300263?via%3Dihub>. Acesso em: 31 jul. 2021.

Savdra C. E. 2007. Taphonomy of trace fossils. In: Miller III W. (ed.). *Trace fossils*. concepts, problems, prospects. Amsterdam, Elsevier, p. 96–109.

Savage N. M. 1971. A varvite ichnocoenosis from the Dwyka Series of Natal. *Lethaia*, **4**(2): 217–233. Disponível em: <https://onlinelibrary.wiley.com/doi/abs/10.1111/j.1502-3931.1971.tb01290.x>. Acesso em: 31 jul. 2021.

Schlirf M., Uchman A., Kümmel M. 2001. Upper triassic (Keuper) non-marine trace fossils from the Haßberge area (Franconia, South-eastern Germany). *Paläontologische Zeitschrift*, **75**(1): 71–96.

- Scott J. J., Buatois L. A., Mangano M. G. 2012. Lacustrine environments. *In*: Knaust D. R. & Bromley G. (eds.). *Fossils as indicators of sedimentary environments*. Part II Continental and Glacial Systems. Amsterdam, Elsevier, p. 379–417. (Developments in Sedimentology 64).
- Scott J. J. & Smith M. E. 2015. Trace fossils of the Eocene Green River lake basins, Wyoming, Utah, and Colorado. *In*: Smith M. E & Carroll A. R. (eds.). *Stratigraphy and paleolimnology of the Green River Formation, Western U.S.* Dordrecht, Springer, p. 313–350.
- Scherer C. M. S., Lavina E. L. C., Dias Filho D. C., Oliveira F. M., Bongioiolo D. E., Aguiar E. S. 2007. Stratigraphy and facies architecture of the fluvial–aeolian–lacustrine Sergi Formation (Upper Jurassic), Recôncavo Basin, Brazil. *Sedimentary Geology*, **194**(3–4): 169–193.  
Disponível em:  
<https://www.sciencedirect.com/science/article/abs/pii/S0037073806001692?via%3Dihub>.  
Acesso em: 31 jul. 2021.
- Seilacher A. 1967. Bathymetry of trace fossils. *Marine geology*, **5**(5–6), 413–428.
- Seilacher A. 1964. Biogenic sedimentary structures. *In*: Imbrie J. & Newell N. (Eds.). *Approaches to Paleocology*. New York, John Wiley and Sons Inc, p. 296–316.
- Seilacher A. 1963. Lebensspuren und saunitatsfazies. *Fortschritte in der Geologie Rheinland und Westfalen*, **10**: 81–94.
- Seilacher A. 1953. Studien zur palichnologie. I. Über die methoden der palichnologie. *Neues Jahrbuch für Geologie und Palaontologie, Abhandlungen*, **96**: 421–452.
- Seilacher A. & Seilacher E. 1994. Bivalvian trace fossils: a lesson from actuopaleontology. *Courier Forschungsinstitut Senckenberg*, **169**: 5–15.
- Spence G. H. & Tucker M. E. 2007. A proposed integrated multi-signature model for peritidal cycles in carbonates. *Journal of Sedimentary Research*, **77**(10): 797–808. Disponível em:  
<https://pubs.geoscienceworld.org/sepm/jrsedres/article-abstract/77/10/797/330339/A-Proposed-Integrated-Multi-Signature-Model-for?redirectedFrom=fulltext>. Acesso em: 31 jul. 2021.
- Stanley D. C. A. & Pickerill R. K. 1998. *Systematic ichnology of the Late Ordovician Georgian Bay Formation of southern Ontario Canada*. Toronto, Royal Ontario Museum, 56 p. (Life Sciences Contributions 162).
- Talbot M. R. & Allen P. A. 1996. *Sedimentary environments: processes, facies and stratigraphy*. 3rd ed. Oxford, Blackwell Science Oxford, p. 83–124.
- Torsvik T. H. & Cocks L. R. M. 2013. Gondwana from top to base in space and time. *Gondwana Research*, **24**(3–4), 999–1030. Disponível em:  
<https://www.sciencedirect.com/science/article/abs/pii/S1342937X13002165>. Acesso em: 04 ago. 2021.

- Uchman A., Pika-Biolzi M., Hochuli P. A. 2004. Oligocene trace fossils from temporary fluvial plain ponds: an example from the Freshwater Molasse of Switzerland. *Eclogae Geologicae Helveticae*, **97**: 133–148. Disponível em: <https://sjg.springeropen.com/articles/10.1007/s00015-004-1111-z>. Acesso em: 31 jul. 2021.
- Vaz P. T., Rezende N. G. A. M., Wanderley Filho J. R., Travassos W. A. S. 2007. Bacia do Parnaíba. *Boletim de Geociências da Petrobras*, **15**(2): 253–263.
- Walker R. G. 1992. Facies, facies models and modern stratigraphic concepts. In: Walker R. G. & James N. P. (eds.). *Facies models – response to sea level change*. 1st. ed. Ontario, Geological Association of Canada, p. 1–14.
- Wang C., Wang Hu, J. B., Lu X. 2015. Trace fossils and sedimentary environments of the upper cretaceous in the Xixia Basin, Southwestern Henan Province, China. *Geodinamica Acta*, **28**(1–2): 53–70. Disponível em: <https://www.tandfonline.com/doi/full/10.1080/09853111.2015.1065307>. Acesso em: 31 jul. 2021.
- Weiss W. 1941. Die entstehung der ‘zöpfe’ im schwarzen und braunen jura. *Natur und Volk*, **71**: 179–184.
- White D. S. & Miller M. F. 2008. Benthic invertebrate activity in lakes: linking present and historical bioturbation patterns. *Aquatic Biology*, **2**(3): 269–277.
- Zaleha M. J. 1997. Fluvial and lacustrine palaeoenvironments of the Miocene Siwalik Group, Khaur area, northern Pakistan. *Sedimentology*, **44**(2): 349–368. Disponível em: <https://onlinelibrary.wiley.com/doi/10.1111/j.1365-3091.1997.tb01529.x>. Acesso em: 31 jul. 2021.